

DEC 10 1992

ornl

**OAK RIDGE
NATIONAL
LABORATORY**

MARTIN MARIETTA

**ORNL
MASTER COPY**

ORNL/TM-12152

**Criticality Safety Studies for the
Storage of Waste from Nuclear
Fuel Services in Intercell Storage
Wells 2 and 3 of Building 3019**

R. T. Primm, III
C. M. Hopper
G. R. Smolen

MANAGED BY
MARTIN MARIETTA ENERGY SYSTEMS, INC.
FOR THE UNITED STATES
DEPARTMENT OF ENERGY

This report has been reproduced directly from the best available copy.

Available to DOE and DOE contractors from the Office of Scientific and Technical Information, P.O. Box 62, Oak Ridge, TN 37831; prices available from (615) 576-8401, FTS 626-8401.

Available to the public from the National Technical Information Service, U.S. Department of Commerce, 5285 Port Royal Rd., Springfield, VA 22161.

This report was prepared as an account of work sponsored by an agency of the United States Government. Neither the United States Government nor any agency thereof, nor any of their employees, makes any warranty, express or implied, or assumes any legal liability or responsibility for the accuracy, completeness, or usefulness of any information, apparatus, product, or process disclosed, or represents that its use would not infringe privately owned rights. Reference herein to any specific commercial product, process, or service by trade name, trademark, manufacturer, or otherwise, does not necessarily constitute or imply its endorsement, recommendation, or favoring by the United States Government or any agency thereof. The views and opinions of authors expressed herein do not necessarily state or reflect those of the United States Government or any agency thereof.

Engineering Physics and Mathematics Division

CRITICALITY SAFETY STUDIES FOR THE STORAGE OF WASTE FROM
NUCLEAR FUEL SERVICES IN INTERCELL STORAGE WELLS 2 AND 3
OF BUILDING 3019

R. T. Primm, III, C. M. Hopper, and G. R. Smolen

DATE PUBLISHED — November 1992

Research sponsored by the
Office of Environmental Restoration
and Waste Management
U.S. Department of Energy

Prepared by the
OAK RIDGE NATIONAL LABORATORY
Oak Ridge, Tennessee 37831
managed by
MARTIN MARIETTA ENERGY SYSTEMS, INC.
for the
U.S. DEPARTMENT OF ENERGY
under contract DE-AC05-84OR21400

TABLE OF CONTENTS

ACKNOWLEDGEMENTS	ix
ABSTRACT	xi
1. INTRODUCTION	1
2. FACILITY DESCRIPTION	1
2.1 WASTE MATERIALS	2
2.2 CONTINGENT CONDITIONS	2
3. ANALYSIS METHODS	2
3.1 PROGRAMS AND CROSS SECTIONS	2
3.2 COMPUTATIONAL ADEQUACY	10
3.3 MARGINS OF SAFETY (COMPUTED SUBCRITICALITY)	10
4. COMPUTATIONS PERFORMED BY C. M. HOPPER (1985)	10
4.1 ASSUMPTIONS IN COMPUTATIONAL MODELS	10
4.2 COMPUTATIONAL RESULTS	10
4.3 SUBCRITICAL LOAD LIMITS FOR SINGLE CONTAINERS	11
5. INVESTIGATION OF HOPPER CALCULATIONS	11
5.1 COMPUTATIONAL MODEL	11
5.2 VERIFICATION OF ASSUMPTIONS FOR SECTION 4 CALCULATIONS	15
6. COMPUTATIONS AND SAFETY ANALYSES SPECIFIC TO NFS WASTE	18
6.1 METHODOLOGY	18
6.2 COMPUTATIONAL MODELS	18
6.3 RESULTS	19
7. CONDITIONS FOR STORAGE WELL USE AND ASSIGNMENT OF SAFE FISSILE MATERIAL LIMITS	20
7.1 INITIAL CONDITIONS	20
7.2 MATERIAL DEFINITION AND CONTAINMENT	20
7.3 FISSILE MATERIAL TRANSFERS TO, FROM, AND AMONG STORAGE WELLS	20
8. CONCLUSIONS	21
REFERENCES	22

TABLE OF CONTENTS (continued)

APPENDIX A	23
A.1 INTRODUCTION	24
A.2 COMPUTATIONAL METHODS	24
A.3 CALCULATION OF K-EFFECTIVE FOR MIXED URANIUM AND PLUTONIUM OXIDE EXPERIMENTS	24
A.3.1 Unpoisoned Experiments with Little Moderation	24
A.3.2 Poisoned Experiments with Little Moderation	26
A.3.3 Unpoisoned, High-Moderation Mixed-Oxide Critical Experiments	29
A.4 INTERACTING ARRAY EXPERIMENTS	36
A.5 CONCRETE-REFLECTED EXPERIMENTS	36
A.6 STATISTICAL ANALYSES OF CRITICAL EXPERIMENTS	38
A.7 CORRECTIONS TO DERIVED SUBCRITICALITY LIMITS TO ACCOUNT FOR UNCERTAINTIES IN EXPERIMENTAL MEASUREMENTS	41
A.8 COMMENTS ON APPLICABILITY OF CRITICAL EXPERIMENTS AND MARGIN OF SUBCRITICALITY	42
REFERENCES FOR APPENDIX A	47
APPENDIX B	49
APPENDIX C	55
APPENDIX D	61
APPENDIX E	63
E.1 REACTIVITY AND PHYSICAL PARAMETERS OF THE WASTE MATERIAL	64
E.2 INTERPOLATIONS OF SUBCRITICAL FISSILE MATERIAL MASS LOADINGS	65
REFERENCES FOR APPENDIX E	68
APPENDIX F	69

LIST OF TABLES

Table 1.	NFS plutonium sources	7
Table 2.	Summary of plutonium activity for fuels with greater than 80 wt % ^{239}Pu	8
Table 3.	Summary of plutonium activity for fuels with less than 80 wt % ^{239}Pu	9
Table 4.	Considered ^{239}Pu material characteristics	11
Table 5.	Intercell 2 and 3 ^{239}Pu results	12
Table 6.	Maximum subcritical fully water reflected single infinite cylinders of ^{239}Pu metal . .	14
Table 7.	Comparison of Intercell 2 and 3 calculations for ^{239}Pu	15
Table 8.	Atom densities in Barytes concrete	17
Table 9.	Impact of concrete composition on calculated k-effective	18
Table 10.	Reactivity parameters for abnormal intercell 2 and 3 storage configurations	20
Table A.1.	Description of experimental fuel and reflector for experiments 1453-01 to 15	25
Table A.2.	Critical assembly configurations for 29.3 wt % Pu, 2.8 H:(Pu+U), $\text{PuO}_2\text{-UO}_2$ -polystyrene fuel compacts	26
Table A.3.	Reflected critical assembly configuration for 15 wt % Pu, 2.86 H:(Pu+U), $\text{PuO}_2\text{-UO}_2$ -polystyrene fuel compacts	26
Table A.4.	Calculated k-effectives for unpoisoned, low-moderation experiments	27
Table A.5.	Description of experimental fuel and reflector material	28
Table A.6.	Composition of neutron poison plates	28
Table A.7.	Critical assembly configurations of poisoned, plexiglas-reflected 2.8 H:(Pu+U) mixed-oxide compacts	29
Table A.8.	Critical assembly configurations of poisoned, plexiglas-reflected 30.6 H:(Pu+U) mixed-oxide compacts	30
Table A.9.	Calculated k-effectives for poisoned, low-moderation experiments with H:(Pu+U) ratio = 2.8	32
Table A.10.	Calculated k-effectives for poisoned, low-moderation experiments with H:(Pu+U) ratio = 30.6	33

LIST OF TABLES (continued)

Table A.11. Composition and atom densities of fuels and reflector for high-moderation, mixed-oxide critical experiments	34
Table A.12. Criticality data for mixed-oxide assemblies containing 30 wt % Pu with H:(Pu + U) = 47.4	34
Table A.13. Criticality data for mixed-oxide assemblies containing 14.62 wt % Pu with H:(Pu + U) = 30.6	35
Table A.14. Calculated k-effectives for high-moderation, mixed-oxide critical experiments	35
Table A.15. Average calculated k-effectives for high-moderation mixed-oxide critical experiments	36
Table A.16. Experimental criticality data for concrete reflected type 3.2 FTR fuel pins in water	36
Table A.17. Comparison of concrete compositions	37
Table A.18. Calculated parameters for arrays of FTR pins	37
Table A.19. Categorized mean calculated k-effectives	38
Table A.20. Calculated Pearson product moment correlation coefficients for KENO-Va, Hansen-Roach calculations	39
Table A.21. Sources of experimental uncertainties	41
Table A.22. Reactivity worth of experimental uncertainties	44
Table E.1. Fitted constants of proportionality for ^{239}Pu in Intercell 2 and 3	65

LIST OF FIGURES

Fig. 1. Vertical inter-cells solid storage	3
Fig. 2. Intercell 2 and 3 storage wells	4
Fig. 3. Top view of cells 3, 2, and 1 (from left to right)	5
Fig. 4. Side view of cell 2	6
Fig. A.1. K-effectives from mixed-oxide criticals (KENO-Va, Hansen-Roach)	40
Fig. A.2. Computed spectral comparison. Nominal case to critical experiments	45
Fig. A.3. Calculated spectral comparison. Credible abnormal storage to critical experiment . . .	46
Fig. C.1. Analyses of concrete walls in Building 3019	57
Fig. C.2. FORTRAN program to calculate atom densities for constituents of concrete	59
Fig. C.3. Input to FORTRAN program to calculate concrete atom densities	60
Fig. C.4. Output from FORTRAN program to calculate concrete atom densities	60
Fig. E.1. Deviation of fit value from calculated k-eff	66
Fig. E.2. Intercell 2 and 3 ^{239}Pu storage well loadings	67

ACKNOWLEDGEMENTS

Gratitude is expressed to J. C. Turner for his coding of the numerous cases from the 1985 studies. Also, thanks go to J. T. Thomas for his constructive comments and reviews of the 1985 results. R. M. Westfall and E. C. Crume, Jr. provided helpful reviews of this document. R. D. Lawson performed excellently in handling all publication aspects of this report.

ABSTRACT

This report provides computational evaluation results demonstrating that mixed oxide waste can be safely stored in Intercell Storage Wells 2 and 3 of Building 3019 at the Oak Ridge National Laboratory. Existing, verified computational techniques are validated with applicable critical experiments and tolerance limits for safety analyses are derived. Multiplication factors for normal and credible abnormal configurations are calculated and found to be far subcritical when compared to derived safety limits.

CRITICALITY SAFETY STUDIES FOR THE STORAGE OF WASTE FROM NUCLEAR FUEL SERVICES IN INTERCELL STORAGE WELLS 2 AND 3 OF BUILDING 3019

R. T. Primm, III, C. M. Hopper, and G. R. Smolen

1. INTRODUCTION

This report provides computational evaluation results demonstrating that waste materials described herein can be stored in Intercell Storage Wells 2 and 3 of Building 3019 with an acceptably low risk of inadvertent criticality. Normal and credible abnormal conditions for storage are identified. This report does not provide justification for the definitions of normal and credible abnormal conditions. Rather, the purpose of these studies is to show that calculations are valid when given a set of assumptions. Verified and validated computer programs and data libraries are used to determine that all identified configurations are safely subcritical.

A large number of previously unreferable calculations performed by C. M. Hopper are included in this document and thereby made referable. The assumptions upon which these prior analyses are based are examined via the use of verified/validated methods and the creation of new computational models. The calculations themselves are not repeated with the exception of a limited number of "spot" checks using new models. Instead, the methods and data are validated via the work documented in Ref. 1 and in Appendix A. An investigation of assumptions made by Hopper enables previously performed calculations to be referable provided allowances are made for assumptions made in the computational models. Criticality safety requirements derived as a result of these studies are stated, but should be used with caution and do not form the basis of the current evaluation.

The reader should note that this document provides evaluation results of a particular waste material² for a particular storage location. At the time of the preparation of this document, work is under way on another document that would provide evaluations for a broader scope of fissile material operations. It is anticipated that, when completed, the broader, more comprehensive document will supersede this report as a reference for demonstrating subcriticality and criticality safety. This shorter, much more limited document is needed due to programmatic timetables.

2. FACILITY DESCRIPTION

According to A. M. Krichinsky, Chemical Technology Division, all Nuclear Fuel Services (NFS) waste material is to be stored in Intercell Storage 2 and 3 of Building 3019 except for that fraction that is to be shipped directly to a burial site.³ All of Intercell Storage 2 and 3 is currently empty.³ The reference description of Building 3019 is contained in Ref. 4, the "Final Safety Analysis Report for the Radiochemical Processing Plant" hereafter designated the FSAR. Figures 1 and 2 are Figs. 4.9 and 4.10, respectively, from the FSAR and show the configuration of the wells that makeup the Intercell Storage 2 and 3. Figures 3 and 4 are scaled drawings of cells 2 and 3. From these figures the dimensions are obtained that are used in the computational models described subsequently. Inspection of the actual installation was performed by one of the authors, and the documented geometry was confirmed.

The cell walls are believed to be composed of reinforced concrete. The measured concrete composition and derived atom densities are presented in Appendix C. Confirmation of the reinforcing steel content had not been obtained at the time of publication. All intercell storage wells have a 4-in.-diam schedule-

40 carbon steel pipe liner. The inside diameter of the liner is assumed to be 4.026 in. and the thickness of the pipe is 0.273 in.

2.1 WASTE MATERIALS

The actinide content of the waste material to be received from NFS is described in Tables 1 and 2.² In most cases, the form of the waste material is oxide,² but both powder and pellets are present. Some waste containers may contain plutonium metal. The total plutonium content in each shipping container is specified in Ref. 2 and will not exceed 260 g. However, the uncertainty on the plutonium content is $\pm 25\%$ (absolute, not 1 standard deviation) according to Ref. 2. The container is a 2.75-in.-diam by 6.403-in.-tall stainless steel vessel. The moisture content of the waste is specified to be less than 0.2 wt % (uncertainty unknown). It is specified that the waste material shall contain no organic materials (uncertainty unknown).

Examining Tables 1, 2, and 3 it is seen that 92% of the plutonium processed at NFS is from the SEFOR batch, and this batch has the highest percentage plutonium content (20%). This material is the most reactive of the four batches and thus is the reference waste for the safety evaluations. However, for the calculations reported in subsequent sections, the plutonium was assumed to be 100% ^{239}Pu , rather than the isotopic mix shown in Table 2.

2.2 CONTINGENT CONDITIONS

Certain abnormal conditions regarding container integrity must be considered. Doubly loading a single can is evaluated. An increase in the moisture content of the oxide of up to a factor of five is considered (see Appendix D). The container radius is limited by the radius of the storage well and thus is not variable. The effect of waste distribution within a container is studied and will be reported in Section 4.

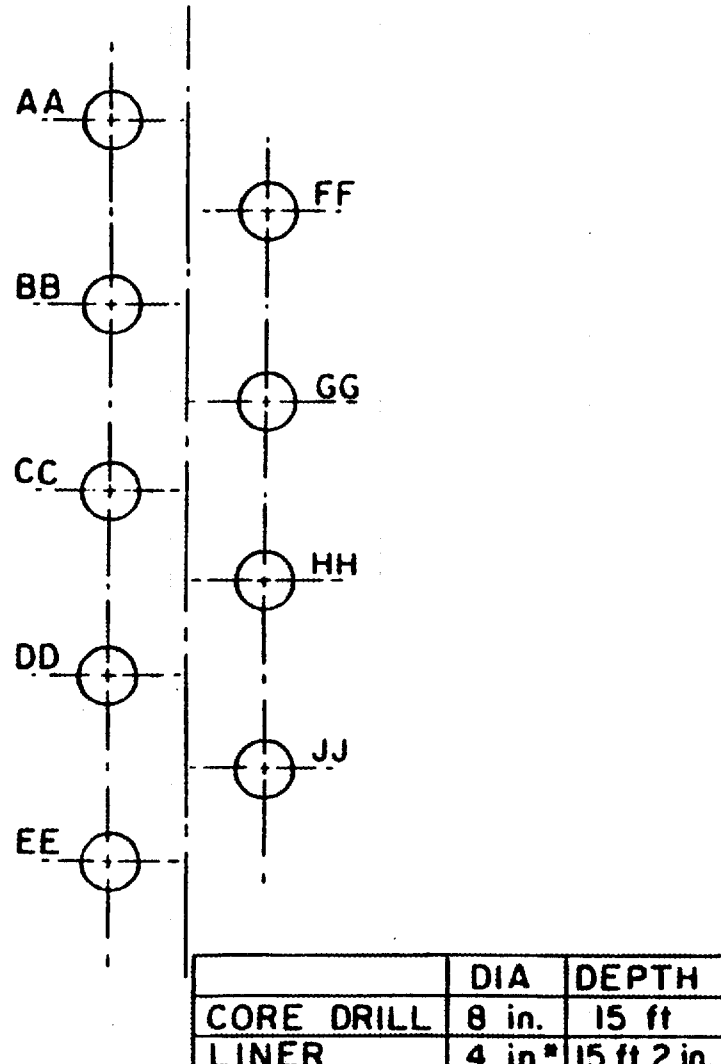
A mechanism for water flooding of the wells is considered. Procedures specify that, at most, only two wells will be open at any given time. Flooding of either one, two, or all wells is considered. Leakage of water into the waste canisters is not considered a credible abnormal event (Appendix D). The effect of uncertain water composition in the cell wall concrete is evaluated.

3. ANALYSIS METHODS

Evaluations are based on standardized Monte Carlo calculational techniques. Confidence in accuracy is gained by comparison with previous computations by Primm, documented in Ref. 1 and by the validation calculations reported in Appendix A.

3.1 PROGRAMS AND CROSS SECTIONS

The nuclear criticality safety analyses of well storage under normal and credible abnormal conditions were performed with the multigroup Monte Carlo criticality program KENO-Va as embodied in the SCALE⁵ computational system. Hopper's work (Sect. 4) included some KENO-IV calculations as well as KENO-Va. All calculations were performed with the 16-energy-group cross sections identified as HANSEN-ROACH as provided within the SCALE system. For the current work, the versions of KENO-Va and SCALE used were those contained in the Martin Marietta Nuclear Criticality Safety Software (NCSS)⁶ procedure on the IBM-3090, unless noted otherwise.



* PIPE SIZE (SCHEDULE 40)

Fig. 1. Vertical inter-cells solid storage.

ORNL Dwg 70-3682R2

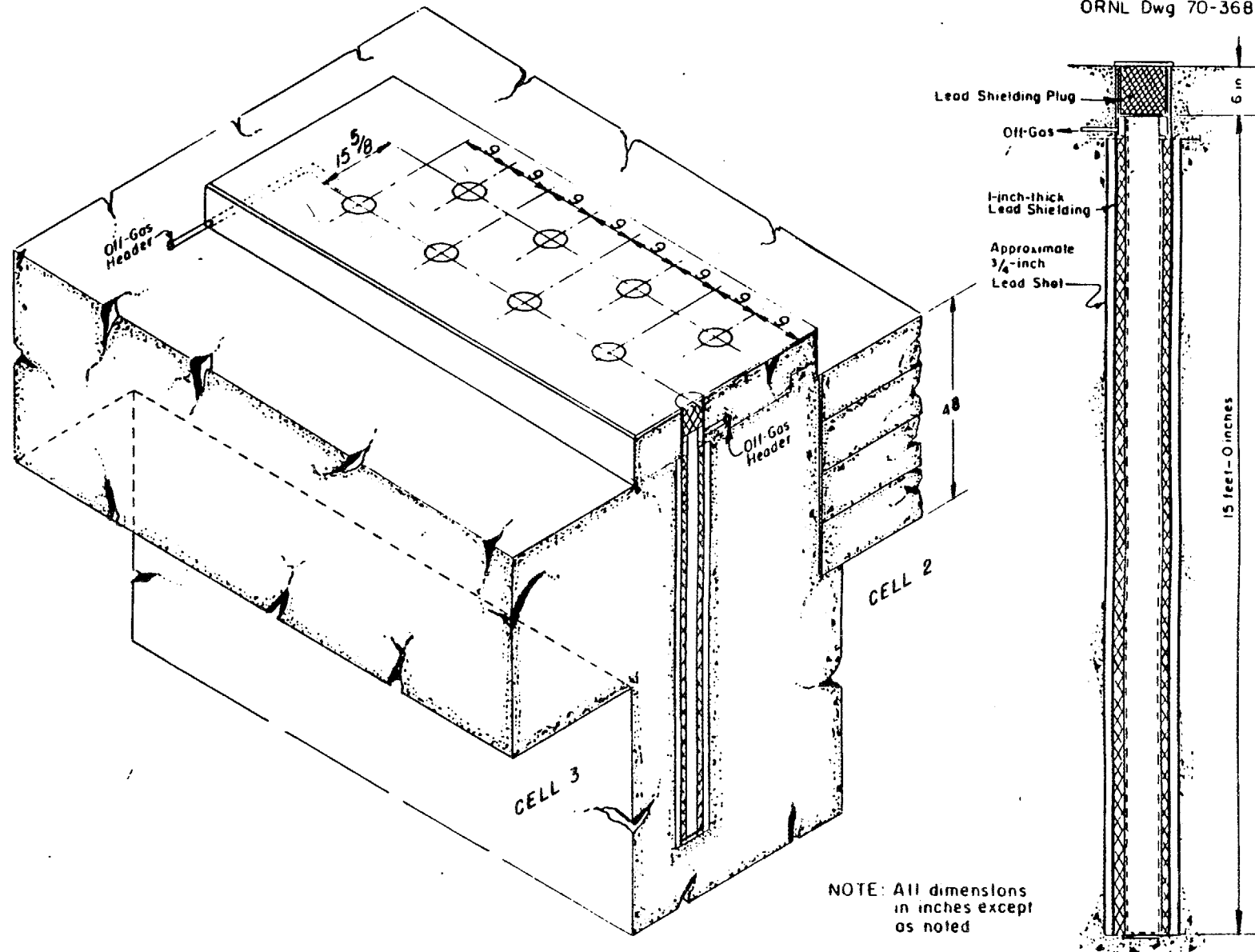
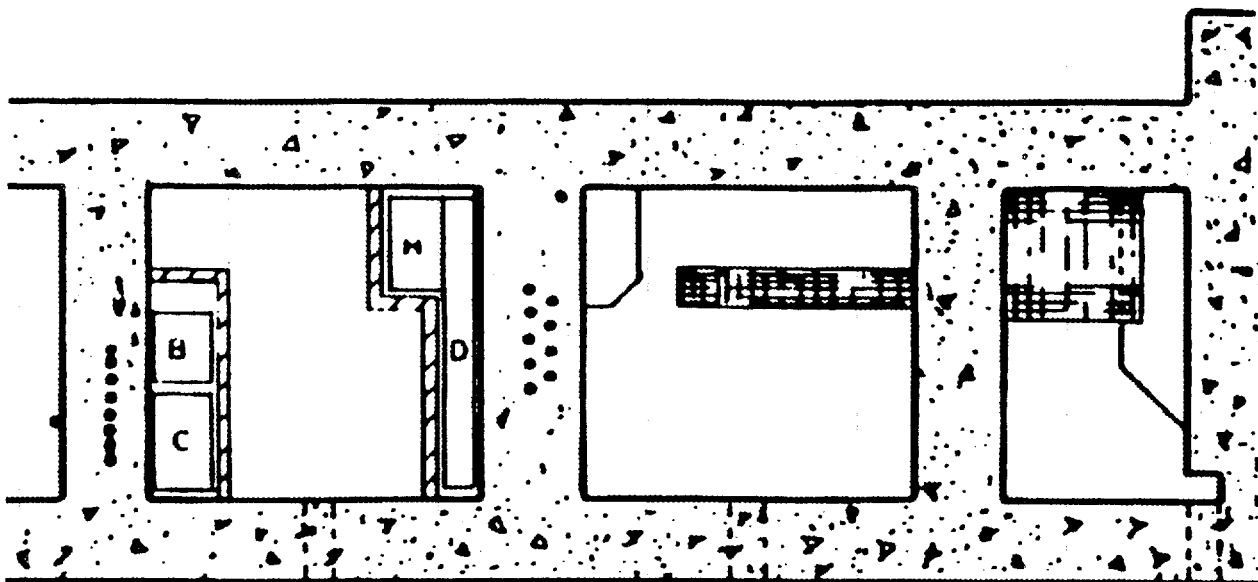
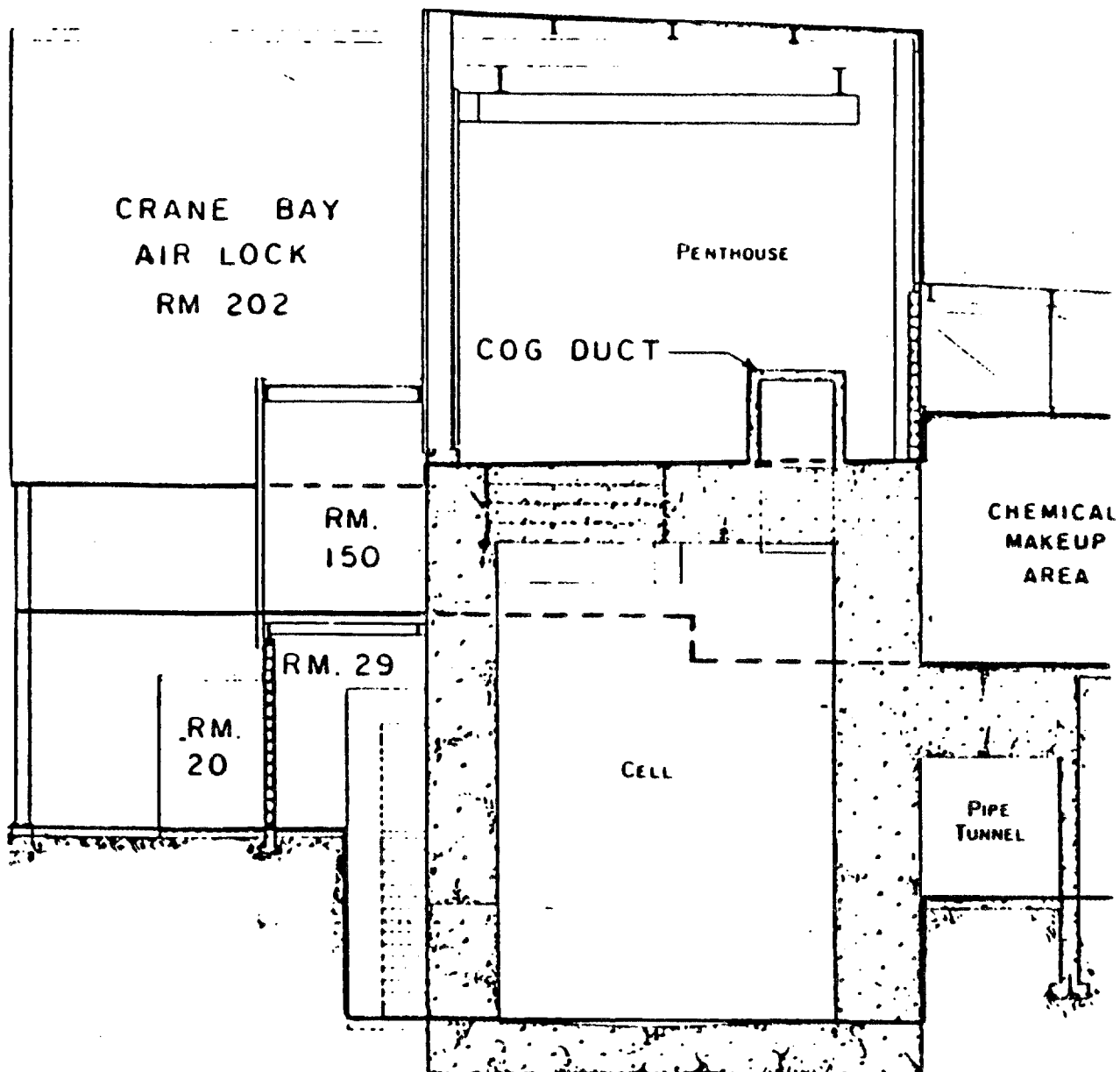


Fig. 2. Intercell 2 and 3 solids storage wells.



Scale: 1 in = 8.9 ft

Fig. 3. Top view of cells 3, 2, and 1 (from left to right).



Scale: 1 in = 8.9 ft

Fig. 4. Side view of cell 2.

Table 1. NFS plutonium sources^a

NFS S.O.	Date	Project/customer	Product	Original Kg-Pu	Mixture	%U	%Pu	Uranium enrichment	
3163	1965-1966	DuPont/SRO (DuPont P.O. AX-2640) (AEC: AT/07/-2/1)	MOX fuel rods	16	Uranium	99.7	0.315	Depleted	
256-A	1967-1971	SEFOR/GE/AEC (GE P.O. 205-58226-NG) (AEC: AT/04-3/-647)	MOX; 2000 fuel rods and scrap dissolution	746	Uranium	80.0	20.0	Depleted	
Subtotal Government Program:					762 (94%)				
945-E	1972	Halden/NFS-RFD (35% of Pu from NPR Fuel)	MOX fuel rods	3	Uranium	98.5 to 97.5	1.5 to 2.5	Depleted and 1.0% to 5.0%	
1021-F	1972-1973	Big Rock Point (Consumers)/NFS-RFD	MOX fuel assemblies	47	Uranium	97.93	Avg 2.27	Avg 2.41%	
Subtotal NFS Program:					50(6%)				
TOTAL					812 (100%)				

^aSource: Ref. 2.

Table 2. Summary of plutonium activity for fuels with greater than 80 wt % ^{239}Pu

SEFOR									
Isotope	Half-life (days)	SpA ($\mu\text{Ci/g}$)	Wt % Jan-70	$\mu\text{Ci/g}$ Jan-70	$\mu\text{Ci/g}$ Aug-90	Wt % Aug-90			
Pu-238	3.16E+04	1.74E+07	0.036	6.26E+03	5.31E+03	0.0305			
Pu-239	8.91E+06	6.13E+04	90.625	5.56E+04	5.56E+04	90.5720			
Pu-240	2.40E+06	2.26E+05	8.334	1.89E+04	1.88E+04	8.3159			
Pu-241	4.82E+03	1.12E+08	0.477	5.36E+05	1.82E+05	0.1617			
Pu-242	1.38E+08	3.90E+03	0.052	2.03E+00	2.03E+00	0.0520			
Am-241	1.67E+05	3.24E+06	0.467	1.51E+04	2.47E+04	0.7621			
SpA	07-Aug-90	$\mu\text{Ci/g}$			Ci/g	g/Ci			
Alpha:		1.04E+05			0.10	9.58			
Beta:		1.82E+05			0.18	5.50			
Alpha/Beta:		2.86E+05 Ratio:			0.57	3.49			
WEST VALLEY (NPR)									
Isotope	Half-life (days)	SpA ($\mu\text{Ci/g}$)	Wt % Jan-70	$\mu\text{Ci/g}$ Jan-70	$\mu\text{Ci/g}$ Aug-90	Wt % Aug-90			
Pu-238	3.16E+04	1.74E+07	0.079	1.37E+04	1.16E+04	0.0670			
Pu-239	8.91E+06	6.13E+04	85.829	5.26E+04	5.26E+04	85.7788			
Pu-240	2.40E+06	2.26E+05	11.531	2.61E+04	2.61E+04	11.5060			
Pu-241	4.82E+03	1.12E+08	1.156	1.30E+06	4.41E+05	0.3919			
Pu-242	1.38E+08	3.90E+03	0.25	9.75E+00	9.75E+00	0.2500			
Am-241	1.67E+05	3.24E+06	1.135	3.68E+04	5.99E+04	1.8500			
SpA	07-Aug-90				Ci/g	g/Ci			
Alpha:		1.50E+05			0.15	6.66			
Beta:		4.41E+05			0.44	2.27			
Alpha/Beta:		5.91E+05 Ratio:			0.34	1.69			

Table 3. Summary of plutonium activity for fuels with less than 80 wt % ^{239}Pu

CONSUMERS POWER						
Isotope	Half-life (days)	SpA ($\mu\text{Ci/g}$)	Wt% Jan-70	$\mu\text{Ci/g}$ Jan-70	$\mu\text{Ci/g}$ Aug-90	Wt% Aug-90
Pu-238	3.16E+04	1.74E+07	0.425	7.39E+04	6.26E+04	0.3603
Pu-239	8.91E+06	6.13E+04	76.241	4.68E+04	4.67E+04	76.1964
Pu-240	2.40E+06	2.26E+05	16.336	3.70E+04	3.69E+04	16.3006
Pu-241	4.82E+03	1.12E+08	2.91	3.27E+06	1.11E+06	0.9866
Pu-242	1.38E+08	3.90E+03	1.17	4.56E+01	4.56E+01	1.1700
Am-241	1.67E+05	3.24E+06	2.857	9.26E+04	1.51E+05	4.6568
SpA	07-Aug-90				Ci/g	g/Ci
Alpha:	2.97E+05				0.30	3.36
Beta:	1.11E+06				1.11	0.90
Alpha/Beta:	1.41E+06		Ratio:	0.27	1.41	0.71
HALDEN FUEL						
Isotope	Half-life (days)	SpA ($\mu\text{Ci/g}$)	Wt% Jan-70	$\mu\text{Ci/g}$ Jan-70	$\mu\text{Ci/g}$ Aug-90	Wt% Aug-90
Pu-238	3.16E+04	1.74E+07	0.294	5.11E+04	4.33E+04	0.2492
Pu-239	8.91E+06	6.13E+04	79.885	4.90E+04	4.90E+04	79.8382
Pu-240	2.40E+06	2.26E+05	14.509	3.29E+04	3.28E+04	14.4776
Pu-241	4.82E+03	1.12E+08	2.243	2.52E+06	8.55E+05	0.7605
Pu-242	1.38E+08	3.90E+03	0.826	3.22E+01	3.22E+01	0.8260
Am-241	1.67E+05	3.24E+06	2.203	7.14E+04	1.16E+05	3.5902
SpA	07-Aug-90				Ci/g	g/Ci
Alpha:	2.41E+05				0.24	4.14
Beta:	8.55E+05				0.85	1.17
Alpha/Beta:	1.10E+06		Ratio:	0.28	1.10	0.91

The benchmark calculations in Appendix A were also performed with the 16-group cross-section library identified as HANSEN-ROACH inside the NCSS version of the SCALE system. The preparation of input data and selection of cross sections for use in the calculations were consistent with the methods outlined in the SCALE manuals. These same procedures were used in the preparation of input data for the Intercell 2 and 3 storage calculations described subsequently.

3.2 COMPUTATIONAL ADEQUACY

Verification of the equations solved by the computer programs that compose the modules of the SCALE-4 system has been discussed in Ref. 6. A review of criticality safety literature revealed that considerable critical experiment data were available for mixed uranium-plutonium systems. Sixty-two critical configurations were identified which had Pu/(Pu + U) ratios ranging from 15 to 30% (bounding the 20% value noted in Table 1). K-effective values were calculated for all these experiments; these results are reported in Appendix A. The same experiments had been analyzed previously,¹ albeit with earlier versions of codes and libraries. Excellent agreement between prior and current work was seen.

3.3 MARGINS OF SAFETY (COMPUTED SUBCRITICALITY)

For the work reported in the next section, Hopper assumed a computed value of k-effective plus 2 standard deviations of the result being less than 0.93 was sufficient to provide an adequate margin of subcriticality for calculated contingent conditions considered. Based on the results reported in Appendix A, this value was judged an adequate margin of subcriticality for the calculated conditions considered. This judgement was based on tolerance limits that have been corrected for experimental uncertainties (derived in Appendix A).

4. COMPUTATIONS PERFORMED BY C. M. HOPPER (1985)

4.1 ASSUMPTIONS IN COMPUTATIONAL MODELS

The computer models reflected the storage configuration shown in Figs. 1 and 2, with a few exceptions. The concrete wall thicknesses in the model were on the order of 10 ft instead of the actual 5 feet thickness (to approximate the effects of cell covers, incidental scattered reflectors in the cells, and other influences). The reactivity contributions of neutrons having migrated out to distances of 5 ft to either side of the fissile material system and reentering the fissile material was considered to be negligible. In all cases, the concrete assumed for the calculations was that identified within the SCALE cross-section library as full-density Oak Ridge concrete. The lead shot surrounding the storage wells was assumed to have a packing fraction of 0.5.

Because of the unknowns in package design and content, a parametric study formed the basis of the criticality safety assessment. Table 4 notes some of the conditions considered in this study.

The maximum material densities and their associated hydrogen-to-fissile isotope atom ratios are derived from volume displacements associated with theoretical densities of water and oxide.

4.2 COMPUTATIONAL RESULTS

Computations were performed to evaluate variations in fissile loading and moderator-to-heavy metal ratio. All calculations were performed with either KENO-IV or KENO-Va and HANSEN-ROACH cross-sections. The results of these calculations are shown in Table 5.

Table 4. Considered ^{239}Pu material characteristics

Material form	Hydrogen to fissile isotope	Maximum fissile isotope density
Metal	0	19.70
Dioxide	1	7.40
Dioxide	3	4.70
Dioxide	10	2.10
Dioxide	20	1.17

4.3 SUBCRITICAL LOAD LIMITS FOR SINGLE CONTAINERS

The safety of a single storage well may be examined by comparison with safe values provided in Ref. 8 and consistent with Ref. 9 for identical to Table 5 theoretical density materials as fully water reflected infinite cylinders. Safe values for the considered materials have been extracted from Ref. 8 and are provided in Table 6. These values offer assurance for the safety of individual well loading and unloading operations of single units.

5. INVESTIGATION OF HOPPER CALCULATIONS

The calculations reported in Sect. 4 were performed in 1985 as part of a criticality safety question brought by Chemical Technology Division. The benchmark calculations in Appendix A were intended to support the calculations of Sect. 4 but due to changes in computer hardware, software, and updates to nuclear data libraries from 1985 to the present, it was felt that confirmation of some of the Sect. 4 calculations was needed. Consequently, a new model of the Intercell Storage Wells 2 and 3 was prepared.

5.1 COMPUTATIONAL MODEL

The programs and cross-section libraries are the same as those mentioned in Sect. 3.1. The waste material was assumed to be either plutonium metal (PLUTONIUMALP in the SCALE library) or plutonium oxide (PuO_2), as appropriate. Water was added to the waste material to provide the desired H/Pu ratios. The SCALE entry CARBON-STEEL was used for the cross-section data for the steel liners of the storage wells. The lead liners were modeled as shown in Fig. 2; SCALE entry was full-density PB. The lead shot was assumed to have a packing fraction of 0.7402, corresponding to a hexagonal close-packed lattice. Again, the SCALE library entry PB was used. The SCALE library entry ORCONCRETE was used for the cross section data for the intercell walls. The calculations were performed on the IBM 3090 using the NCSS procedure.

For the waste material expected to be loaded into the storage wells (see Sect. 2.3) a maximum H/Pu ratio of 0.3 is expected. As noted in Sect. 2, the radius of the individual storage wells is 5.08 cm. Based on the well radius and Hopper's data in Table 5, eight cases were selected for recalculation. Note that the H/Pu ratios of zero and 1 bracket the current waste material. A comparison of the current calculated values to those from Sect. 4 is shown in Table 7. Even though many nuclides in the Hansen-Roach library were updated in 1989, agreement is excellent.

Table 5. Intercell 2 and 3 ^{239}Pu results

Material form	H/Pu atom/ratio	^{239}Pu density (g/cc)	Radius (cm)	k-eff	σ
Metal	0	19.700	3.1	1.287	0.006
		5.910	3.1	0.659	0.004
		12.214	3.1	0.985	0.005
		11.623	3.1	0.958	0.006
		11.426	4.2	1.229	0.006
		3.349	4.2	0.667	0.004
		7.486	4.2	0.991	0.006
		6.698	4.2	0.950	0.005
		8.274	4.8	1.173	0.005
		2.561	4.8	0.640	0.005
		5.910	4.8	0.975	0.006
		5.516	4.8	0.954	0.005
		7.289	5.08	1.160	0.006
		2.187	5.08	0.630	0.004
		5.267	5.08	0.974	0.005
		5.012	5.08	0.953	0.005
Dioxides	1	12.950*	4.2	1.435	0.006
		3.922	4.2	0.749	0.005
		6.512	4.2	1.001	0.004
		5.994	4.2	0.958	0.005
		9.250*	4.8	1.315	0.005
		2.812	4.8	0.716	0.004
		5.328	4.8	1.001	0.005
		4.884	4.8	0.961	0.005
		7.992*	5.08	1.296	0.005
		2.397	5.08	0.705	0.005
		4.712	5.08	0.986	0.005
		4.418	5.08	0.963	0.005

*Value exceeds theoretical density.

Table 5. (continued)

Material form	H/Pu atom/ratio	^{239}Pu density (g/cc)	Radius (cm)	k-eff	σ
Dioxides	3	8.319 ^a	4.2	1.301	0.005
		2.491	4.2	0.657	0.004
		5.170 ^a	4.2	0.993	0.005
		4.794 ^a	4.2	0.967	0.005
		5.828 ^a	4.8	1.200	0.005
		1.739	4.8	0.629	0.005
		4.042	4.8	1.000	0.005
		3.572	4.8	0.932	0.005
		4.940 ^a	5.08	1.154	0.005
		1.482	5.08	0.616	0.004
Dioxides	10	3.423 ^a	4.2	1.102	0.006
		1.029	4.2	0.540	0.004
		2.772 ^a	4.2	0.980	0.005
		2.604 ^a	4.2	0.947	0.005
		2.415 ^a	4.8	1.023	0.005
		0.735	4.8	0.512	0.004
		2.184 ^a	4.8	0.959	0.005
		2.142 ^a	4.8	0.954	0.005
		2.080	5.08	0.994	0.005
		0.624	5.08	0.504	0.004
		1.949	5.08	0.960	0.005
		1.909	5.08	0.950	0.005

^aValue exceeds theoretical density.

Table 5. (continued)

Material form	H/Pu atom/ratio	^{239}Pu density (g/cc)	Radius (cm)	k-eff	σ
Dioxides	20	2.363*	3.1	0.909	0.004
		4.025*	3.1	1.233	0.005
		2.574*	3.1	0.956	0.006
		2.551*	3.1	0.944	0.005
		1.322*	4.2	0.831	0.005
		2.258*	4.2	1.139	0.005
		1.685*	4.2	0.967	0.005
		1.638*	4.2	0.947	0.005
		0.948	4.8	0.791	0.005
		1.615*	4.8	1.059	0.005
		1.346*	4.8	0.972	0.005
		1.275*	4.8	0.934	0.005
		0.808	5.08	0.759	0.005
		1.373*	5.08	1.040	0.005
		1.190*	5.08	0.949	0.005

*Value exceeds theoretical density.

Table 6. Maximum subcritical fully water reflected single infinite cylinders of ^{239}Pu metal

H to Pu	Pu density (g/cc)	Diameter (cm)	Pu loading (kg/ft)
0	19.70	4.19	8.32
1	7.4	7.29	9.44
3	4.7	8.89	8.91
10	2.1	11.00	6.08
20	1.27	11.81	3.90

Table 7. Comparison of Intercell 2 and 3 calculations for ^{239}Pu

Material form	H to Pu atom ratio	^{239}Pu density (g/cc)	Calculated k-eff			
			Hopper (85)		Current	
			k-eff	Std. dev.	k-eff	Std. dev.
Metal	0	2.187	0.630	0.004	0.645	0.003
Metal	0	5.012	0.953	0.005	0.961	0.003
Oxide	1	4.418	0.963	0.005	0.966	0.003
Oxide	3	1.482	0.616	0.004	0.615	0.002
Oxide	3	3.348	0.943	0.004	0.958	0.003
Oxide	10	0.624	0.504	0.004	0.505	0.002
Oxide	10	1.909	0.950	0.005	0.959	0.003
Oxide	20	0.808	0.759	0.005	0.767	0.003

5.2 VERIFICATION OF ASSUMPTIONS FOR SECTION 4 CALCULATIONS

Table 7 provides certification that the Sect. 4 calculations were reproducible. Investigations were conducted to determine if what was intended to be calculated (safety limits) was calculated.

Curious as to the existence of interaction between the wells, a calculation was performed in which all but one of the storage wells was replaced with concrete to estimate the amount of interaction between the wells. The waste material was the same as that listed in the first entry of Table 7. The calculated k-effective was 0.536 ± 0.003 . Thus, there is some interaction between loaded storage wells and it is necessary to model all wells (requiring KENO-Va and CSAS25) rather than model a single well. Had this not been the case, a less expensive and equally as accurate calculation (for an isolated, single well) could have been performed using a one-dimensional, discrete-ordinates model (XSDRNP, CSAS1x).

Upon examination of the input for the cases listed in Table 7, one minor difference was found. The packing fraction for the lead shot in the older, Hopper models was assumed to be 0.5. The value for the current model was 0.7405. Even though the worth of this zone was believed to be small, the first case in Table 7 was recalculated with a lead shot packing fraction of 0.5. The calculated value of k-effective was 0.643 ± 0.003 . Thus the difference between k-effectives for the two packing fractions is statistically insignificant.

It was noted earlier that the concrete walls in the KENO-Va model were assumed to be 10 ft thick to account for room return of neutrons. Since the actual walls are 5 ft thick, a calculation was performed with that concrete thickness to determine the impact of the additional 5 ft of concrete on k-effective. The same CSAS25 model was used for these calculations as was used for the calculations reported in Table 7; however, the fuel was assumed to be a mixture of PuO_2 at 20% of theoretical density and UO_2 at 80% of theoretical density. The water content of the fuel was zero. The value of k-effective for a 5-ft-thick wall was 0.673 ± 0.002 . The value for a 10-ft-thick wall was 0.672 ± 0.002 . One can conclude that the number of neutrons leaking from the 5-ft system is small and one can ignore the possibility of interactions with other materials that might be stored in either cell 2 or 3.

Even though the actual uranium-to-plutonium ratio of the waste to be received in Building 3019 is not known, the data supplied in Table 1 imply that the ratio of Pu/(Pu + U) will be less than or equal to 0.20. Since all of Hopper's calculations had been for pure plutonium systems, an investigation of the effect of uranium on calculated k-effective was conducted. The 5-ft-thick wall case described in the previous paragraph was rerun with the uranium (natural uranium isotopes) removed. The calculated value of k-effective decreased to 0.618 ± 0.002 .

The 8% decrease in k-effective due to the removal of natural uranium implied that material was contributing in a significant manner to the reactivity of the system. Investigation of the number of fissions per energy group revealed that 27% of the fissions were occurring at neutron energies above 1.4 MeV, an energy range where the ^{238}U fission cross section is about 1 barn. Investigation of the ^{235}U , ^{238}U , and ^{239}Pu atom densities and fast cross sections revealed that in this energy range, ^{239}Pu accounted for about 55% of the total fissions, and ^{238}U accounted for 45%.

The finding that ^{238}U has a significant reactivity impact for dry systems—when the H/Pu ratio rises to 20, the percentage of fissions occurring above 1.4 MeV drops to 5%—instigated an extension of Hopper's work. The input for second entry in Table 7 (^{239}Pu density = 5.012) was modified via the addition of natural uranium dioxide. With a plutonium metal density of 19.84 g/cc, the maximum theoretical uranium dioxide density is $0.7474 \times 10.95 = 8.184$ g/cc. This quantity of uranium was added to the input for the second entry, and k-effective was calculated to be 1.005 ± 0.003 . In this case, the addition of natural uranium has driven a subcritical system critical. Establishing the limiting plutonium concentration based on calculations that only include plutonium oxide would be nonconservative.

The third entry in Table 7 (^{239}Pu density = 4.418) was also recalculated with added uranium. The voided region (39.6% of the waste volume) was replaced with natural uranium dioxide. The calculated k-effective was 0.991 ± 0.003 . This is a statistically significant increase over the case with no uranium present, albeit less of an increase than for the case where H/Pu = 0.

A third examination of the effect of added uranium was conducted using the dataset corresponding to the fifth entry in Table 7 (plutonium density of 3.348 g/cc). A review of the atom densities showed that there was 25% void in this waste material. Uranium dioxide at 25% of theoretical density was added to the CSAS2 model, and k-effective was calculated to be 0.943 ± 0.002 . Statistically, this value is not greater than the case in Table 7 (no uranium present). Consequently, an H/Pu ratio of at least 3 removes the positive worth.

The purpose of the uranium study relates to the assumptions regarding the material that fills the void when the plutonium loading is less than theoretical density. If the void is assumed to be filled with water, then the H/Pu ratio will be sufficiently high such that the increase in reactivity due to the assumed increase in moderation will outweigh the fast fission effect due to any ^{238}U which may be present. However, if the analyst accepts the certified water content as input to the k-effective calculation, then the uranium content of the waste MUST be included in the computational model because it may have a positive reactivity effect. If the uranium is not accurately known, then all of the remaining "void" region in the waste should be assumed to be uranium.

An alternative, simpler, but much more conservative procedure is to treat all fissionable materials as if they were ^{239}Pu when the water content is below H/Pu = 3. Since the expected well loadings from the waste described in Tables 1 and 2 are quite small, about 0.5 kg per linear foot, this practice could be adopted were it not for the results of concrete induced reactivity studies described subsequently.

For the specific waste being addressed in this report, the presence of uranium in the waste is not a problem. Because the Pu/(Pu + U) ratio will always be less than or equal to 0.20, the maximum possible plutonium content is 2.209 g/cc. Given that the water content of the waste is less than 0.2 wt %, examination of relevant cases from Table 5 (H/Pu ratios of 0 and 1) reveal that this configuration is far subcritical (k-effectives of about 0.70). The added reactivity due to the presence of uranium in a dry system will be far less than the amount needed to violate a safety limit.

As noted previously, the 1985 Hopper calculational models had assumed the cell wall concrete to be the composition specified as ORCONCRETE in the SCALE System. At the start of this study it was speculated that the 3019 cell walls were probably composed of Barytes concrete. An investigation into the reactivity effect of substituting Barytes for ORCONCRETE and varying the water content in the concrete was conducted. Atom densities were calculated using Ref. 10 and are reported in Table 8.

Table 8. Atom densities in Barytes concrete

Element	Atom Density (atoms/bn · cm) ^a	
	With Rebar	No Rebar
H	1.40844E-2 ^b	1.45200E-2 ^c
O	4.16247E-2 ^b	4.29121E-2 ^c
Mg	9.51809E-5	9.81246E-5
Al	3.00953E-4	3.10261E-4
Si	7.32168E-4	7.54812E-4
S	6.57595E-3	6.77933E-3
Ca	2.45317E-3	2.52904E-3
Fe	4.16972E-3	1.71648E-3
Ba	6.59790E-3	6.80196E-3

^aE-2 should be read as $\times 10^{-2}$.

^bValues shown are for 100% water retention. Using ANSI/ANS Standard 6.4-1977, the minimum bound water content would be 0.064 g/cm³, yielding H atom density of 4.15055E-3 and O atom density of 3.66152E-2 (some O is from concrete mix).

^cValues shown are for 100% water retention. Using ANSI/ANS Standard 6.4-1977, the minimum bound water content would be 0.064 g/cm³, yielding H atom density of 4.27892E-3 and O atom density of 3.77476E-2 (some O is from concrete mix).

The second and seventh entries from Table 7 were recalculated using atom densities from Table 8. Those results, along with calculated k-effectives for other types of concrete, are shown in Table 9. The final entries in the table are for the actual concrete composition as determined in June 1992 and reported in Appendix C.

It is apparent that the drier the concrete, the more reactive the system. If the intercell 2 and 3 concrete could have been certified as Barytes with 3% rebar, then Hopper's previous calculations would have been referable by comparison to the verified, validated calculations presented in this memorandum.

With the provision of the measured concrete data given in Appendix C, the 1985 calculations are shown to be nonconservative. Consequently, the derived fits to these data — presented in Appendix E for instructive purposes only, not for use — cannot provide assurance of subcriticality for the storage of the NFS waste material.

Table 9. Impact of concrete composition on calculated k-effective

Concrete types	k-effectives	
	Table 7, Case 2 ^a	Table 7, Case 7 ^b
Oak Ridge ^c	0.961 ± 0.003	0.959 ± 0.003
Magnuson (very dry) ^{d,e}	1.05052 ± 0.00311	1.02408 ± 0.00287
Barytes, No Rebar; All H ₂ O ^e	0.86293 ± 0.00291	0.87591 ± 0.00283
Barytes, No Rebar; Bound H ₂ O ^e	0.98607 ± 0.00291	0.97262 ± 0.00304
Barytes, Rebar; All H ₂ O ^e	0.84555 ± 0.00300	0.86241 ± 0.00286
Barytes, Rebar; Bound H ₂ O ^e	0.96068 ± 0.00321	0.96275 ± 0.00281
Appendix C Concrete (0.5 wt% H)	1.04725 ± 0.00312	1.01862 ± 0.00292

^aMetal, H/Pu=0, Pu-239 den. = 5.012 g/cc.^bOxide, H/Pu=10, Pu-239 den. = 1.909 g/cc.^cHopper assumption, SCALE id is ORCONCRETE.^dA SCALE composition, id is MGCONCRETE.^eCalculation performed with unverified version of SCALE4 on the ucray, Spring 1992.

6. COMPUTATIONS AND SAFETY ANALYSES SPECIFIC TO NFS WASTE

The discussions in Sects. 4 and 5 provide support for the conclusion that NFS waste can be safely stored in the proposed fashion. However, uncertainty exists in the safety margin due to the recently determined cell wall composition. In an attempt to provide further assurance that the proposed storage configuration is safely subcritical, a set of calculations was performed for the Intercell 2 and3 storage array under "normal" and abnormal NFS storage conditions.

6.1 METHODOLOGY

The CSAS25 module of the SCALE system⁵ was used to compute k-effectives for several storage configurations. The analyses were performed with the same code system and cross section library as were used in the validation calculations, which were discussed in Appendix A. All of the datasets for the cases presented in this section are stored on the floppy disk attached to the back cover of this report. They are in the subdirectory named *section6.dir*.

6.2 COMPUTATIONAL MODELS

The dimensions and positions in Figs. 1 and 2 were used to create the Monte Carlo (KENO) model. Unlike the models used to generate the calculations reported in Sect. 4, these models incorporated the actual concrete thickness (5 ft) and composition as given in Appendix C.

The steel bottles that contain the waste were not included in the KENO model, and the waste material was assumed to occupy the entire volume of the storage well. Calculations in Sect. 4 showed that spreading the fissile material over the entire volume was conservative.

The normal configuration was defined to be a fuel loading of 260/g ²³⁹Pu per canister. The water content was set at 0.2 wt %. Full-density graphite was added to the waste region to simulate the reactivity impact of unknown waste constituents. A listing of the normal case input is given in Appendix F.

Ten abnormal configurations were considered. In all cases, the fuel density was set at 1.2 kg ^{239}Pu per foot (2.5 times the expected value). This is the current maximum fissile loading limit for intercell storage in Building 3019.

For the first abnormal case, the Pu/(Pu+U) ratio was 0.2. The fuel form was oxide. The water content of the fuel was 0.1 wt %—the value specified in Ref. 2 for pellets. The carbon steel liner in each well was modeled, but the waste containers were not modeled. Unlike the normal case, no graphite was mixed with the waste. A second case was executed with the water content increased to 0.2 wt %—the value specified in Ref. 2 for all forms of mixed oxide other than pellets. To examine the effect of miscellaneous and/or unknown materials mixed with the waste material, full-density graphite was added to the model that contained 0.2 wt % water. Note that this third configuration is physically impossible to obtain, but is conservative. To protect against uncertainty in the water content of the waste material, two cases were examined in which the water content was increased to 0.4 wt % (Case 4, a doubling of expected water content) and 1.0 wt % (Case 5, a conservative water content as identified in Appendix D).

A sixth abnormal case was considered in which a centrally located storage well was assumed to be flooded. Based on the dimensions of the waste storage canister as contained in Ref. 2, the free volume in the storage well was computed. The waste container was assumed to be water-tight, but all free volume in the storage well was assumed to be flooded (see Appendix D). The water content of the waste was 0.2 wt % and full density graphite was mixed with the fuel. In the seventh case, the water content of the cell wall concrete was set to zero. This case was considered due to the fact that the concrete analysis presented in Appendix C did not provide a lower bound for the water content.

In Case 8, two adjacent storage wells were flooded. This case corresponds to the maximum number of storage wells which might be open at anytime during the waste loading or unloading procedures.

In Cases 9 and 10 (1.0 and 0.2 wt % water, respectively), all of the storage wells are assumed to be flooded. While it is uncertain if this is a credible abnormal configuration, it is considered in order to relieve concern regarding possible, unidentified water ingress pathways.

6.3 RESULTS

Calculated k-effective for the normal case was $0.34795 \pm .00171$. The average fission group value was 13.2, within the validated range as shown in Appendix A. K-effectives for the ten abnormal cases are shown in Table 10. Average fission group (avg) values are also shown. Note that all configurations are far subcritical and all average values are within the validated range. Note that, contrary to trends derived from Table 9, when all water is removed from actual cell wall concrete, k-effective remains unchanged relative to the nominal concrete condition. Note also that flooding of ALL storage wells yields no significant reactivity increase compared with flooding a single well.

Table 10. Reactivity parameters for abnormal intercell 2 and 3 storage configurations

ID No.	Case				k-effective	Average fission group
	gr $^{239}\text{Pu}/\text{ft}$	H_2O wt %	H/Pu ratio	C present		
1	1200	0.1	0.283	No	0.420 ± 0.002	11.5
2	1200	0.2	0.566	No	0.420 ± 0.002	11.5
3	1200	0.2	0.566	Yes	0.450 ± 0.002	11.5
4	1200	0.4	1.134	No	0.426 ± 0.002	11.5
5	1200	1.0	2.854	No	0.436 ± 0.002	11.6
6	1200 ^a	0.2	0.566	Yes	0.451 ± 0.002	11.6
7	1200 ^{a,b}	0.2	0.566	Yes	0.450 ± 0.002	9.3
8	1200 ^c	0.2	0.566	Yes	0.447 ± 0.002	11.5
9	1200 ^a	1.0	2.854	Yes	0.446 ± 0.002	11.5
10	1200 ^d	0.2	0.566	Yes	0.446 ± 0.002	11.5

^aCentral storage well flooded.

^bWater content in cell wall concrete set to zero.

^cTwo central storage wells flooded.

^dAll storage wells flooded.

7. CONDITIONS FOR STORAGE WELL USE AND ASSIGNMENT OF SAFE FISSILE MATERIAL LIMITS

The following conditions must be met.

7.1 INITIAL CONDITIONS

Intercell 2 and 3 storage wells shall be confirmed as empty before loading waste canisters.

7.2 MATERIAL DEFINITION AND CONTAINMENT

The safe storage limits noted in Sects. 5 and 6 are predicated upon the specified hydrogen to fissile isotope atom ratios and material containment. Material definition and quality and material containment integrity should be controlled or limited such that unlikely, yet credible, changes in material form and/or containment will not exceed the safe load limits and respective hydrogen to fissile isotope atom ratios as set forth in Ref. 2. It should be noted that the Pu loading and hydrogen moderation parameters based upon the waste acceptance criteria are much lower than those used in the earlier, and more general, qualification of the facility (Section 4).

7.3 FISSILE MATERIAL TRANSFERS TO, FROM, AND AMONG STORAGE WELLS

The safe mass values in Sect. 6 are predicated on the assumption that the fissile material primary containment is leaktight to water in the event of accidental water flooding. Interim storage of fissile materials outside the wells during transfer to, from, and among storage wells may be accomplished near the storage wells in an authorized manner with approved storage/transfer containers. An important administrative control in this procedure is the limit of an approved maximum number of waste canisters exterior to the storage containers or storage wells at any time.

8. CONCLUSIONS

An adequate number of criticality computations were performed to permit the characterization of fissile materials interactions for storage in Building 3019 Intercell 2 and 3 Storage Wells. Verified and validated methods and libraries were used to evaluate subcriticality in Intercell 2 and 3 wells for NFS waste. Extension of the evaluation to other, undefined, fissile waste materials would require recalculation of parametric studies performed during the 1985 time frame. Results from the 1985 parametric studies of Intercell 2 and 3 are included in this report (1) to demonstrate the nonconservative effect of using the SCALE Oak Ridge concrete for inappropriately modeling the cell wall concrete composition, and (2) to review the adequacy of using an empirical model for interpreting the KENO Monte Carlo results.

REFERENCES

1. R. T. Primm, III, *Validation Studies for KENO-IV with Mixed Plutonium-Uranium Critical Experiments*, ORNL/TM-9668, November 1985.
2. *Oak Ridge National Laboratory Waste Acceptance Criteria for Transuranic Waste from Nuclear Fuel Services, Inc.*, WM-WMCO-202/R1, April 7, 1992.
3. Personal Communication from A. M. Krichinsky, Chemical Technology Division, Martin-Marietta Energy Systems, Inc., September 22, 1992.
4. *Final Safety Analysis Report for the Radiochemical Processing Plant (RPP)*, ORNL/CF-81/37, Draft version, cover letter from R. S. Wiltshire to J. A. Lenhard, August 30, 1984.
5. *SCALE - A Modular Code System for Performing Standardized Computer Analyses for Licensing Evaluation*, NUREG/CR-0200, Rev. 4 (ORNL/NUREG/CSD-2/R4), Vols. I, II, and III (draft February 1990). Available from Radiation Shielding Information Center, Oak Ridge National Laboratory, as CCC-545.
6. N. F. Landers, L. M. Petrie and J. C. Turner, "Martin Marietta Energy Systems Nuclear Criticality Safety Software Verification Plan SRR-0," December 31, 1991, contained in *Martin Marietta Energy Systems Nuclear Criticality Safety Software Configuration Control Plan*, K/ESH-3, December 18, 1991.
7. American National Standards Institute, *Design Criteria for an Independent Spent Fuel Storage Installation (Water Pool Type)*, Standard Number ANSI/ANS-57.7-1981, 1981.
8. J. T. Thomas, Ed., *Nuclear Safety Guide, TID-7016, Revision 2*, NUREG/CR-0095, ORNL/NUREG/CSD-6, June 1978.
9. H. C. Paxton and N. L. Pruvost, *Critical Dimensions of Systems Containing ^{235}U , ^{239}Pu , and ^{233}U , 1986 Revision*, LA-15860-MS, UC-46, Los Alamos National Laboratory, July 1987.
10. E. P. Blizzard and L. S. Abbott, Reactor Handbook, Oak Ridge National Laboratory, 1962.

APPENDIX A

VALIDATION STUDIES WITH URANIUM AND PLUTONIUM OXIDE EXPERIMENTS

APPENDIX A

VALIDATION STUDIES WITH URANIUM AND PLUTONIUM OXIDE EXPERIMENTS

A.1 INTRODUCTION

Four publicly available documents contain data for critical experiments that have been performed with mixed uranium and plutonium oxide.¹⁻⁴ All these experiments utilize plastic powder as a moderator, and all critical configurations are rectangular parallelepipeds. This section includes a description of the k-effective calculations of these mixed-oxide critical experiments. A brief review of computational methods is also provided, along with a short discussion of each experimental series. This section is organized such that the calculated k-effectives are grouped according to the articles in which the data are provided. The datasets for all of the critical experiments are stored on the floppy disk attached to the inside of the back cover of this report.

A.2 COMPUTATIONAL METHODS

Calculations were performed with cross sections from the 16-group Hansen-Roach library.⁵ The SCALE⁶ module, CSAS25 was used to process cross-section data and generate k-effectives for the mixed-oxide critical experiments. Atom densities for input to these codes were provided in the articles that describe the critical configurations. All calculations were performed with the same configuration control software as was used to perform the calculations for Intercell Storage 2 and 3 wells of Building 3019.

A.3 CALCULATION OF K-EFFECTIVE FOR MIXED URANIUM AND PLUTONIUM OXIDE EXPERIMENTS

A.3.1 Unpoisoned Experiments with Little Moderation

References 1, 7, and 8 provide descriptions of several critical experiments conducted at the Battelle-Pacific Northwest Laboratories (PNL). These experiments were conducted with fuel mixtures containing depleted uranium (0.2 wt % ^{235}U) homogenized with plutonium oxide. The ^{240}Pu content of the plutonium was 11.5 wt %. Three Pu:(Pu+U) ratios were examined (0.29, 0.15, and 0.08). Atom densities for the three fuel mixtures are reported in Table A.1.¹

The mixed oxide was blended with polystyrene powder to achieve the desired H:(U+Pu) atom ratios. This fuel mixture was compressed to form two types of fuel compacts: some measured 5.1 by 5.1 by 5.1 cm, and the remainder measured 5.1 by 5.1 by 1.3 cm. Each compact was then clad in the 3M Company's 471 tape.

An approach to critical was performed by stacking the compacts in a rectangular parallelepiped configuration. Some configurations had no reflector; others were fully reflected with methacrylate plastic. Critical sizes are provided in Tables A.2 and A.3.

Table A.1. Description of experimental fuel and reflector for experiments 1453-01 to 15
 (Values are 10^{24} atoms per cubic centimeter)

Material	29.3 wt % Pu fuel; 2.8 H:(Pu + U) atomic ratio	15.0 wt % Pu fuel; 2.86 H:(Pu + U) atomic ratio	8.1 wt % Pu fuel; 7.3 H:(Pu + U) atomic ratio
Fuel*			
^{241}Am	1.019×10^{-5}	2.765×10^{-5}	3.132×10^{-5}
^{238}Pu	1.833×10^{-6}	5.737×10^{-7}	3.809×10^{-7}
^{239}Pu	2.203×10^{-3}	1.118×10^{-3}	3.490×10^{-4}
^{240}Pu	2.931×10^{-4}	1.478×10^{-4}	4.678×10^{-5}
^{241}Pu	4.934×10^{-5}	2.221×10^{-5}	7.745×10^{-6}
^{242}Pu	5.636×10^{-6}	2.370×10^{-6}	1.116×10^{-6}
^{235}U	9.401×10^{-6}	1.365×10^{-5}	9.116×10^{-6}
^{238}U	6.172×10^{-3}	7.549×10^{-3}	4.606×10^{-3}
O	1.869×10^{-2}	1.840×10^{-2}	1.178×10^{-2}
C	2.666×10^{-2}	2.653×10^{-2}	3.567×10^{-2}
H	2.417×10^{-2}	2.534×10^{-2}	3.680×10^{-2}
Cladding			
H	4.489×10^{-2}	4.489×10^{-2}	4.489×10^{-2}
C	3.111×10^{-2}	3.111×10^{-2}	3.111×10^{-2}
Cl	7.240×10^{-3}	7.240×10^{-3}	4.240×10^{-3}
Reflector			
H	5.666×10^{-2}	5.666×10^{-2}	5.666×10^{-2}
C	3.510×10^{-2}	3.510×10^{-2}	3.510×10^{-2}
O	1.428×10^{-2}	1.428×10^{-2}	1.428×10^{-2}

*Concentration at time of experiments.

According to Beirman and Clayton:¹

To provide a more simplified geometry for use in calculations, the reactivity worth of the 1.3-cm-thick fuel compacts with respect to the full-sized fuel compacts was determined for each fuel mixture by replacement measurements. The critical height in terms of the full-sized compacts is presented in (Tables A.2 and A.3) for each of the experimental assemblies.

In the KENO-Va model of these experiments, each compact in the array was represented discretely. The fractional height was represented as a single, full layer with a thickness equal to the fraction times the height of the compact (5.1 cm).

Calculated k-effectives for the 11 described experiments are reported in Table A.4. The calculations show good agreement with the experimentally determined value of k-effective (1.0) for the 29 wt % Pu experiments.

**Table A.2. Critical assembly configurations for 29.3 wt % Pu,
2.8 H:(Pu+U), PuO₂-UO₂-polystyrene fuel compacts**

Experiment designation	Reflected	Critical number of compacts		
		Length	Width	Height ^a
1453-01	No	10	10	8.888
1453-02	No	10	11	8.252
1453-03	Yes	7	7	7.060
1453-04	Yes	8	8	5.615
1453-05	Yes	9	9	4.997
1453-06	Yes	10	10	4.316
1453-07	Yes	12	10	3.948
1453-08	Yes	12	12	3.668
1453-09	Yes	12	13	3.578
1453-10	Yes	14	13	3.487

^aThe 1.3-cm-thick fuel is expressed as 5.1 fuel by using its measured reactivity worth in terms of the full-size fuel.

**Table A.3. Reflected critical assembly configuration for 15 wt % Pu,
2.86 H:(Pu+U), PuO₂-UO₂-polystyrene fuel compacts**

Experiment designation	Critical number of compacts		
	Length	Width	Height ^a
1453-11	10	10	10.749

^aThe 1.3-cm-thick fuel is expressed as 5.1 fuel by using its measured reactivity worth in terms of the full-size fuel.

A.3.2 Poisoned Experiments with Little Moderation

References 2 and 9 provide descriptions of series of experiments conducted with mixed-oxide and heterogeneously distributed neutron poison materials. The relative worths of plates of aluminum, copper, and copper containing 1 wt % Cd were measured for two different mixed oxides. Both sets of fuel were homogeneous mixtures of PuO₂-UO₂-polystyrene in the form of 5- by 5-cm compacts having varying thicknesses.²

One fuel had a H:(Pu+U) atomic ratio of 2.8; the oxide mixture contained 30.3 wt % PuO₂. The plutonium in this fuel had a ²⁴⁰Pu-to-total-plutonium atomic ratio of 0.115. The second fuel had a H:(Pu+U) ratio of 30.6, and the oxide mixture contained 14.62 wt % PuO₂. The plutonium in this fuel contains 7.97 at. % ²⁴⁰Pu. A complete description of each fuel, including cladding, is shown in Table A.5. Atom densities for the three poison plates are shown in Table A.6.

**Table A.4. Calculated k-effectives for unpoisoned,
low-moderation experiments**

Experiment designation	k-effective ^a	Average energy group for fissions ^b
1453-01	0.99229 ± 0.00223	8.97497
1453-02	0.99076 ± 0.00224	8.97252
1453-03	0.99905 ± 0.00223	10.6919
1453-04	0.99827 ± 0.00216	10.6876
1453-05	1.00715 ± 0.00227	10.6908
1453-06	0.99958 ± 0.00247	10.7358
1453-07	0.99245 ± 0.00248	10.7985
1453-08	0.99343 ± 0.00243	10.8220
1453-09	0.99562 ± 0.00230	10.8093
1453-10	1.00106 ± 0.00239	10.8307
1453-11	0.98991 ± 0.00241	11.5014

^aValue shown is for KENO-Va using Hansen-Roach cross sections. Uncertainty reported is 1 standard deviation.

^b16-energy group, Hansen-Roach structure, 1 σ uncertainty is approximately 0.003.

According to Bierman and Clayton,²

The critical assemblies consisted of rectangular parallelepipeds of fuel fully reflected with 15 cm of a methacrylate plastic (Plexiglas). All assemblies had a base of nine fuel compacts on a side. The plates, having thicknesses up to approximately 2½ cm and the same cross-section dimensions as the assemblies, were positioned horizontally in the assemblies. Except for one series of experiments to measure the worth of a plate as a function of position in the assembly, the position of the plates, relative to the bottom of the assembly, was constant for each fuel. This distance from the bottom was such that the plates were approximately centered in the fuel for all the experiments.

In addition to the measurements with copper or copper-cadmium plates, measurements were similarly made without any plates and with aluminum plates to provide a measure of the void effects relative to the poison effects caused by the plates being present in the assemblies.

Some critical configurations were achieved by using two poison plates in the assembly. These configurations were generally symmetric with one layer of oxide compacts between the two poison plates.

A summary of the experimental data presented in Ref. 2 is provided in Tables A.7 and A.8. The fractional blocks were treated computationally as full layers of thinner fuel compacts having a thickness equal to the fractional layer times the full-sized compact. In the KENO-Va models of these experiments, each compact in the array was represented discretely.

**Table A.5. Description of experimental fuel and reflector material
(Values are atoms per barncentimeter^a)**

Material	2.8 H:(Pu+U) Fueled experiments	30.6 H:(Pu+U) Fueled experiments
Cladding		
H	4.489×10^{-2}	4.489×10^{-2}
C	3.110×10^{-2}	3.110×10^{-2}
Cl	0.724×10^{-2}	0.724×10^{-2}
Reflector		
H	5.712×10^{-2}	5.712×10^{-2}
C	3.570×10^{-2}	3.570×10^{-2}
O	1.428×10^{-2}	1.428×10^{-2}
Fuel Compacts		
²⁴¹ Am	1.472×10^{-5}	5.801×10^{-7}
²³⁹ Pu	2.186×10^{-3}	1.954×10^{-4}
²³⁸ Pu	2.288×10^{-6}	0.0
²⁴⁰ Pu	2.927×10^{-4}	1.702×10^{-5}
²⁴¹ Pu	5.420×10^{-5}	1.034×10^{-6}
²⁴² Pu	6.751×10^{-6}	0.0
O	1.864×10^{-2}	3.023×10^{-3}
²³⁸ U	6.162×10^{-3}	1.252×10^{-3}
²³⁵ U	9.269×10^{-6}	1.904×10^{-6}
H	2.432×10^{-2}	4.489×10^{-2}
C	2.660×10^{-2}	4.412×10^{-2}

^a1 barn = 10^{-24} cm.

Table A.6. Composition of neutron poison plates

Element	Atom Density (atom/bcm) ^a		
	Cu plate	Cu-Cd plate	Al plate
Cu	8.44384×10^{-2}	8.33333×10^{-2}	
O	1.00651×10^{-4}		
C	1.78929×10^{-5}		
Cd		4.71679×10^{-4}	
Sn		1.13027×10^{-4}	
Al			5.88742×10^{-2}
Fe			2.03213×10^{-4}
Si			2.30900×10^{-4}

^a1 barn = 10^{-24} cm.

Table A.7. Critical assembly configurations of poisoned, plexiglas-reflected 2.8 H:(Pu + U) mixed-oxide compacts

Experiment designation	Layers of fuel below plate 5.09 cm	Type of poison plate	Layers of fuel above plate	
			5.09 cm	1.339 cm
1547-1	3	1/8 in. Cu	2	0.502
1547-2	3	3/8 in. Cu	2	1.321
1547-3	3	3/4 in. Cu	2	2.536
1547-4	3	1/8 in. Cu-Cd	2	0.738
1547-5	3	3/8 in. Cu-Cd	2	1.827
1547-6	3	3/4 in. Cu-Cd	2	3.468
1547-7	3	1/8 in. Al	2	0.342
1547-8	3	3/8 in. Al	2	0.873
1547-9	3	3/4 in. Al	2	1.688

Calculated k-effectives for the nine experiments conducted with the 2.8 H:(Pu + U) oxide are shown in Table A.9. No trends in k-effective as a function of either type of poison or poison-plate thickness were observed. Thus, it appears that the fixed poisons examined in these experiments can be modeled accurately with this particular code and library combination.

Calculated k-effectives for the 22 experiments conducted with 30.6 H:(Pu + U) oxide are shown in Table A.10. The results are somewhat higher than those reported in Table A.9.

Comparison of calculated k-effectives in Table A.10 with the physical data provided in Table A.8 reveals only one trend in k-effectives. The presence of Cu plates seems to slightly lower calculated k-effective. Considering experiments 1547-10 through 1547-15 and 1547-25 through 1547-28, the value of k-effective decreases from 1.015 to 1.0 as the plate thickness increases. Generally, it appears that the fixed poisons examined in the 30.6 H:(Pu + U) ratio experiments can be modeled accurately with the code and library combination.

A.3.3 Unpoisoned, High-Moderation Mixed-Oxide Critical Experiments

Reference 3 contains data for low-moderation oxide critical experiments with high ^{240}Pu content (23 wt %). However, these experiments were not calculated due to their low Pu:(Pu + U) ratio (0.08).

References 4, 7, 10, and 11 provide information on three series of critical experiments. These experiments were conducted with mixed-oxide fuel having 30.0 and 14.62 wt % Pu and H:(Pu + U) ratios of 47.4 and 30.6 respectively. In all three fuels, the plutonium contained 8 wt % ^{240}Pu , and the uranium was depleted to 0.151 wt % ^{235}U .

**Table A.8. Critical assembly configurations of poisoned, plexiglas-reflected
30.6 H:(Pu+U) mixed-oxide compacts**

Experiment designation	Layers of fuel below plate 3.4 cm	Type of poison plate	Layers of fuel above plate		Type of second poison plate	Layers of fuel above second plate	
			5.09 cm	1.384 cm		5.09 cm	1.384 cm
1547-10	3	None	2	1.276			/
1547-11	3	1/8 in. Cu	2	2.415			
1547-12	3	1/4 in. Cu	2	3.110			
1547-13	3	1/2 in. Cu	3	0.463			
1547-14	3	3/4 in. Cu	3	1.136			
1547-15	3	1 in. Cu	3	1.746			
1547-16	3	1/8 in. Cu-Cd	3	0.757			
1547-17	3	3/4 in. Cu-Cd	3	2.698			
1547-18	3	1/8 in. Al	2	1.548			
1547-19	3	1/4 in. Al	2	1.739			
1547-20	3	3/4 in. Al	2	2.713			
1547-21	3	1 in. Al	2	3.158			
1547-22	a	1/8 in. Cu	1	2.349			
1547-23	a	1/8 in. Cu-Cd	2	0.952			
1547-24	b	1/8 in. Cu-Cd	0	3.463			
1547-25	3	1/8 in. Cu	1	0	1/8 in. Cu	1	3.603

Table A.8. (continued)

Experiment designation	Layers of fuel below plate 3.4 cm	Type of poison plate	Layers of fuel above plate		Type of second poison plate	Layers of fuel above second plate	
			5.09 cm	1.384 cm		5.09 cm	1.384 cm
1547-26	3	1/2 in. Cu	1	0	1/2 in. Cu	2	3.584
1547-27	3	3/4 in. Cu	1	0	3/4 in. Cu	3	1.129
1547-28	3	1 in. Cu	1	0	1 in. Cu	3	2.092
1547-29	3	1/8 in. Cu-Cd	1	0	1/8 in. Cu-Cd	3	0.331
1547-30	3	1/8 in. Al	1	0	1/8 in. Al	1	1.812
1547-31	3	1 in. Al	1	0	1 in. Al	2	1.151

*Three layers of 3.4 cm plus one layer of 5.09-cm-thick fuel compacts below poison plate.

^bThree layers of 3.4 cm plus two layers of 5.09-cm-thick fuel compacts below poison plate.

Table A.9. Calculated k-effectives for poisoned, low-moderation experiments with H:(Pu+U) ratio = 2.8

Experiment designation	k-effective ^a	Average energy group for fissions ^b
1547-1	0.99644 ± 0.00239	10.739
1547-2	0.99679 ± 0.00236	10.682
1547-3	0.99823 ± 0.00226	10.695
1547-4	1.00222 ± 0.00244	10.6997
1547-5	0.99371 ± 0.00237	10.6767
1547-6	0.99367 ± 0.00234	10.6108
1547-7	1.00391 ± 0.00248	10.7062
1547-8	1.00414 ± 0.00228	10.7083
1547-9	1.00300 ± 0.00247	10.7166

^aValue shown is for KENO-Va using Hansen-Roach cross-sections. Uncertainty reported is one standard deviation.

^b16-energy-group, Hansen-Roach structure, 1σ uncertainty is approximately 0.003.

Bierman, Clayton, and Hansen⁴ report:

Each of the fuels consisted of a homogeneous mixture of PuO₂-UO₂-polystyrene in the form of 2- X 2-in. compacts having thicknesses of 2-, 1½- and ½-in. Each compact was clad with 6-mil-thick tape (MM&M #471). Nuclide composition and densities are given in (Table A.11) for each of the three fuels and for the Plexiglas reflector used in the experiments.

The critical assemblies were formed by stacking the oxide compacts into rectangular parallelepiped configurations. The Plexiglas reflector had a thickness of 15 cm. The measured critical assembly parameters are given in Tables A.12 and A.13. The critical sizes given in these two tables are for solid assemblies of fuel only. Experimentally determined corrections have been applied in each case to account for the effects of the cladding material and the presence of voids in the assembly of stacked blocks. Reference 10 provides the actual experimental data in terms of the number of polycubes in the length, width, and height of the assemblies. However, the computer calculations to be described in this section were based on the simpler, solid assembly data.

The calculated k-effectives are shown in Table A.14. To provide for easier comparison, the experiments were grouped according to fuel type and reflector, and the means of the calculated k-effectives were tabulated. These mean values are shown in Table A.15. It appears that the bare, 30 wt % Pu experiments calculate somewhat lower than the Plexiglas-reflected 30 wt % Pu experiments. This trend is not as pronounced in the 14.6 wt % Pu experiments.

Table A.10. Calculated k-effectives for poisoned, low-moderation experiments with H:(Pu+U) ratio = 30.6

Experiment designation	k-effective ^a	Average energy group for fissions ^b
1547-10	1.01640 ± 0.00273	15.0134
1547-11	1.01597 ± 0.00251	14.9997
1547-12	1.00939 ± 0.00256	14.9959
1547-13	1.00513 ± 0.00274	14.9859
1547-14	1.00532 ± 0.00271	14.9899
1547-15	1.00365 ± 0.00290	14.9788
1547-16	1.01563 ± 0.00235	14.982
1547-17	1.00850 ± 0.00261	14.9715
1547-18	1.01557 ± 0.00271	15.0203
1547-19	1.01759 ± 0.00264	15.0106
1547-20	1.01486 ± 0.00261	15.0187
1547-21	1.02042 ± 0.00263	15.0193
1547-22	1.01625 ± 0.00264	15.0024
1547-23	1.01081 ± 0.00257	14.9833
1547-24	1.01480 ± 0.00279	14.9848
1547-25	1.01074 ± 0.00265	14.9992
1547-26	1.00046 ± 0.00249	14.9688
1547-27	0.99617 ± 0.00245	14.9619
1547-28	1.00096 ± 0.00244	14.9607
1547-29	1.02132 ± 0.00228	14.9561
1547-30	1.01427 ± 0.00258	15.0171
1547-31	1.01583 ± 0.00267	15.0163

^aValue shown is for KENO-Va using Hansen-Roach cross sections. Uncertainty reported is 1 standard deviation.

^b16-energy-group, Hansen-Roach structure, 1σ uncertainty is approximately 0.003.

Table A.11. Composition and atom densities of fuels and reflector for high-moderation, mixed-oxide critical experiments

Nuclide	Atom density (atom/bcm) ^a			
	426 g/L oxide; atomic H:(U+Pu) = 47.4; 30.0 wt % Pu	660 g/L oxide; atomic H:(U+Pu) = 30.6; 14.62 wt % Pu	408 g/L oxide; atomic H:(U+Pu) = 51.8; 7.89 wt % Pu	Reflector
²⁴¹ Am	3.511×10^{-7}	4.036×10^{-7}	1.741×10^{-7}	
²³⁹ Pu	2.578×10^{-4}	1.954×10^{-4}	6.528×10^{-3}	
²⁴⁰ Pu	2.257×10^{-5}	1.702×10^{-5}	5.941×10^{-6}	
²⁴¹ Pu	1.756×10^{-6}	1.211×10^{-6}	3.481×10^{-7}	
O	1.974×10^{-3}	3.023×10^{-3}	1.830×10^{-3}	1.428×10^{-2}
²³⁸ U	6.604×10^{-4}	1.252×10^{-3}	8.376×10^{-4}	
²³⁵ U	1.008×10^{-5}	1.904×10^{-6}	1.285×10^{-6}	
H	4.468×10^{-2}	4.489×10^{-2}	4.719×10^{-2}	5.712×10^{-2}
C	4.537×10^{-2}	4.412×10^{-2}	4.540×10^{-2}	3.570×10^{-2}

^a1 barn = 10^{-24} cm.

Table A.12. Criticality data for mixed-oxide assemblies containing 30 wt % Pu with H:(Pu+U) = 47.4

Experiment designation	Reflector	Critical dimensions (cm)		
		Length	Width	Height
1677-1	Plexiglas	30.54	30.54	30.89
1677-2	Plexiglas	35.63	35.63	23.95
1677-3	Plexiglas	40.72	40.72	20.22
1677-4	Plexiglas	50.90	45.81	17.14
1677-5	Plexiglas	61.08	50.90	15.53
1677-6	Plexiglas	61.08	55.99	15.16
1677-7	Plexiglas	66.17	61.08	14.43
1677-8	Plexiglas	50.90	50.90	16.49
1677-9	Bare	45.81	40.72	37.98
1677-10	Bare	40.72	40.72	42.24
1677-11	Bare	45.81	50.90	32.49

Table A.13. Criticality data for mixed-oxide assemblies containing 14.62 wt % Pu with H:(Pu + U) = 30.6

Experiment designation	Reflector	Critical dimensions (cm)		
		Length	Width	Height
1677-12	Plexiglas	30.54	40.72	29.81
1677-13	Plexiglas	40.72	40.72	23.84
1677-14	Plexiglas	45.81	50.90	19.82
1677-15	Plexiglas	50.90	50.90	18.92
1677-16	Plexiglas	61.08	50.90	17.72
1677-17	Plexiglas	61.08	61.08	16.63
1677-18	Bare	40.72	40.76	52.39
1677-19	Bare	40.72	45.86	45.10
1677-20	Bare	50.90	45.86	36.99

Table A.14. Calculated k-effectives for high-moderation, mixed-oxide critical experiments

Experiment designation	k-effective ^a	Average energy group for fissions ^b
1677-01	1.02477 ± 0.00278	14.9263
1677-02	1.01451 ± 0.00299	14.9141
1677-03	1.01987 ± 0.00279	14.9227
1677-04	1.01802 ± 0.00284	14.9362
1677-05	1.01897 ± 0.00295	14.9428
1677-06	1.01956 ± 0.00305	14.9474
1677-07	1.01923 ± 0.00256	14.9460
1677-08	1.01606 ± 0.00286	14.9359
1677-09	1.00541 ± 0.00307	14.6429
1677-10	1.00453 ± 0.00298	14.6434
1677-11	1.00126 ± 0.00319	14.6395
1677-12	1.02493 ± 0.00291	15.0215
1677-13	1.02348 ± 0.00290	15.0122
1677-14	1.02111 ± 0.00282	15.0246
1677-15	1.01779 ± 0.00273	15.0212
1677-16	1.02193 ± 0.00282	15.0300
1677-17	1.02112 ± 0.00279	15.0370
1677-18	1.02008 ± 0.00283	14.8003
1677-19	1.01874 ± 0.00293	14.7966
1677-20	1.01335 ± 0.00290	14.7958

^aValue shown is for KENO-Va using Hansen-Roach cross sections. Uncertainty reported is one standard deviation.

^b16-energy-group, Hansen Roach structure, 1σ uncertainty is approximately 0.003.

Table A.15. Average calculated k-effectives for high-moderation mixed-oxide critical experiments

Fuel type	Reflector	Average k-effective
30 wt % Pu	Plexiglas	1.019
30 wt % Pu	Bare	1.004
14.6 wt % Pu	Plexiglas	1.022
14.6 wt % Pu	Bare	1.017

A.4 INTERACTING ARRAY EXPERIMENTS

Few array experiments were found which would be applicable to this problem. The most applicable data are documented in Ref. 12. An investigation of these experiments revealed that the uncertainty in the fuel distribution was so large as to make these data unusable.

A.5 CONCRETE-REFLECTED EXPERIMENTS

Appendix C contains a description of the composition of the cell wall concrete. The most applicable data are believed to be a series of experiments conducted with Fast Flux Test Reactor (FTR) pins immersed in water and reflected with concrete (Ref. 13) and a second series conducted with a water reflector. Critical experiment data for nine experiments are shown in Table A.16. The composition of the concrete reflector is shown in Table A.17. Also shown is the cell wall concrete composition from Appendix C. Even though the densities of the two mixtures are quite different, the relative abundances of various elements are similar. Thus, a significant error in cross-section data for any of the constituents of the 3019 cell wall concrete might appear in the k-effective calculations for the critical experiments provided similar neutron spectra exist in both configurations. Any bias due to the presence of concrete can be isolated by comparing equivalent pitches for water and concrete reflected experiments. Calculated k-effectives are reported in Table A.18.

Table A.16. Experimental criticality data for concrete reflected type 3.2 FTR fuel pins in water

Koponen Citation ID	PNL Experiment reference no.	Square lattice pitch ^a (mm)	Lattice width (fuel pins)	Critical number of fuel pins ^a	Critical rows of fuel pins	Reflector
2116-1	010	9.53 ± 0.13	28	554 ± 1	19.79	Concrete
2116-2	007	12.64 ± 0.13	18	260 ± 1	14.44	Concrete
2116-3	012	15.41 ± 0.13	18	191 ± 1	10.61	Concrete
2116-4	011	19.06 ± 0.18	14	152 ± 1	10.86	Concrete
2117-1	021	0.968 ± 0.001	25	571.9 ± 0.2	22.88	Water
2117-9	043	1.242 ± 0.001	20	293.9 ± 0.1	14.70	Water
2117-17	013	1.537 ± 0.001	15	196.7 ± 0.2	13.11	Water
----	068R	1.537 ± 0.001	15	199.7 ± 0.3	13.31	Water
2117-25	032	1.935 ± 0.002	15	165.1 ± 0.4	11.01	Water

^aError limits shown are standard deviations and are for the indicated measured parameter only.

Table A.17. Comparison of concrete compositions

Chemical element	Wt % in concrete ^a	
	Critical experiments ^b	3019 cell walls ^c
Al	2.32 ± 0.01	2.26 ± 0.15
Ca	7.27 ± 0.28	7.51 ± 0.28
Fe	0.28 ± 0.02	1.40 ± 0.03
Si	34.68 ± 0.39	38.19 ± 1.21
Mg	1.45 ± 0.05	0.31 ± 0.03
K	0.75 ± 0.15	0.92 ± 0.26
Na	0.17 ± 0.01	0.24 ± 0.03
O	52.26 ± 0.58	48.01 ± 1.56
H	0.82 ± 0.07	0.50 ^d
C	-----	0.50 ^d
S	-----	0.08 ± 0.02

^aErrors are 1σ standard deviations based on three analyses.

^bDensity of concrete immersed in water = 2.452 g/cm³.

^cDensity of cell wall concrete = 1.523 ± 0.036 g/cm³.

^dMaximum value assumed from Appendix C.

Table A.18. Calculated parameters for arrays of FTR pins

Koponen Citation ID	Pitch (cm)	Reflector	K-effective	Avg. fission group
2117-1	0.968	water	0.98491 ± 0.00286	13.61
2117-9	1.242	water	0.99373 ± 0.00339	14.48
2117-7	1.537 ^a	water	0.99217 ± 0.00318	14.89
---- ^b	1.537 ^{c,d}	water	0.99522 ± 0.00303	14.88
2117-25	1.935	water	1.00712 ± 0.00304	15.18
2116-1	0.953	concrete	0.99199 ± 0.00267	13.53
2116-2	1.264	concrete	1.00091 ± 0.00327	14.52
2116-3	1.541	concrete	1.00409 ± 0.00306	14.90
2116-4	1.906	concrete	1.01019 ± 0.00303	15.16

^aPNL experiment number 013.

^bComputer input dataset designated 2117.X.

^cPNL experiment number 068r.

^dAverage k-effective for 1.537 cm pitch is 0.993769 ± 0.002194.

For comparable pitches, average fission group values are in excellent (with 1%) agreement. While the calculated k-effectives for concrete reflected experiments are slightly higher than comparable water reflected cases, comparison of the differences using student's *t* test reveals that the differences are not significant.

Considering the range of average fission group values, the presence of concrete as a moderator and reflector in intercell 2 and 3 configurations should not lead to any bias in k-effective under nominal conditions. Applicable data do not exist for credible abnormal conditions but extrapolation from existing data does not yield any trends.

A.6 STATISTICAL ANALYSES OF CRITICAL EXPERIMENTS

The data presented in Sect. A.3 were grouped into various categories and tested for trends and biases. The first procedure was to simply calculate the means of the various data sets and visually inspect them for trends. Table A.19 shows the calculated mean value of k-effective for the various series of experiments.

Table A.19. Categorized mean calculated k-effectives

Category	Mean value of k-effective
All experiments	1.009
All 1453 experiments Pu % = 29.3, H/X = 2.8, Pu-240 = 11.5% Pu % = 15, H/X = 2.86, Pu-240 = 11.5%	0.996 0.997 0.990
All 1547 experiments Pu % = 30.3, H/X = 2.8, Pu-240 = 11.5% Pu % = 14.6, H/X = 30.6, Pu-240 = 7.97%	1.008 0.999 1.011
All 1677 experiments Pu % = 30.0, H/X = 47.4, Pu-240 = 8% Pu % = 14.62, H/X = 30.6, Pu-240 = 8%	1.017 1.015 1.020
All Bare	1.004
All Plexiglas Ref.	1.010

Considering all the data as a group, a 1% bias exists in calculated k-effective. In order to quantitatively examine the calculations for trends, some statistical analyses were performed with the SAS procedure CORR.¹⁴ A search for a linear relationship between a given variable and calculated k-effective was performed by calculating the Pearson product moment correlation and its level of significance. If a variable, *x*, can be expressed exactly as a linear function of another variable, *y*, then the correlation is 1 or -1 depending on whether the two variables are directly related or inversely related. The lower the value of the significance level, the higher the degree of confidence that the computed correlation value represents a true phenomena. Calculated product moments for the critical experiment parameters are presented in Table A.20. All of the values in Table A.20 have a high degree of confidence.

It should be noted that there is no physical reason to suspect that k-effective would be correlated in any way with any of the parameters listed in Table A.16. The justification for selecting the product moment formulation is simply observation of the trends summarized in Table A.19.

Considering the first four entries of Table A.20, it appears that k-effective is directly correlated with H/(Pu + U) ratio and average fission group and inversely correlated with the quantity of Pu-240 in the plutonium. Note, however, that average fission group and H/(Pu + U) ratio are strongly correlated. Intuitively, it is obvious that both of these correlations represent the same physical phenomena — degree of moderation in the system.

The strong negative correlation between H/(Pu + U) ratio and ^{240}Pu content reveals a need for additional experimental data if one is to discern whether k-effective is correlated to either a degree-of-moderation parameter or to ^{240}Pu content or both. Note that examination of plutonium oxide critical experiments and/or low plutonium content mixed oxide experiments might resolve this situation.

For this study, it was decided to correlate k-effective with average fission group. Among the correlations to k-effective, the value for average fission group was largest. Perhaps more importantly, in all the criticality safety calculations for Intercell 2 and 3 storage wells, the ^{240}Pu content was assumed to be zero. This assumption is conservative since maximum reactivity is derived from assuming that all plutonium is present as ^{239}Pu but the safety limit, derived subsequently, is based on critical experiments which have been conducted with fuels ranging in ^{240}Pu content from 8—11.5%. Note in Table 2, that most of the NFS waste contains 8.3 wt % ^{240}Pu in the plutonium.

Table A.20. Calculated Pearson product moment correlation coefficients for KENO-Va, Hansen-Roach calculations

Correlated variables	Correlation coefficient	Significance level
Average fission group, k-eff	.765	.0001
$^{240}\text{Pu}/\text{Total Pu}$, k-eff	-.753	.0001
Pu/(Pu + U), k-eff	-.421	.0007
H/(Pu + U), k-eff	.699	.0001
H/(Pu + U), average fission group	.898	.0001
H/(Pu + U), ^{240}Pu	-.917	.0001

From Table A.16, reflectors appear to add a positive bias to calculated k-effectives. Note, however, that the 3019 Intercell 2 and 3 wells have large concrete reflectors.

Correlating with average fission group allows the moderation provided by interstitial concrete in Intercell Storage 2 and 3 to be compared to the polystyrene moderated and reflected oxide critical experiments. A plot of k-effective versus average fission group is given in Fig. A.1. Note that the expected average fission group value for the NFS waste under "normal" conditions would be 12-13, within the range spanned by the critical experiment data. The average fission group values for all credible abnormal conditions considered also are within the range of the data.

A linear regression of k-effective to average fission group, AFG, was performed and the resulting linear function was

$$\text{k-effective} = 0.957397 + 0.003797 \text{ (average Hansen-Roach fission group).}$$

The R^2 value (goodness-of-fit) was 0.601. This equation is plotted as a solid line in Fig. A.1. Inclusion of all of the other variables noted in Tables A.19 and A.20 into the correlation yielded an insignificant increase in the R^2 value to 0.680.

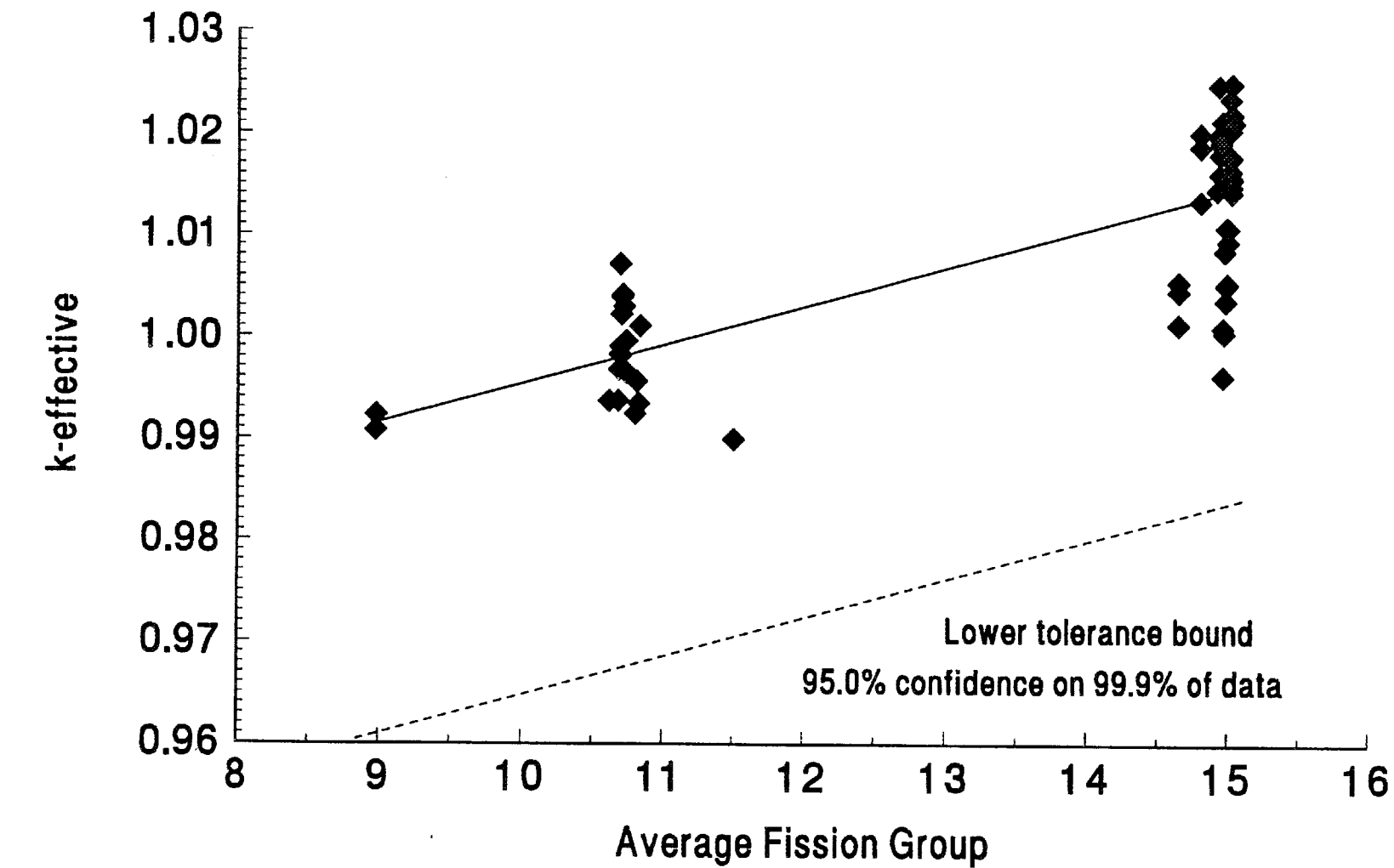


Fig. A.1. K-effectives from mixed-oxide criticales (KENO-Va, Hansen-Roach).

Note that correlating k-effective to powers of the AFG values — specifically the cube of these values — yielded correlations with the same R^2 values but with significantly higher y intercepts ($k_{\text{eff}} = 0.988$ at average fission group of 1). This finding would be important if it were necessary to extrapolate beyond the range of the critical experiment data.

Also shown in Fig. A.1 is a dashed line representing the lower tolerance bound for inclusion of 99.9% of the calculated k-effectives at the 95% confidence level. The equation of this line is $k_{\text{effective}} = 0.92674 + 0.003797$ (average Hansen-Roach fission group). The derivation of the tolerance bound is based on the treatment presented in Refs. 15–17. Note that for nominal NFS conditions, a k-effective of 0.97 yields a tolerance bound of at least 99.9/95.

Earlier in the report it was noted that possible negative biases exist regarding the presence of copper plates in critical experiments or the absence of a reflector. Nevertheless, these experiments have been retained in the database shown in Fig. A.1 because their impact is conservative (leads to a lower tolerance bound).

A.7 CORRECTIONS TO DERIVED SUBCRITICALITY LIMITS TO ACCOUNT FOR UNCERTAINTIES IN EXPERIMENTAL MEASUREMENTS

The critical experiments parameters that are input to the SCALE calculations have associated uncertainties. The impact of these uncertainties must be accommodated in the margin of subcriticality. Yet, it would be untractable to examine the impact of every experimental uncertainty on each of the critical experiments examined in this study. Consequently, two experiments were selected for study.

Experiment 1453-10 is the low-moderation-oxide experiment with the minimum critical height. Uncertainty in the critical height should have the greatest impact in the minimum height configuration. Likewise, experiment 1677-7 has the minimum critical height for the high-moderation experiments. Selecting these two experiments allowed for observation of impact of uncertainties over the range of moderation available. An assessment of possible experimental errors and comments are provided in Table A.21.

Table A.21. Sources of experimental uncertainties

Source	Remarks
Measured size of oxide blocks	Uncertainties provided by experimenters
Extrapolation of critical thickness of final row	Uncertainties provided by experimenters
Density of fuel	Uncertainties provided by experimenters
Isotopic ratios	Uncertainties provided by experimenters, Appendix B.
Impurities in fuel	Spark source check performed by experimenters, but no data available for calculations.
Moderator density in fuel	Uncertainties provided by experimenters
Reflector impurities	1960's plexiglas, no fire-retarding agents present, spark source check performed but no data available for calculations

Most of the experimental uncertainty data were reported in the references containing the critical experiment data. However, some data regarding uncertainty in the plutonium concentration were obtained from the log books for the experiments. A letter provides reference for these data and is included as Appendix B.

Where possible, the uncertainties noted in Table A.21 were investigated. Because of cost considerations, these investigations were not performed with verified software. However, since only perturbations from a reference case were being investigated, this is not believed to be a problem, especially in light of the results which are presented in Table A.21.

If the experimental uncertainties have no impact on calculated k-effectives, all the differences reported on the right-hand side of Table A.22 should be zero. One can use student's *t* distribution¹⁸ to determine whether the calculated differences are significantly different from zero. Defining the *t* statistic to be

$$t = \frac{\text{difference}_i - 0}{\sigma_i} ,$$

and assuming one degree of freedom then for the "worst case," in Table A.22, $t = 0.00403/0.00215 = 1.874$. The probability of $t > 1.874$ is 0.19. Thus, it is unlikely that, taken independently, the experimental uncertainties have any statistically significant impact on calculated k-effectives. Considering that not all experimental uncertainties were well-known (see Table A.20), a reactivity bias of 0.01 to account for these unknowns should be quite conservative.

A.8 COMMENTS ON APPLICABILITY OF CRITICAL EXPERIMENTS AND MARGIN OF SUBCRITICALITY

It has been stated previously that the actinide content, moderator content, and physical form of the materials in the critical experiments are representative of the waste expected to be stored in the Intercell 2 and 3 wells. It has also been noted that the span of the values of the average fission group (afg) for the critical experiments includes the range expected to exist for normal and credible abnormal configurations in the storage wells. It seemed possible, however, for two configurations to have the same afgs but have different neutron spectra. Consequently, qualitative comparisons of spectra were made and are shown in Figs. A.2 and A.3.

As noted in Sect. 6.3, the "normal" storage configuration has an afg of 13.2. The two critical experiments whose afg values are closest to the normal configuration are 1453-11 (afg=11.5) and 1677-11 (afg=14.64). Note that 1453-11 is a methacrylate-plastic-reflected experiment and 1677-11 is a "bare" experiment.

For all the fast and epithermal groups, shown in Fig. A.2, the fission fraction for the storage configuration lies between the two experiments. The storage configuration appears to have a more thermalized spectra than either of the critical experiments, but the overall spectral shape is similar.

Spectra for the abnormal configuration corresponding to Case 6 in Table 10 is shown in Fig. A.3. The afg value for this case, 9.2, is the lowest of all calculated abnormal configurations. Experiment 1453-01 has an almost identical afg — 9.0.

The shapes of the two spectra in Fig. A.3 are quite similar. All significant peaks in groupwise fission fraction for the storage case are matched in the critical experiment spectra.

The spectral comparisons in Figs. A.2 and A.3, taken with previous comparisons of fuel composition and moderator content, provide support for the conclusion that the storage configurations which have been evaluated are within the range of applicability defined by the critical experiments. Given the relatively large number of experiments, the small variability among calculated k-effectives for the experiments, and the well-defined storage configuration being considered, there seems to be no need to apply an additional subcritical margin to the corrected (for experimental uncertainties) tolerance bound derived in Sect. A.6. Note that other, undefined, mixed-oxide storage configurations might not satisfy these criteria and would require an additional subcritical margin applied to the corrected tolerance bound.

During safety reviews, it is sometimes questioned as to the degree of subcriticality to which a particular configuration is designed. Using results from Sects. 6.6, 6.7 and Table 10, the degree of subcriticality for Intercell 2 and 3 storage wells for NFS waste is at least 0.447 ($0.96 - 0.01 - 0.453 = 0.447$).

Table A.22. Reactivity worth of experimental uncertainties^a

Case	k-effective		Difference from base case ^b	
	1453-10	1677-7	1453-10	1677-7
Reference	1.00377 ± 0.00162	1.02055 ± 0.00164	0.0	0.0
Critical height increased ^c	1.00228 ± 0.00136	1.02232 ± 0.00159	0.00149 ± 0.00212	-0.00177 ± 0.00228
Fissile density increased ^d	1.00013 ± 0.00144	1.02068 ± 0.00163	0.00364 ± 0.00216	-0.00013 ± 0.00231
Fuel isotopics modified ^e	1.0078 ± 0.00141	1.02149 ± 0.00163	0.00403 ± 0.00215	-0.00094 ± 0.00231
Hydrogen in fuel increased ^f	1.00596 ± 0.00136	1.02251 ± 0.00162	-0.00219 ± 0.00212	-0.00196 ± 0.00231
Carbon in fuel increased ^f	1.00233 ± 0.00136	1.02326 ± 0.00168	0.00144 ± 0.00212	-0.00271 ± 0.00235

^aAll calculations performed with unvalidated SCALE4 procedure on the ucry with Hansen-Roach cross sections.

^bValue is (reference-perturbation). Uncertainty is $\sqrt{\sigma_{\text{ref}}^2 + \sigma_{\text{pert}}^2}$.

^cHeight of assembly increased by 1σ . Note that experimental uncertainty is derived from variations in the dimensions of individual fuel blocks and thus should be conservative.

^dFuel density increased by 2σ and fissile isotope wt. percentages increased by 2σ .

^ePu-239 increased by 1σ uncertainty on fissile Pu isotopes, Pu-240 decreased by corresponding amount.

^fModerator nuclide increased by 1σ .

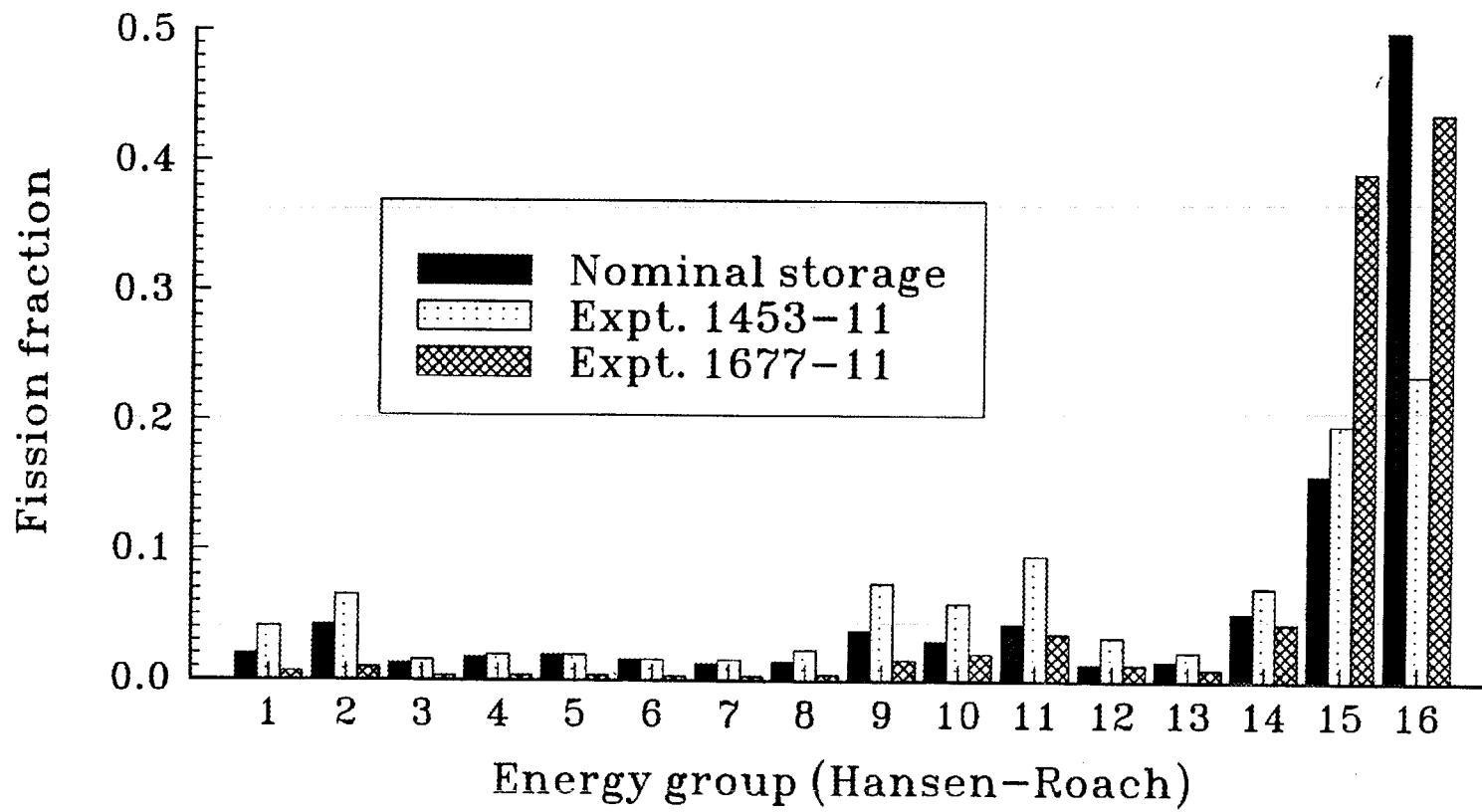


Fig. A.2. Computed spectral comparison. Nominal case to critical experiments.

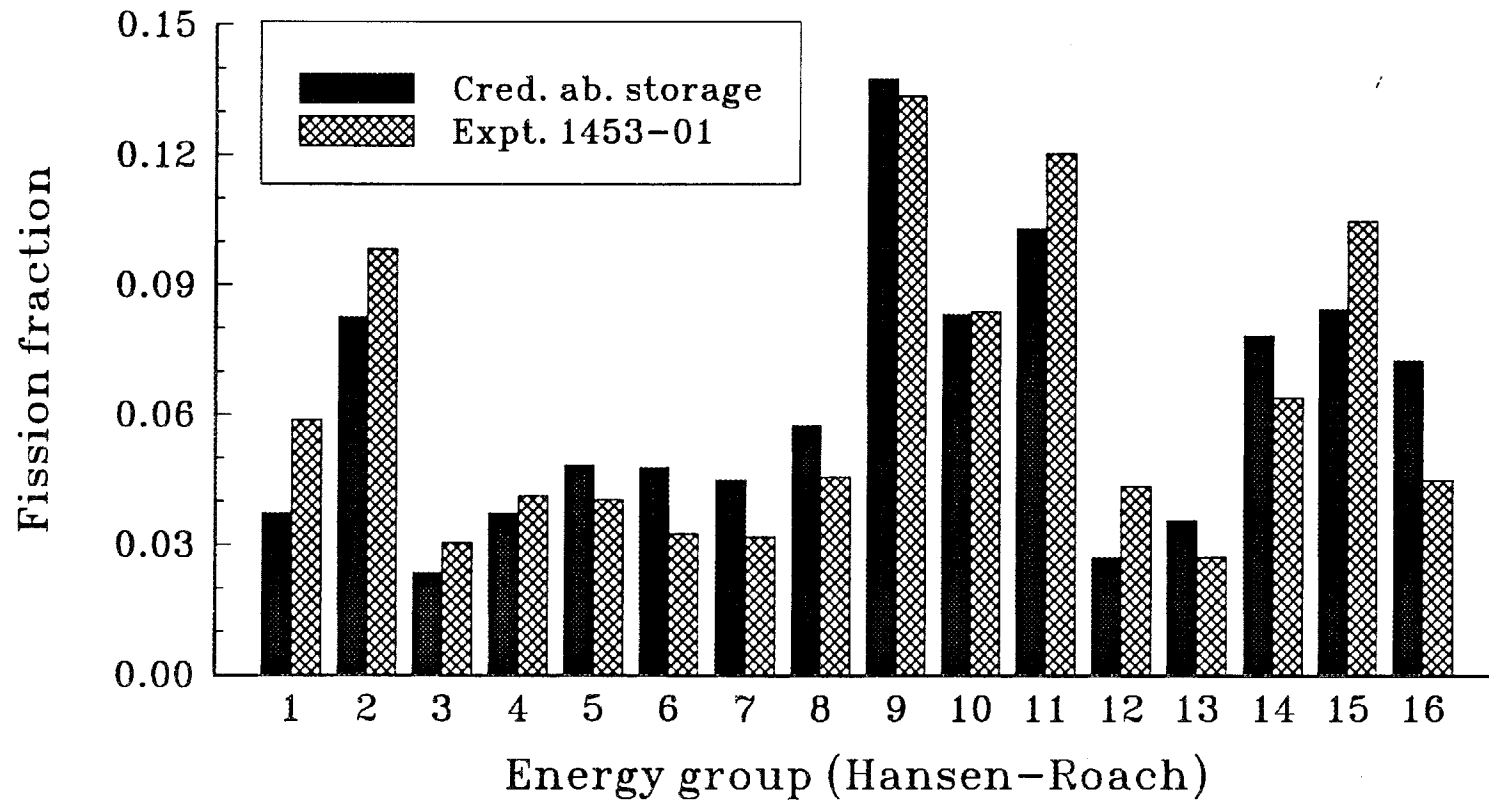


Fig. A.3. Calculated spectral comparison. Credible abnormal storage to critical experiment.

REFERENCES FOR APPENDIX A

1. S. R. Bierman and E. D. Clayton, "Critical Experiments with Low-Moderated Homogeneous Mixtures of Plutonium and Uranium Oxides Containing 8, 15, and 30 wt % Plutonium," *Nucl. Sci. Eng.* **61**, 370-76 (1976).
2. S. R. Bierman and E. D. Clayton, "Critical Experiments to Measure the Neutron Poisoning Effects of Copper and Copper-Cadmium Plates," *Nucl. Sci. Eng.* **55**, 58-66 (1974).
3. R. C. Lloyd, S. R. Bierman, and E. D. Clayton, "Criticality of Plutonium-Uranium Mixtures Containing 5 to 8 wt % Plutonium," *Nucl. Sci. Eng.* **55**, 51-57 (1974).
4. S. R. Bierman, E. D. Clayton, and L. E. Hansen, "Critical Experiments with Homogeneous Mixtures of Plutonium and Uranium Oxides Containing 8, 15, and 30 Wt % Plutonium," *Nucl. Sci. Eng.* **50**, 115-26 (1973).
5. G. E. Hansen and W. H. Roach, *Six and Sixteen Group Cross Sections for Fast and Intermediate Critical Systems*, LAMS-2543, December 1961.
6. *SCALE - A Modular Code System for Performing Standardized Computer Analyses for Licensing Evaluation*, NUREG/CR-0200, Rev. 4 (ORNL/NUREG/CSD-2/R4), Vols. I, II and III (draft February 1990). Available from Radiation Shielding Information Center, Oak Ridge National Laboratory, as CCC-545.
7. S. R. Bierman and E. D. Clayton, "Critical Experiments with Mixed Oxides of Pu and U Containing 8 and 30 wt % Plutonium," *Trans. Am. Nucl. Soc.* **15**, 307-309 (1972).
8. S. R. Bierman and E. D. Clayton, "Critical Experiments with Low Moderated Homogeneous Mixtures of Plutonium and Uranium Containing 8 and 15 Wt % Plutonium," *Trans. Am. Nucl. Soc.* **23**, 235-37 (November 1976).
9. S. R. Bierman, R. C. Lloyd, and E. D. Clayton, "Critical Experiments to Measure the Neutron Poisoning Effects of Cu and Cu-Cd Plates," *Trans. Am. Nucl. Soc.* **17**, 265 (1973).
10. S. R. Bierman, "Critical Experiments-Benchmarks (Pu+U Systems)," *Nucl. Technol.* **26**, 352-81 (July 1975).
11. S. R. Bierman and E. D. Clayton, "Critical Experiments with Mixed Oxides of Pu and U Containing 15 and 30 Wt % Pu," *Trans. Am. Nucl. Soc.* **14**, 40-41 (June 1971).
12. J. T. Thomas, "Critical Experiments with UF₆ Cylinder Model 8A Containers," Y-DR-128 (September 1974).
13. B. M. Durst, et al., "Summary of Experimental Data for Critical Arrays of Water Moderated Fast Test Reactor Fuel," PNL-3313, ORNL/Sub-81/97731/7, May 1981.

REFERENCES (continued)

14. J. P. Sall and D. M. Delong, "The CORR Procedure," *SAS User's Guide: Basics 1982 Edition*, 501-512, SAS Institute, Inc. (1982).
15. H. R. Dyer, W. C. Jordan, and V. R. Cain, "A Technique for Code Validation for Criticality Safety Calculations," *Trans. Am. Nucl. Soc.*, **63**, pg. 238-239 (June 1991).
16. D. C. Bowden and F. A. Graybill, "Confidence Bands of Uniform and Proportional Width for Linear Models," *Am. Stat. Assoc. J.*, **61**, 182 (March 1966).
17. D. C. Bowden, "Query, Tolerance Interval in Regression," *Technometrics* **10**, 207-209 (February 1968).
18. G. E. P. Box, W. G. Hunter, and J. S. Hunter, *Statistics for Experimenters* (1978).

APPENDIX B

UNCERTAINTIES IN ACTINIDE CONTENT FOR LOW-MODERATED OXIDE CRITICAL EXPERIMENTS



Pacific Northwest Laboratories
Battelle Boulevard
P.O. Box 999
Richland, Washington 99352
Telephone (509) 376-9589

June 29, 1992

Facsimile: (509) 376-9200
Verification: (509) 376-9589

Mr. Trent Primm
ORNL
MS-6363
P.O. Box 2008
Oak Ridge, TN 37831-6370

Dear Trent:

As we discussed by phone today, I have enclosed the Pu isotopic analyses for the three batches of oxides used in the 11.5-30-3 mixed oxide fuel. As compacts were made from each batch of oxide a composite sample was accumulated. The enclosed analyses are the results obtained on each composite sample.

Although the weighted average one sigma deviation quoted in the report reflects the spread in the composition between batches, the experimental assembly was a homogeneous mix of these batches. Therefore, I agree with you that the error limits should be based on those quoted in the three analyses. Fortunately these are essentially the same for all three batches.

I have also enclosed copies of the uranium isotopic analyses obtained from two samples. However, there should not be a similar problem since all of the uranium came from the same source.

Sincerely Yours,


S.R. Bierman
Staff Scientist
Reactor Systems Analyses

WADCO
Corporation

1453 expts
RTP

From: Applied Chemistry and Analysis
Date: November 29, 1971
Subject: ISOTOPIC ANALYSIS OF PLUTONIUM

F.com 115-30-3 Fuel comission
D-Series Co-2000 Dose

TO: R. R. King, Jr.

Sid Burnam

CC: MW Goheen
File

$95.7\% \text{CC} = 1.96\%$

M. S. #	Lab. No.	Cust. I. D.	Wt. %	wt. %
1271177	P-3110	D-310-478	$238 = 0.088 \pm 0.004$	$0.088 \pm .02$
		<i>ATR NCO OXID</i>	$239 = 85.67 \pm 0.06$	$85.761 \pm .03$
			$240 = 11.53 \pm 0.06$	$11.542 \pm .03$
			$241 = 2.32 \pm 0.01$	$2.322 \pm .01$
			$242 = 0.286 \pm 0.009$	$0.2863 \pm .01$
			<u>99.884</u>	<u>99.947</u>

M. A. Goheen
M. A. Goheen, Supervisor
Mass and Emission Spec. Laboratories

BATTELLE B NORTHWEST
BATTELLE MEMORIAL INSTITUTE

DISTRIBUTION OF COPIES

DATE July 1, 1970

1637 copies
RTP

TO Sid Bierman

FROM H. W. Gobain *MWG*

SUBJECT Isotopic Determination of Plutonium

<u>H. S. #</u>	<u>Lab. #</u>	<u>Customer I. D.</u>	<u>Wt. %</u>	<u>T = 0.0153</u>
1270165	P-1584	PuO ₂ UO ₂ Dyline	238 - 0.015 ± 0.001, 239 - 90.89 ± 0.04, 240 - 8.37 ± 0.04, 241 - 0.571 ± 0.005, 242 - 0.049 ± 0.001,	238 - 0.015 ± 0.001, 239 - 90.89 ± 0.04, 240 - 8.37 ± 0.04, 241 - 0.571 ± 0.005, 242 - 0.049 ± 0.001,
				238 - 90.89 ± 0.04, 240 - 8.37 ± 0.04, 241 - 0.571 ± 0.005, 242 - 0.049 ± 0.001,
				238 - 90.89 ± 0.04, 240 - 8.37 ± 0.04, 241 - 0.571 ± 0.005, 242 - 0.049 ± 0.001,
				238 - 90.89 ± 0.04, 240 - 8.37 ± 0.04, 241 - 0.571 ± 0.005, 242 - 0.049 ± 0.001,

*Pm & U from
same material
- White feed*

Uncertainties are of the 95% confidence level.

BATTELLE B NORTHWEST
BATTELLE MEMORIAL INSTITUTE

DISTRIBUTION OF COPIES

DATE July 8, 1970.

TO Sidney Bierman

FROM H. W. Gobain *MWG*

SUBJECT ISOTOPIC DETERMINATION OF URANIUM

<u>H.S. #</u>	<u>Lab #</u>	<u>Cust. I.D.</u>	<u>Wt %</u>	<u>T = 0.0153</u>
1170142	P-1584	PuO ₂ UO ₂ Dyline	238 = 99.85 ± 0.003, 236 = 0.0039 ± 0.0003, 235 = 0.151 ± 0.003, 234 < 0.001	238 = 99.85 ± 0.003, 236 = 0.0039 ± 0.0003, 235 = 0.151 ± 0.003, 234 < 0.001
				238 = 99.85 ± 0.003, 236 = 0.0039 ± 0.0003, 235 = 0.151 ± 0.003, 234 < 0.001
				238 = 99.85 ± 0.003, 236 = 0.0039 ± 0.0003, 235 = 0.151 ± 0.003, 234 < 0.001
				238 = 99.85 ± 0.003, 236 = 0.0039 ± 0.0003, 235 = 0.151 ± 0.003, 234 < 0.001

1.96%
Uncertainties are the 95% confidence level.

BATTELLE IN NORTHWEST

DATE November 17, 1969
TO V. C. Assmund/S. R. Bierman
FROM M. H. Goheen

1677 expt.

HA Treibs
File

Isotopic Analysis of Uranium and Plutonium - COMPOSITE SAMPLE
OF SD H/X Pd₂-W₂-S₃
BLOCKS AT 30/70. PROJECT

Plutonium

<u>M.S.#</u>	<u>Chem #</u>	<u>Customer I.D.</u>	<u>Weight %</u>	<u>T</u>
1269245	3325	231-Z/209 E	229 = 91.38 ±0.04	±.02
		B-43377	-240 = 8.00 ±0.04	±.02
		Poly-UHM	241 = 0.592 ±0.0015	±.03
		Polystyrene	242 = 0.0360 ±0.0009	0.0045

Uncertainties are the 95% confidence level. $1.96\sigma_{x-y}$

Uranium

Beth 325-.

<u>M S #</u>	<u>Chem #</u>	<u>Customer I. D.</u>	<u>Weight g</u>
1169274	3325	231 Z/209 E	233 = 99.844 ±0.002 ± 0.0010
		S-43317	235 = 0.0042 ±0.0004 ± 0.0002
		PoO ₂ VO ₂	235 = 0.151 ±0.002 ± 0.0010
		Polystyrene	234 = >0.001

Uncertainties are the 95% confidence level.

(1) SEE 30 1/2% FUEL, PAGE 34, FOR 24.1 AM
(2) SEE 30 1/2% FUEL PAGE 33, FOR REPRODUCTION
OF ABOVE NUMBER. ~~THE~~ MATERIAL USED IN 50+30
1/2% FUEL COMES FROM SAME ~~SOURCE~~

ME-2100

SIEB-

APPENDIX C

CONCRETE COMPOSITION IN CELL WALLS OF BUILDING 3019

APPENDIX C

CONCRETE COMPOSITION IN CELL WALLS OF BUILDING 3019

Four samples were sent for analyses. Sample number P25 pit wall was sent as a standard and does not reflect the composition of 3019 cell walls. Data from the three RM samples were averaged to determine cell wall atom densities. Figure C.1 is the report of the concrete analyses as supplied by Galbraith Laboratories.

Figure C.2 shows the FORTRAN program used to calculate atom densities. Figures C.3 and C.4 show the program input and output, respectively. Note that all percentages were confirmed by Galbraith Laboratories to be wt % and that the unreported constituent of the concrete samples was confirmed by A. M. Krichinsky, ORNL Chemical Technology Division, to be oxygen. Note that atom densities are in units of atoms/(bn · cm).

From the data shown in Fig. C.1, it is apparent that sample 4 differs from the other RM samples. Inspection revealed that the Si content of the third RM sample is much lower than that of the first two samples. Galbraith Laboratories was asked to reevaluate Sample 4 and provide an update to A. M. Krichinsky. Sample 4 was reanalyzed twice, and the silicon content was reported to be 37.48 and 36.27 wt % respectively (average = 36.875). This average value was used along with the other weight percentages reported in Fig. C.1 to calculate atom densities shown in Fig. C.4.

Sensitivity studies showed that maximum reactivity was obtained with minimum water content. Because only an upper limit was provided for hydrogen, a second set of atom densities was generated with the hydrogen contents of all three samples set to zero. For the no hydrogen case, the atom density of oxygen increases from that shown in Fig. C.4 to 2.78196×10^{-2} .

The bulk density measurement was performed using gravimetric techniques and has a reported accuracy of 0.001 g/ml (1σ value). The weight fractions were determined using an inductively coupled plasma analysis technique which has a 2σ uncertainty of 5% of the analyzed value for higher weight percentage measurements (> a few weight percent) and 10% of the analyzed value for lower weight percentage measurements. Note that sampling differences usually exceed these uncertainties.

CALBRAITH
Laboratories, Inc.

QUANTITATIVE MICROANALYSES
ORGANIC - INORGANIC
 PHONE 615/546-1335 FAX 615/546-7209

HARRY W. CALBRAITH, Ph.D.
 CHAIRMAN OF THE BOARD
 KENNETH S. WOODS
 PRESIDENT
 VELMA M. RUSSELL
 SECRETARY/TREASURER
 DAVID J. STROM
 SENIOR VICE-PRESIDENT
 GAIL R. HUTCHENS
 EXECUTIVE VICE-PRESIDENT
 WILLIAM M. LONGMIRE
 VICE-PRESIDENT
 TECHNICAL SERVICES

Ms. Marion Ferguson
 Oak Ridge National Lab 4500S
 Post Office Box 2008
 Oak Ridge, Tennessee 37831-6131

June 8, 1992

Received: June 1st
 PO#: 36XG184

Dear Ms. Ferguson:

Analysis of your compound gave the following results:

Your #,	Our #,	Analyses,	
RM25 East Wall	W-3376	# Carbon	<0.5
		# Hydrogen	<0.5
		# Sulfur	0.10
		# Sodium	0.21
		# Magnesium	0.31
		# Aluminum	2.33
		# Silicon	39.24
		# Potassium	1.18
		# Calcium	7.19
		# Iron	1.29
		# Zinc	<0.077
		Bulk Density, g/ml	1.492
		Pounds/Cu. Ft.	93.15
P25 Pitch Wall	W-3377	# Carbon	<0.5
Small side CGU side rock		# Hydrogen	<0.5
		# Sulfur	10.08
		# Sodium	0.011
		# Magnesium	0.12
		# Aluminum	0.32
		# Silicon	4.45
		# Potassium	<0.054
		# Calcium	3.71
		# Iron	0.70
		# Zinc	<0.06
		Bulk Density, g/ml	2.270
		Pounds/Cu. Ft.	141.72

Fig. C.1. Analyses of concrete walls in Building 3019.

Mr. Marion Ferguson
Page 2
June 8, 1992

Your #,	Our #,	Analyses,	
<u>RM160 W Wall</u>	W-3378	# Carbon	<0.5
		# Hydrogen	<0.5
		# Sulfur	0.10
		# Sodium	0.27
		# Magnesium	0.34
		# Aluminum	2.37
		# Silicon	38.46
		# Potassium	0.90
		# Calcium	7.65
		# Iron	1.70
		# Zinc	<0.074
		Bulk Density, g/ml	1.515
		Pounds/Cu. Ft.	94.58
<u>RM150 N Wall</u>	W-3379	# Carbon	<0.5
		# Hydrogen	<0.5
		# Sulfur	0.066
		# Sodium	0.24
		# Magnesium	0.29
		# Aluminum	2.09
		# Silicon	32.02
		# Potassium	0.69
		# Calcium	7.69
		# Iron	1.20
		# Zinc	<0.05
		Bulk Density, g/ml	1.562
		Pounds/Cu. Ft.	97.52

Sincerely yours,

GALBRAITH LABORATORIES, INC.

Gail R. Hutchens
Gail R. Hutchens
Exec. Vice-President

GRH:sla

Fig. C.1 (continued).

```

dimension znum(3,13),ave(12),atw(12)
character*2 name(12)
data (atw(i),i=1,12)/12.0,1.0079,32.06,22.98977,24.305,26.98154,
     28.0855,39.0983,40.08,55.847,65.38,15.9994/
data (name(i),i=1,12)/*C ','H ','S ','Na','Mg','Al','Si','K ',
     'Ca','Fe','Zn','O */
open(5,file='concrete',status='unknown')
open(6,file='answer',status='unknown')
rewind 6
read(5,*)((znum(i,j),j=1,12),i=1,3)
do i=1,3
    znum(i,13)=znum(i,12)
    sum=0.0
    do j=1,11
        sum=sum+znum(i,j)
    enddo
    write(6,101)i,sum
    znum(i,12)=100-sum
    enddo
do i=1,3
    do j=1,12
        znum(i,j)=znum(i,j)*znum(i,13)/100.0
    enddo
enddo
do i=1,12
    ave(i)=0.0
    do j=1,3
        ave(i)=ave(i)+znum(j,i)
    enddo
    ave(i)=ave(i)/3.0
    enddo
    write(6,102)
    write(6,100)(name(i),ave(i),i=1,12)
do i=1,12
    ave(i)=ave(i)*.602214/atw(i)
    enddo
    write(6,103)
    write(6,100)(name(i),ave(i),i=1,12)
100  format(10x,a2,5x,1p,e11.5)
101  format(' For sample # ',i2,' sum of percentages is ',f6.3)
102  format(//12x,' Grams/cc')
103  format(//12x,'atom density')
stop
end

```

Fig. C.2. FORTRAN program to calculate atom densities for constituents of concrete.

```

0.5 0.5 0.1 0.21 0.31 2.33 39.24 1.18 7.19 1.29 0.077 1.492
0.5 0.5 0.10 0.27 0.34 2.37 38.46 0.90 7.65 1.70 0.074 1.515
0.5 0.5 0.066 0.24 0.29 2.09 36.875 0.69 7.69 1.20 0.05 1.562

```

Fig. C.3. Input to FORTRAN program to calculate concrete atom densities.

```

For RM sample # 1 sum of percentages is 52.927
For RM sample # 2 sum of percentages is 52.864
For RM sample # 3 sum of percentages is 50.191

```

	Grams/cc
C	7.61500E-03
H	7.61500E-03
S	1.34597E-03
Na	3.65750E-03
Mg	4.76867E-03
Al	3.44383E-02
Si	5.81372E-01
K	1.40061E-02
Ca	1.14430E-01
Fe	2.12486E-02
Zn	1.01698E-03
O	7.31485E-01

	atom density (atoms/(barn*cm))
C	3.82155E-04
H	4.54991E-03
S	2.52827E-05
Na	9.58077E-05
Mg	1.18155E-04
Al	7.68645E-04
Si	1.24659E-02
K	2.15730E-04
Ca	1.71935E-03
Fe	2.29130E-04
Zn	9.36739E-06
O	2.75330E-02

Fig. C.4. Output from FORTRAN program to calculate concrete atom densities.

APPENDIX D

ASSUMPTIONS FOR SPECIFYING WATER CONTENT FOR MIXED OXIDE WASTE

Internal Correspondence

MARTIN MARIETTA ENERGY SYSTEMS, INC.

September 25, 1992

R.T. Primm, III

Assumptions for specifying Water Content for NFS MOX Waste

The following assumptions for water content in NFS MOX waste are appropriate for use in nuclear criticality safety evaluations for the indicated reasons:

1. Initial water content of material is less than 1%. MOX waste will be subjected to heat treatment for the specific purpose of driving off moisture and volatile components. These treatments include heating to 600+/-25 deg C for 4 hours with cooldown and packaging in an inert atmosphere. The waste acceptance criteria for this material is actually <0.2%; however, the more conservative value (<1%) may be assumed for these evaluations.
2. Water ingress into the primary container will be prevented during handling. Packaging will be performed within an inert atmosphere into a stainless steel container with a bolted, flanged closure. Bolts will be secured in a specified sequence and to a specified torque (8 ft-lbs) to ensure closure consistent with a 150 psig hydro-test procedure.
3. Water ingress into the primary container will be prevented during storage. Closed primary containers will be encased into a welded-shut overpack capsule prior to storage. Welding procedures and welders will be qualified and certified for use on this package. Welded closures will be visually inspected and subjected to dye penetrant testing to provide a quality control check of the welds.

Please call me if any additional information is needed on these assumptions.



Alan M. Krichinsky, 3019, MS-6046 (4-6940) - RC

AMK:dsc

cc: B.D. Patton
C.E. Pepper
B.W. Starnes

APPENDIX E
INTERPRETATIONS OF 1985 RESULTS

APPENDIX E

INTERPRETATIONS OF 1985 RESULTS

Hopper has noted that the selected subcritical value of k-effective < or = 0.93 has little relevance to "margins of safety" without an understanding of the changes in k-effective with respect to changes in operational conditions. Consequently, a model was developed to relate operational values (material density, degree of moderation, geometry, etc.) to system reactivity. Thus operational parameters were related directly to safety limits.

Though the calculations reported in Table 5 are nonconservative, these analyses of them are presented as a model for future derivations. To interpret and interpolate from the computational results of Sect. 4, an algorithm was used to relate fissile material density and cylinder radius to array reactivity for the considered materials. The behavior of the algorithm in predicting array reactivity was examined.

The following sections provide the development of the algorithm and interpolation of calculated results relevant to operational limits and variations for the storage wells.

E.1 REACTIVITY AND PHYSICAL PARAMETERS OF THE WASTE MATERIAL

It has been demonstrated (Refs. 1 and 2) that array reactivity can be related to array unit mass/reactivity for uniform arrays of fissile material even with the presence of interunit moderating and absorbing materials. That is to say, the array and unit reactivities are proportional to the unit mass (i.e., $k_{\text{eff}} \propto (\text{Unit Mass})^{1/3}$). For near-infinite-length cylindrical units of variable density and geometry, the mass per unit length or reactivity can be expressed as a relation with density:

$$\text{Array } k_{\text{eff}} = (A1) * (\text{Material Density})^{1/3} + B1,$$

or to geometry,

$$\text{Array } k_{\text{eff}} = (A2) * (\text{Material Radius})^{2/3} + B2,$$

where A and B are constants of proportionality. Where both the material density and geometry vary, the array reactivity may be expressed as

$$\begin{aligned} k_{\text{eff}} = & (A3) * [(\text{Material Density})^{1/3}] \\ & + (B3) * [(\text{Material Density})^{1/3}] * [(\text{Material Radius})^{2/3}] \\ & + (C3) * [(\text{Material Radius})^{2/3}], \end{aligned}$$

where A3, B3, and C3 are combined constants of proportionality.

This last relationship was used to interpret intermediate KENO V.a search results to interpolate variable loading conditions (material densities and radii) having equivalent array reactivities. A multiple linear regression fit of this relationship to the results of Table 5 reproduces the KENO calculated results between k-effs of 0.88 and 1.02 with a standard deviation of about 1% for the range of variables considered. Figure 5 is a scatter graph of the deviation between k-effs predicted by the above relationship and about 300 KENO calculated k-effs between the values of 0.88 and 1.02. Note that the values which fall above and below the two standard deviation values are not unique to a specific material or storage configuration.

Combined constants of proportionality (multiple linear regression coefficients) for the considered materials are presented in Table D.1 for Intercell 2 and 3.

Table E.1. Fitted constants of proportionality for ^{239}Pu in Intercell 2 and 3

Material form	H/X atom ratio	Coefficients		
		A3	B3	C3
Metal	0	-0.10970477	0.32883389	-0.17464236
Oxides	1	-0.14458998	0.36506649	-0.19289005
	3	-0.22096846	0.41614497	-0.18779307
	10	-0.26247951	0.49957564	-0.18691215
	20	-0.18640133	0.59263783	-0.24259676

E.2 INTERPOLATIONS OF SUBCRITICAL FISSILE MATERIAL MASS LOADINGS

The relationship in Sect. D.1, with the associated coefficients, predicts the calculated values with a standard deviation of about 1% in k-eff for the range of intended application (i.e., k-effs between 0.90 and 0.96). It is judged from Appendix A that a calculated k-eff plus 2 standard deviations which is less than 0.93 may be considered subcritical for the materials evaluated.

Figure 5 is a graph that was generated using the algorithm presented in Sect. D.1 such that the plotted loadings would have a predicted k-eff of 0.93. It depicts fissile material linear mass loadings vs fissile isotope density. Note that all the limiting values presented in Fig. 6 are significantly less than the single unit subcritical values provided in Table 6. If one ignores the cell wall concrete composition, then the predicted "safe" linear Pu density at 0.2 wt % water (H/Pu ratio of 0.05) — corresponding to NFS waste is 10 kg Pu/ft. Furthermore, if one assumes, as recommended in Sect. 5, that U-238 be treated as ^{239}Pu , then the limit is 2 kg Pu/ft. This is approximately 4 times larger than the expected value of 0.48 kg Pu/ft, allowing a sufficient margin for the more reactive, Appendix C concrete composition.

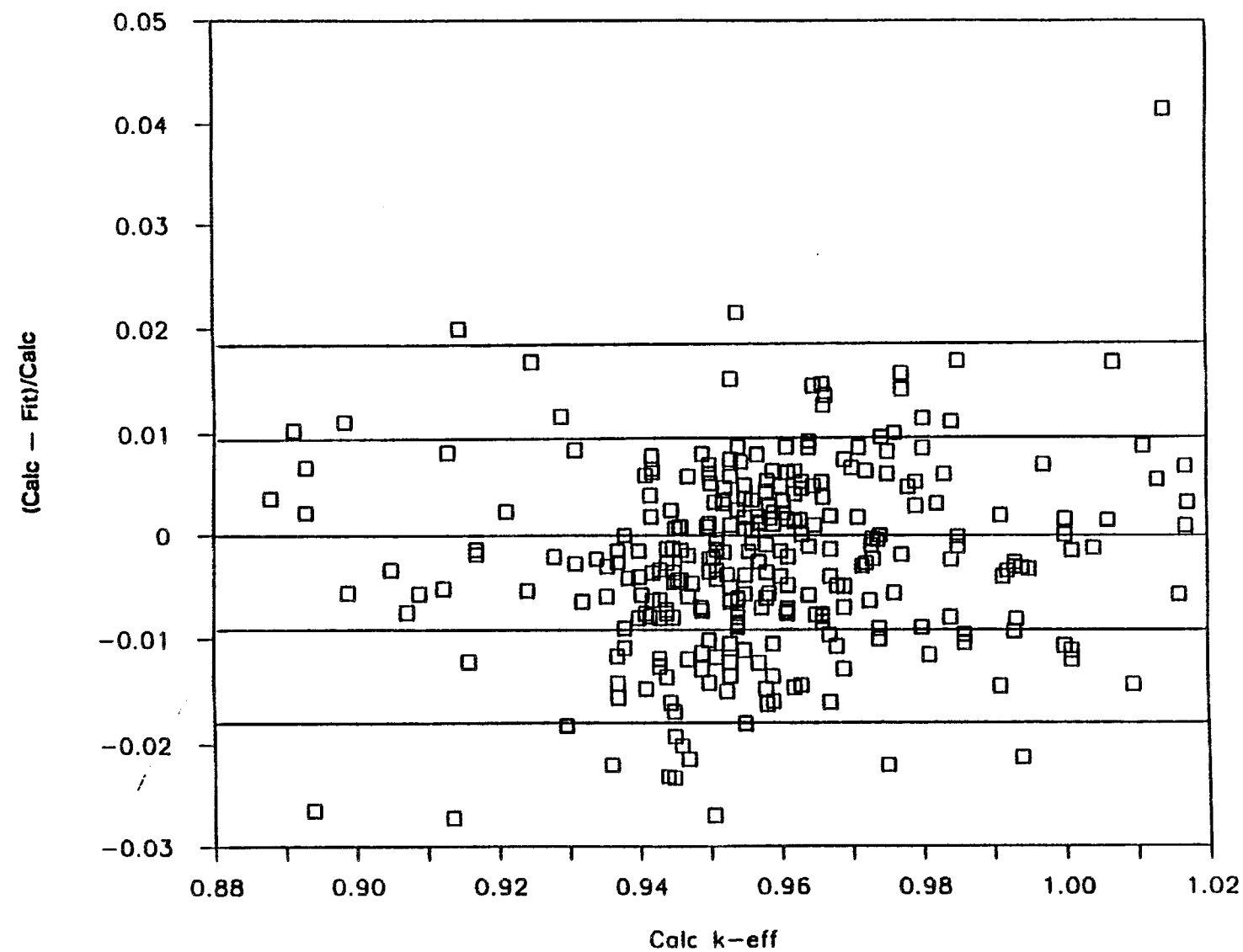


Fig. E.1. Deviation of fit value from calculated k_{eff} .

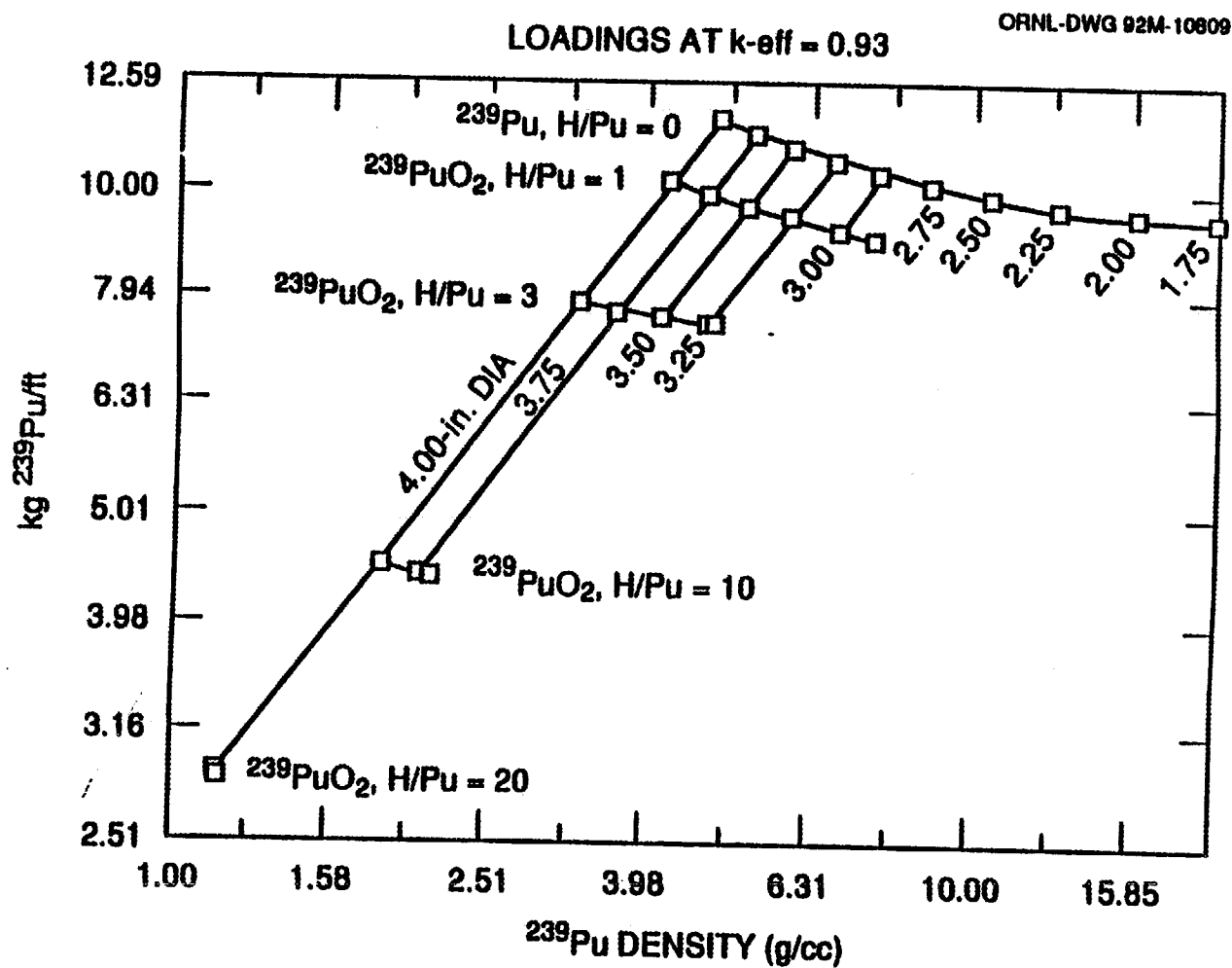


Fig. E.2. Intercell 2 and 3 ^{239}Pu storage well loadings.

REFERENCES FOR APPENDIX E

1. J. T. Thomas, "Review of Criteria for Nuclear Criticality Safety Control in Transportation," in Proceedings of the Fifth International Symposium on Packaging and Transportation of Radioactive Materials, Las Vegas, Nevada, May 7-12, 1978.
2. J. T. Thomas, "Generic Array Criticality," Y-CDC-13, Union Carbide Corporation-Nuclear Division, Y-12 Plant, Oak Ridge, TN, August 1, 1973.

APPENDIX F

SCALE INPUT FOR "NORMAL" OPERATION OF NFS WASTE STORAGE IN INTERCELL 2 AND 3 WELLS

```

#csas25
Intercell storage 2 & 3; 7/27/92, 260 gr Pu/can, Full C, 0.2 wt % h2o
hansen-roach
multiregion
am-241 1 0.0 1.0e-30 end
puo2 1 1.81221e-2 end
uo2 1 7.58154e-2 end
h 1 0.0 1.39372e-4 end
c 1 1.0 end
o 1 0.0 6.96158e-4 end
carbonsteel 2 1.0 end
pb 3 1.0 end
pb 4 0.7405 end
c 5 0.0 3.82155E-04 end
h 5 0.0 4.54991E-03 end
s 5 0.0 2.52827E-05 end
na 5 0.0 9.58077E-05 end
mg 5 0.0 1.18155E-04 end
al 5 0.0 7.68645E-04 end
si 5 0.0 1.19239E-02 end
k 5 0.0 2.15730E-04 end
ca 5 0.0 1.71935E-03 end
fe 5 0.0 2.29130E-04 end
zn 5 0.0 9.36739E-06 end
o 5 0.0 2.84844E-02 end
n 6 0.0 1.98881e-5 end
o 6 0.0 5.33497e-6 end
end comp
buckledcyl vacuum reflected 0.0 457.2 end
1 5.08 oneextermod 2 5.68 oneextermod 3 8.22 twoextermod 4 10.13 twoextermod
5 56.356 noextermod 6 58.0 noextermod
end zone
Intercell storage 2 & 3; 7/27/92, 260 gr Pu/can, Full C, 0.2 wt % h2o
read para gen=303 tme=60 flx=yes fdn=yes pki=yes nub=yes end para
read geom
box type 1
cylinder 1 1 5.08 457.2 0.0
cylinder 2 1 5.68 457.2 0.0
cylinder 3 1 8.22 457.2 0.0
cylinder 4 1 10.13 457.2 0.0
cuboid 5 1 19.8438 -19.8438 11.43 -11.43 457.2 0.0
box type 2
cuboid 5 1 19.8438 -19.8438 11.43 -11.43 457.2 0.0
box type 3
cylinder 6 1 7.62 10.0 0.0
cylinder 3 1 7.62 25.0 0.0
cylinder 5 1 9.525 25.0 0.0
cuboid 5 1 19.8438 -19.8438 11.43 -11.43 25.0 0.0
box type 4
cuboid 5 1 19.8438 -19.8438 11.43 -11.43 25.0 0.0
corebdy 0 1 0.0 0.0 0.0
reflector 5 -1 36.5124 36.5124 495.3 495.3 0.0 737.0 1
end geom
read array
nux=2 nuy=9 nuz=2
loop
1 1 1 1 1 9 2 1 1 1
1 2 2 1 2 8 2 1 1 1
3 1 1 1 1 9 2 2 2 1
3 2 2 1 2 8 2 2 2 1
2 1 1 1 2 8 2 1 1 1
2 2 2 1 1 9 2 1 1 1
4 1 1 1 2 8 2 2 2 1
4 2 2 1 1 9 2 2 2 1
end loop
end array
read bias id=301 2 2 end bias
end data
end

```

INTERNAL DISTRIBUTION

- | | |
|-------------------------|---------------------------------|
| 1. H. L Adair | 26. W. H. Pechin |
| 2. J. E. Bigelow | 27-28. C. E. Pepper |
| 3. S. D. Clinton | 29. L. M. Petrie |
| 4. E. C. Crume, Jr. | 30-34. R. T. Primm, III |
| 5-6. H. L. Dodds | 35-39. G. R. Smolen |
| 7. H. R. Dyer | 40. S. G. Snow |
| 8. P. B. Fox | 41. B. W. Starnes |
| 9. R. K. Genung | 42. D. W. Turner |
| 10-14. C. H. Hopper | 43. J. C. Turner |
| 15. D. T. Ingersoll | 44. R. C. Ward |
| 16. W. C. Jordan | 45. R. M. Westfall |
| 17. G. Q. Kirk | 46. G. E. Whitesides |
| 18-19. A. M. Krichinsky | 47-51. B. A. Worley |
| 20. N. F. Landers | 52. EPMD Reports Office |
| 21. R. D. Lawson | 53-54. Laboratory Records Dept. |
| 22. K. H. Lin | 55. Laboratory Records, ORNL-RC |
| 23. P. E. Mueller | 56. Document Reference Section |
| 24. C. V. Parks | 57. Central Research Library |
| 25. B. D. Patton | 58. ORNL Patent Section |

EXTERNAL DISTRIBUTION

- 59-60. Office of Scientific and Technical Information, P.O. Box 62, Oak Ridge, TN 37831.
61. Office of Assistant Manager for Energy Research and Development, Department of Energy-Oak Ridge Field Office, P.O. Box 2008, Oak Ridge, TN 37831.
62. Professor Roger W. Brockett, Harvard University, Pierce Hall, 29 Oxford Street, Cambridge, MA 02138.
63. Dr. James E. Leiss, Rt. 2, Box 142C, Broadway, VA 22815.
64. Professor Neville Moray, Dept. of Mechanical and Industrial Engineering, University of Illinois, 1206 West Green Street, Urbana, IL 61801.
65. Professor Mary F. Wheeler, Department of Mathematics, Rice University, P.O. Box 1892, Houston, TX 77251.

Information from Floppy Disk

```

#csas25
EXPT 1453-01; CSAS25; 2/7/92; Hansen-Roach CROSS SECTIONS
hansen-roach
multiregion
am-241 1 0.0 1.019e-5 end
pu-238 1 0.0 1.833e-6 end
pu-239 1 0.0 2.203e-3 end
pu-240 1 0.0 2.931e-4 end
pu-241 1 0.0 4.934e-5 end
pu-242 1 0.0 5.636e-6 end
u-235 1 0.0 9.401e-6 end
u-238 1 0.0 6.172e-3 end
o 1 0.0 1.869e-2 end
c 1 0.0 2.666e-2 end
h 1 0.0 2.417e-2 end
h 2 0.0 4.489e-2 end
c 2 0.0 3.111e-2 end
cl 2 0.0 7.240e-3 end
n 3 0.0 1.98881e-5 end
o 3 0.0 5.33497e-6 end
c 4 0.0 3.1691e-4 end
crss 4 0.0 1.6471e-2 end
mn 4 0.0 1.7321e-3 end
fess 4 0.0 6.036e-2 end
niss 4 0.0 6.4834e-3 end
si 4 0.0 1.694e-4 end
end comp
buckledslab vacuum reflected 0.0 51.80 51.80 end
1 22.6644 noextermod
end zone
EXPT 1453-01; CSAS25/KENO-Va; 2/7/92
read para
gen=303 tme=60 flx=yes fdn=yes pki=yes nub=yes
end para
read geom
box type 1
cuboid 1 1 5.09 0.0 5.09 0.0 5.083 0.0
cuboid 2 1 5.102 -0.012 5.102 -0.012 5.1265 -0.0435
cuboid 3 1 5.104 -0.014 5.104 -0.014 5.1285 -0.0455
box type 2
cuboid 1 1 5.090 0.0 5.090 0.0 .448528e+01 0.0
cuboid 2 1 5.102 -0.012 5.102 -0.012 .448728e+01 -0.0435
cuboid 3 1 5.104 -0.014 5.104 -0.014 .449928e+01 -0.0455
corebdy 0 1 0.0 0.0 0.0
cuboid 4 1 51.180 0.0 51.180 0.0 45.93678 -0.15875
end geom
read array
nux=10 nuy=10 nuz=9
loop
1 1 10 1 1 10 1 1 8 1
2 1 10 1 1 10 1 9 9 1
end loop
end array
end data
end

```

```

#csas25
EXPT 1453-02; CSAS25; 2/6/92; Hansen-Roach CROSS SECTIONS
hansen-roach
multiregion
am-241 1 0.0 1.019e-5 end
pu-238 1 0.0 1.833e-6 end
pu-239 1 0.0 2.203e-3 end
pu-240 1 0.0 2.931e-4 end
pu-241 1 0.0 4.934e-5 end
pu-242 1 0.0 5.636e-6 end
u-235 1 0.0 9.401e-6 end
u-238 1 0.0 6.172e-3 end
o 1 0.0 1.869e-2 end
c 1 0.0 2.666e-2 end
h 1 0.0 2.417e-2 end
h 2 0.0 4.489e-2 end
c 2 0.0 3.111e-2 end
cl 2 0.0 7.240e-3 end
n 3 0.0 1.98881e-5 end
o 3 0.0 5.33497e-6 end
c 4 0.0 3.1691e-4 end
crss 4 0.0 1.6471e-2 end
mn 4 0.0 1.7321e-3 end
fess 4 0.0 6.036e-2 end
niss 4 0.0 6.4834e-3 end
si 4 0.0 1.694e-4 end
end comp
buckledslab vacuum reflected 0.0 51.00 55.10 end
1 21.0426 noextermod
end zone
EXPT 1453-02; CSAS25/KENO-Va; 2/6/92
read para
gen=303 tme=60 flx=yes fdn=yes pkis=yes nub=yes
end para
read geom
box type 1
cuboid 1 1 5.09 0.0 5.09 0.0 5.083 0.0
cuboid 2 1 5.102 -0.012 5.102 -0.012 5.1265 -0.0435
cuboid 3 1 5.104 -0.014 5.104 -0.014 5.1285 -0.0455
box type 2
cuboid 1 1 5.090 0.0 5.090 0.0 .128092e+01 0.0
cuboid 2 1 5.102 -0.012 5.102 -0.012 .132442e+01 -0.0435
cuboid 3 1 5.104 -0.014 5.104 -0.014 .132642e+01 -0.0455
corebdy 0 1 0.0 0.0 0.0
cuboid 4 2 51.180 0.0 56.298 0.0 42.764 -0.15875
end geom
read array
nux=10 nuy=11 nuz=9
loop
1 1 10 1 1 11 1 1 8 1
2 1 10 1 1 11 1 9 9 1
end loop
end array
read bias
id=400 2 2 end bias
end data
end

```

```

#csas25
EXPT 1453-03; CSAS25; 2/7/92; Hansen-Roach CROSS SECTIONS
hansen-roach
multiregion
am-241 1 0.0 1.019e-5 end
pu-238 1 0.0 1.833e-6 end
pu-239 1 0.0 2.203e-3 end
pu-240 1 0.0 2.931e-4 end
pu-241 1 0.0 4.934e-5 end
pu-242 1 0.0 5.636e-6 end
u-235 1 0.0 9.401e-6 end
u-238 1 0.0 6.172e-3 end
o 1 0.0 1.869e-2 end
c 1 0.0 2.666e-2 end
h 1 0.0 2.417e-2 end
h 2 0.0 4.489e-2 end
c 2 0.0 3.111e-2 end
cl 2 0.0 7.240e-3 end
n 3 0.0 1.98881e-5 end
o 3 0.0 5.33497e-6 end
h 4 0.0 0.05666 end
c 4 0.0 0.03510 end
o 4 0.0 0.01428 end
end comp
buckledslab vacuum reflected 0.0 35.70 35.70 end
1 18.003 oneextermod
2 33.003 noextermod
end zone
EXPT 1453-03; CSAS25/KENO-Va; 2/7/92
read para
gen=303 tme=60 flx=yes fdn=yes pki=yes nub=yes
end para
read geom
box type 1
cuboid 1 1 5.09 0.0 5.083 0.0 5.09 0.0
cuboid 2 1 5.102 -0.012 5.1265 -0.0435 5.102 -0.012
cuboid 3 1 5.104 -0.014 5.1285 -0.0455 5.104 -0.014
box type 2
cuboid 1 1 5.090 0.0 5.083 0.0 .305400E+00 0.0
cuboid 2 1 5.102 -0.012 5.1265 -0.0435 .317400E+00 -0.012
cuboid 3 1 5.104 -0.014 5.1285 -0.0455 .319400E+00 -0.014
corebdy 0 1 0.0 0.0 0.0
cuboid 4 2 .510660E+02 -15.24 .514580E+02 -15.24 .513994E+02 -15.24
end geom
read array
nux=7 nuy=7 nuz=8
loop
1 1 7 1 1 7 1 1 7 1
2 1 7 1 1 7 1 8 8 1
end loop
end array
read bias
id=400 2 2 end bias
end data
end

```

```

#csas25
EXPT 1453-04; CSAS25; 2/7/92; Hansen-Roach CROSS SECTIONS
hansen-roach
multiregion
am-241 1 0.0 1.019e-5 end
pu-238 1 0.0 1.833e-6 end
pu-239 1 0.0 2.203e-3 end
pu-240 1 0.0 2.931e-4 end
pu-241 1 0.0 4.934e-5 end
pu-242 1 0.0 5.636e-6 end
u-235 1 0.0 9.401e-6 end
u-238 1 0.0 6.172e-3 end
o 1 0.0 1.869e-2 end
c 1 0.0 2.666e-2 end
h 1 0.0 2.417e-2 end
h 2 0.0 4.489e-2 end
c 2 0.0 3.111e-2 end
cl 2 0.0 7.240e-3 end
n 3 0.0 1.98881e-5 end
o 3 0.0 5.33497e-6 end
h 4 0.0 0.05666 end
c 4 0.0 0.03510 end
o 4 0.0 0.01428 end
end comp
buckledslab vacuum reflected 0.0 40.8 40.8 end
1 14.3182 oneextermod
2 29.3182 noextermod
end zone
EXPT 1453-04; CSAS25/KENO-Va; 3/26/92
read para
gen=303 tme=60 flx=yes fdn=yes pkis=yes nub=yes
end para
read geom
box type 1
cuboid 1 1 5.09 0.0 5.083 0.0 5.09 0.0
cuboid 2 1 5.102 -0.012 5.1265 -0.0435 5.102 -0.012
cuboid 3 1 5.104 -0.014 5.1285 -0.0455 5.104 -0.014
box type 2
cuboid 1 1 5.090 0.0 5.083 0.0 .313035E+01 0.0
cuboid 2 1 5.102 -0.012 5.1265 -0.0435 .314235E+01 -0.012
cuboid 3 1 5.104 -0.014 5.1285 -0.0455 .314435E+01 -0.014
corebdy 0 1 0.0 0.0 0.0
cuboid 4 2 56.072 -15.24 56.268 -15.24 43.6544 -15.24
end geom
read array
nux=8 nuy=8 nuz=6
loop
1 1 8 1 1 8 1 1 5 1
2 1 8 1 1 8 1 6 6 1
end loop
end array
read bias
id=400 2 2 end bias
end data
end

```

```

#csas25
EXPT 1453-05; CSAS25; 2/7/92; Hansen-Roach CROSS SECTIONS
hansen-roach
multiregion
am-241 1 0.0 1.019e-5 end
pu-238 1 0.0 1.833e-6 end
pu-239 1 0.0 2.203e-3 end
pu-240 1 0.0 2.931e-4 end
pu-241 1 0.0 4.934e-5 end
pu-242 1 0.0 5.636e-6 end
u-235 1 0.0 9.401e-6 end
u-238 1 0.0 6.172e-3 end
o 1 0.0 1.869e-2 end
c 1 0.0 2.666e-2 end
h 1 0.0 2.417e-2 end
h 2 0.0 4.489e-2 end
c 2 0.0 3.111e-2 end
cl 2 0.0 7.240e-3 end
n 3 0.0 1.98881e-5 end
o 3 0.0 5.33497e-6 end
h 4 0.0 0.05666 end
c 4 0.0 0.03510 end
o 4 0.0 0.01428 end
end comp
buckledslab vacuum reflected 0.0 45.9 45.9 end
1 12.7424 oneextermod
2 27.7424 noextermod
end zone
EXPT 1453-05; CSAS25/KENO-Va; 2/7/92
read para
gen=303 tme=60 flx=yes fdn=yes pki=yes nub=yes
end para
read geom
box type 1
cuboid 1 1 5.09 0.0 5.083 0.0 5.09 0.0
cuboid 2 1 5.102 -0.012 5.1265 -0.0435 5.102 -0.012
cuboid 3 1 5.104 -0.014 5.1285 -0.0455 5.104 -0.014
box type 2
cuboid 1 1 5.090 0.0 5.083 0.0 .507473E+01 0.0
cuboid 2 1 5.102 -0.012 5.1265 -0.0435 .508673E+01 -0.012
cuboid 3 1 5.104 -0.014 5.1285 -0.0455 .508873E+01 -0.014
corebdy 0 1 0.0 0.0 0.0
cuboid 4 2 .613020E+02 -15.24 .618060E+02 -15.24 .408147E+02 -15.24
end geom
read array
nux=9 nuy=9 nuz=5
loop
1 1 9 1 1 9 1 1 4 1
2 1 9 1 1 9 1 5 5 1
end loop
end array
read bias
id=400 2 2 end bias
end data
end

```

```

#csas25
EXPT 1453-06; CSAS25; 2/7/92; Hansen-Roach CROSS SECTIONS
hansen-roach
multiregion
am-241 1 0.0 1.019e-5 end
pu-238 1 0.0 1.833e-6 end
pu-239 1 0.0 2.203e-3 end
pu-240 1 0.0 2.931e-4 end
pu-241 1 0.0 4.934e-5 end
pu-242 1 0.0 5.636e-6 end
u-235 1 0.0 9.401e-6 end
u-238 1 0.0 6.172e-3 end
o 1 0.0 1.869e-2 end
c 1 0.0 2.666e-2 end
h 1 0.0 2.417e-2 end
h 2 0.0 4.489e-2 end
c 2 0.0 3.111e-2 end
cl 2 0.0 7.240e-3 end
n 3 0.0 1.98881e-5 end
o 3 0.0 5.33497e-6 end
h 4 0.0 0.05666 end
c 4 0.0 0.03510 end
o 4 0.0 0.01428 end
end comp
buckledslab vacuum reflected 0.0 51.18 51.74 end
1 11.0542 oneextermod
2 26.0542 noextermod
end zone
EXPT 1453-06; CSAS25/KENO-Va; 2/7/92
read para
gen=303 tme=60 flx=yes fdn=yes pki=yes nub=yes
end para
read geom
box type 1
cuboid 1 1 5.09 0.0 5.083 0.0 5.09 0.0
cuboid 2 1 5.102 -0.012 5.1265 -0.0435 5.102 -0.012
cuboid 3 1 5.104 -0.014 5.1285 -0.0455 5.104 -0.014
box type 2
cuboid 1 1 5.090 0.0 5.083 0.0 .160844E+01 0.0
cuboid 2 1 5.102 -0.012 5.1265 -0.0435 .162044E+01 -0.012
cuboid 3 1 5.104 -0.014 5.1285 -0.0455 .162244E+01 -0.014
corebdy 0 1 0.0 0.0 0.0
cuboid 4 2 .664200E+02 -15.24 .669800E+02 -15.24 .373484E+02 -15.24
end geom
read array
nux=10 nuy=10 nuz=5
loop
1 1 10 1 1 10 1 1 4 1
2 1 10 1 1 10 1 5 5 1
end loop
end array
read bias
id=400 2 2 end bias
end data
end

```

```

#csas25
EXPT 1453-07; CSAS25; 2/7/92; Hansen-Roach CROSS SECTIONS
hansen-roach
multiregion
am-241 1 0.0 1.019e-5 end
pu-238 1 0.0 1.833e-6 end
pu-239 1 0.0 2.203e-3 end
pu-240 1 0.0 2.931e-4 end
pu-241 1 0.0 4.934e-5 end
pu-242 1 0.0 5.636e-6 end
u-235 1 0.0 9.401e-6 end
u-238 1 0.0 6.172e-3 end
o 1 0.0 1.869e-2 end
c 1 0.0 2.666e-2 end
h 1 0.0 2.417e-2 end
h 2 0.0 4.489e-2 end
c 2 0.0 3.111e-2 end
cl 2 0.0 7.240e-3 end
n 3 0.0 1.98881e-5 end
o 3 0.0 5.33497e-6 end
h 4 0.0 0.05666 end
c 4 0.0 0.03510 end
o 4 0.0 0.01428 end
end comp
buckledslab vacuum reflected 0.0 61.416 51.74 end
1 10.1036 oneextermod
2 25.1036 noextermod
end zone
EXPT 1453-07; CSAS25/KENO-Va; 2/7/92
read para
gen=303 tme=60 flx=yes fdn=yes pki=yes nub=yes
end para
read geom
box type 1
cuboid 1 1 5.09 0.0 5.083 0.0 5.09 0.0
cuboid 2 1 5.102 -0.012 5.1265 -0.0435 5.102 -0.012
cuboid 3 1 5.104 -0.014 5.1285 -0.0455 5.104 -0.014
box type 2
cuboid 1 1 5.090 0.0 5.083 0.0 .482532E+01 0.0
cuboid 2 1 5.102 -0.012 5.1265 -0.0435 .483732E+01 -0.012
cuboid 3 1 5.104 -0.014 5.1285 -0.0455 .483932E+01 -0.014
corebdy 0 1 0.0 0.0 0.0
cuboid 4 2 .766560E+02 -15.24 .669800E+02 -15.24 .354473E+02 -15.24
end geom
read array
nux=12 nuy=10 nuz=4
loop
1 1 12 1 1 10 1 1 3 1
2 1 12 1 1 10 1 4 4 1
end loop
end array
read bias
id=400 2 2 end bias
end data
end

```

```

#csas25
EXPT 1453-08; CSAS25; 2/8/92; Hansen-Roach CROSS SECTIONS
hansen-roach
multiregion
am-241 1 0.0 1.019e-5 end
pu-238 1 0.0 1.833e-6 end
pu-239 1 0.0 2.203e-3 end
pu-240 1 0.0 2.931e-4 end
pu-241 1 0.0 4.934e-5 end
pu-242 1 0.0 5.636e-6 end
u-235 1 0.0 9.401e-6 end
u-238 1 0.0 6.172e-3 end
o 1 0.0 1.869e-2 end
c 1 0.0 2.666e-2 end
h 1 0.0 2.417e-2 end
h 2 0.0 4.489e-2 end
c 2 0.0 3.111e-2 end
cl 2 0.0 7.240e-3 end
n 3 0.0 1.98881e-5 end
o 3 0.0 5.33497e-6 end
h 4 0.0 0.05666 end
c 4 0.0 0.03510 end
o 4 0.0 0.01428 end
end comp
buckledslab vacuum reflected 0.0 61.416 62.0880 end
1 9.39105 oneextermode
2 24.391 noextermode
end zone
EXPT 1453-08; CSAS25/KENO-Va; 2/8/92
read para
gen=303 tme=60 flx=yes fdn=yes pki=yes nub=yes
end para
read geom
box type 1
cuboid 1 1 5.09 0.0 5.083 0.0 5.09 0.0
cuboid 2 1 5.102 -0.012 5.1265 -0.0435 5.102 -0.012
cuboid 3 1 5.104 -0.014 5.1285 -0.0455 5.104 -0.014
box type 2
cuboid 1 1 5.090 0.0 5.083 0.0 .340012E+01 0.0
cuboid 2 1 5.102 -0.012 5.1265 -0.0435 .341212E+01 -0.012
cuboid 3 1 5.104 -0.014 5.1285 -0.0455 .341412E+01 -0.014
corebdy 0 1 0.0 0.0 0.0
cuboid 4 2 .766560E+02 -15.24 .773280E+02 -15.24 .340221E+02 -15.24
end geom
read array
nux=12 nuy=12 nuz=4
loop
1 1 12 1 1 12 1 1 3 1
2 1 12 1 1 12 1 4 4 1
end loop
end array
read bias
id=400 2 2 end bias
end data
end

```

```

#csas25
EXPT 1453-09; CSAS25; 2/8/92; Hansen-Roach CROSS SECTIONS
hansen-roach
multiregion
am-241 1 0.0 1.019e-5 end
pu-238 1 0.0 1.833e-6 end
pu-239 1 0.0 2.203e-3 end
pu-240 1 0.0 2.931e-4 end
pu-241 1 0.0 4.934e-5 end
pu-242 1 0.0 5.636e-6 end
u-235 1 0.0 9.401e-6 end
u-238 1 0.0 6.172e-3 end
o 1 0.0 1.869e-2 end
c 1 0.0 2.666e-2 end
h 1 0.0 2.417e-2 end
h 2 0.0 4.489e-2 end
c 2 0.0 3.111e-2 end
cl 2 0.0 7.240e-3 end
n 3 0.0 1.98881e-5 end
o 3 0.0 5.33497e-6 end
h 4 0.0 0.05666 end
c 4 0.0 0.03510 end
o 4 0.0 0.01428 end
end comp
buckledslab vacuum reflected 0.0 61.416 67.2620 end
1 9.162 oneextermod
2 24.162 noextermod
end zone
EXPT 1453-09; CSAS25/KENO-Va; 2/8/92
read para
gen=303 tme=60 flx=yes fdn=yes pki=yes nub=yes
end para
read geom
box type 1
cuboid 1 1 5.09 0.0 5.083 0.0 5.09 0.0
cuboid 2 1 5.102 -0.012 5.1265 -0.0435 5.102 -0.012
cuboid 3 1 5.104 -0.014 5.1285 -0.0455 5.104 -0.014
box type 2
cuboid 1 1 5.090 0.0 5.083 0.0 .294202E+01 0.0
cuboid 2 1 5.102 -0.012 5.1265 -0.0435 .295402E+01 -0.012
cuboid 3 1 5.104 -0.014 5.1285 -0.0455 .295602E+01 -0.014
corebdy 0 1 0.0 0.0 0.0
cuboid 4 2 .766560E+02 -15.24 .825020E+02 -15.24 .335640E+02 -15.24
end geom
read array
nux=12 nuy=13 nuz=4
loop
1 1 12 1 1 13 1 1 3 1
2 1 12 1 1 13 1 4 4 1
end loop
end array
read bias
id=400 2 2 end bias
end data
end

```

```

#csas25
EXPT 1453-10; CSAS25; 2/8/92; Hansen-Roach CROSS SECTIONS
hansen-roach
multiregion
am-241 1 0.0 1.019e-5 end
pu-238 1 0.0 1.833e-6 end
pu-239 1 0.0 2.203e-3 end
pu-240 1 0.0 2.931e-4 end
pu-241 1 0.0 4.934e-5 end
pu-242 1 0.0 5.636e-6 end
u-235 1 0.0 9.401e-6 end
u-238 1 0.0 6.172e-3 end
o 1 0.0 1.869e-2 end
c 1 0.0 2.666e-2 end
h 1 0.0 2.417e-2 end
h 2 0.0 4.489e-2 end
c 2 0.0 3.111e-2 end
cl 2 0.0 7.240e-3 end
n 3 0.0 1.98881e-5 end
o 3 0.0 5.33497e-6 end
h 4 0.0 0.05666 end
c 4 0.0 0.03510 end
o 4 0.0 0.01428 end
end comp
buckledslab vacuum reflected 0.0 71.652 67.2620 end
1 8.9304 oneextermod
2 23.9304 noextermod
end zone
EXPT 1453-10; CSAS25/KENO-Va; 2/8/92
read para
gen=303 tme=60 flx=yes fdn=yes pki=yes nub=yes
end para
read geom
box type 1
cuboid 1 1 5.09 0.0 5.083 0.0 5.09 0.0
cuboid 2 1 5.102 -0.012 5.1265 -0.0435 5.102 -0.012
cuboid 3 1 5.104 -0.014 5.1285 -0.0455 5.104 -0.014
box type 2
cuboid 1 1 5.090 0.0 5.083 0.0 .247883E+01 0.0
cuboid 2 1 5.102 -0.012 5.1265 -0.0435 .249083E+01 -0.012
cuboid 3 1 5.104 -0.014 5.1285 -0.0455 .249283E+01 -0.014
corebdy 0 1 0.0 0.0 0.0
cuboid 4 2 .868920E+02 -15.24 .825020E+02 -15.24 .331008E+02 -15.24
end geom
read array
nux=14 nuy=13 nuz=4
loop
1 1 14 1 1 13 1 1 3 1
2 1 14 1 1 13 1 4 4 1
end loop
end array
read bias
id=400 2 2 end bias
end data
end

```

```

#csas25
EXPT 1453-11; CSAS25; 2/11/92; Hansen-Roach CROSS SECTIONS
hansen-roach
multiregion
am-241 1 0.0 2.765E-5 end
pu-238 1 0.0 5.737E-7 end
pu-239 1 0.0 1.118E-3 end
pu-240 1 0.0 1.478E-4 end
pu-241 1 0.0 2.221E-5 end
pu-242 1 0.0 2.370E-6 end
u-235 1 0.0 1.365E-5 end
u-238 1 0.0 7.549E-3 end
o 1 0.0 1.840E-2 end
c 1 0.0 2.653E-2 end
h 1 0.0 2.534E-2 end
h 2 0.0 4.489e-2 end
c 2 0.0 3.111e-2 end
cl 2 0.0 7.240e-3 end
n 3 0.0 1.98881e-5 end
o 3 0.0 5.33497e-6 end
h 4 0.0 0.05666 end
c 4 0.0 0.03510 end
o 4 0.0 0.01428 end
end comp
buckledslab vacuum reflected 0.0 51.29 55.62742 end
1 25.645 oneextermod
2 40.6454 noextermod
end zone
EXPT 1453-11; CSAS25/KENO-Va; 2/11/92
read para
gen=303 tme=60 flx=yes fdn=yes pki=yes nub=yes
end para
read geom
box type 1
cuboid 1 1 5.09 0.0 5.090 0.0 5.082 0.0
cuboid 2 1 5.102 -0.012 5.1020 -0.012 5.126 -0.044
cuboid 3 1 5.1095 -0.0195 5.1095 -0.0195 5.1275 -0.0455
box type 2
cuboid 1 1 5.090 0.0 5.090 0.0 3.80642 0.0
cuboid 2 1 5.102 -0.012 5.102 -0.012 3.85042 -0.044
cuboid 3 1 5.1095 -0.0195 5.1095 -0.0195 3.85192 -0.0455
corebdy 0 1 0.0 0.0 0.0
cuboid 4 2 66.53 -15.24 66.53 -15.24 70.86742 -15.24
end geom
read array
nux=10 nuy=10 nuz=11
loop
1 1 10 1 1 10 1 1 10 1
2 1 10 1 1 10 1 11 11 1
end loop
end array
read bias
id=400 2 2 end bias
end data
end

```

```

#csas25
EXPT 1547-02; CSAS25; 2/10/92; Hansen-Roach CROSS SECTIONS
hansen-roach
multiregion
am-241 1 0.0 .147224e-04 end
pu-238 1 0.0 .2288e-05 end
pu-239 1 0.0 .2186e-02 end
pu-240 1 0.0 .2927e-03 end
pu-241 1 0.0 .541976e-04 end
pu-242 1 0.0 .6751e-05 end
u-235 1 0.0 .9269e-05 end
u-238 1 0.0 .6162e-02 end
o 1 0.0 .1864e-01 end
c 1 0.0 .2660e-01 end
h 1 0.0 .2432e-01 end
h 2 0.0 4.489e-2 end
c 2 0.0 3.110e-2 end
cl 2 0.0 7.240e-3 end
n 3 0.0 1.98881e-5 end
o 3 0.0 5.33497e-6 end
h 4 0.0 0.05712 end
c 4 0.0 0.03570 end
o 4 0.0 0.01428 end
cu 5 0.0 8.44384e-2 end
o 5 0.0 1.00651e-4 end
c 5 0.0 1.78929e-5 end
end comp
buckledslab vacuum reflected 0.0 46.0620 46.5660 end
1 14.1156 oneextermod
2 29.1156 noextermod
end zone
EXPT 1547-02; CSAS25/KENO-Va; 2/10/92
read para
gen=303 tme=60 flx=yes fdn=yes pki=yes nub=yes
end para
read geom
box type 1
cuboid 1 1 5.0900 0.0000 5.0830 0.0000 5.0900 0.0000
cuboid 2 1 5.1020 -0.0120 5.1265 -0.0435 5.1020 -0.0120
cuboid 3 1 5.1040 -0.0140 5.1285 -0.0455 5.1040 -0.0140
box type 2
cuboid 1 1 5.0900 0.0000 5.0830 0.0000 1.5932 0.0000
cuboid 2 1 5.1020 -0.0120 5.1265 -0.0435 1.6052 -0.0120
cuboid 3 1 5.1040 -0.0140 5.1285 -0.0455 1.6072 -0.0140
box type 3
cuboid 5 1 5.1040 -0.0140 5.1285 -0.0455 0.9740 0.0
cuboid 3 1 5.1040 -0.0140 5.1285 -0.0455 0.9970 -0.0230
corebdy 0 1 0.0 0.0 0.0
cuboid 4 2 0.61302E+2 -15.24 0.61806E+2 -15.24 0.434712E+02 -15.24
end geom
read array
nux=9 nuy=9 nuz=7
loop
1 1 9 1 1 9 1 1 3 1
3 1 9 1 1 9 1 4 4 1
1 1 9 1 1 9 1 5 6 1
2 1 9 1 1 9 1 7 7 1
end loop
end array
read bias
id=400 2 2 end bias

```

```
end data  
end
```

```

#csas25
EXPT 1547-03; CSAS25; 2/10/92; Hansen-Roach CROSS SECTIONS
hansen-roach
multiregion
am-241 1 0.0 .147224e-04 end
pu-238 1 0.0 .2288e-05 end
pu-239 1 0.0 .2186e-02 end
pu-240 1 0.0 .2927e-03 end
pu-241 1 0.0 .541976e-04 end
pu-242 1 0.0 .6751e-05 end
u-235 1 0.0 .9269e-05 end
u-238 1 0.0 .6162e-02 end
o 1 0.0 .1864e-01 end
c 1 0.0 .2660e-01 end
h 1 0.0 .2432e-01 end
h 2 0.0 4.489e-2 end
c 2 0.0 3.110e-2 end
cl 2 0.0 7.240e-3 end
n 3 0.0 1.98881e-5 end
o 3 0.0 5.33497e-6 end
h 4 0.0 0.05712 end
c 4 0.0 0.03570 end
o 4 0.0 0.01428 end
cu 5 0.0 8.44384e-2 end
o 5 0.0 1.00651e-4 end
c 5 0.0 1.78929e-5 end
end comp
buckledslab vacuum reflected 0.0 46.0620 46.5660 end
1 15.3686 oneextermod
2 30.3686 noextermod
end zone
EXPT 1547-03; CSAS25/KENO-Va; 2/10/92
read para
gen=303 tme=60 flix=yes fdn=yes pki=yes nub=yes
end para
read geom
box type 1
cuboid 1 1 5.0900 0.0000 5.0830 0.0000 5.0900 0.0000
cuboid 2 1 5.1020 -0.0120 5.1265 -0.0435 5.1020 -0.0120
cuboid 3 1 5.1040 -0.0140 5.1285 -0.0455 5.1040 -0.0140
box type 2
cuboid 1 1 5.0900 0.0000 5.0830 0.0000 3.0591 0.0000
cuboid 2 1 5.1020 -0.0120 5.1265 -0.0435 3.0711 -0.0120
cuboid 3 1 5.1040 -0.0140 5.1285 -0.0455 3.0731 -0.0140
box type 3
cuboid 5 1 5.1040 -0.0140 5.1285 -0.0455 1.9640 0.0
cuboid 3 1 5.1040 -0.0140 5.1285 -0.0455 2.0120 -0.0480
corebdy 0 1 0.0 0.0 0.0
cuboid 4 2 0.61302E+2 -15.24 0.61806E+2 -15.24 0.459771E+02 -15.24
end geom
read array
nux=9 nuy=9 nuz=7
loop
1 1 9 1 1 9 1 1 3 1
3 1 9 1 1 9 1 4 4 1
1 1 9 1 1 9 1 5 6 1
2 1 9 1 1 9 1 7 7 1
end loop
end array
read bias
id=400 2 2 end bias

```

```
end data  
end
```

```

#csas25
EXPT 1547-04; CSAS25; 2/10/92; Hansen-Roach CROSS SECTIONS
hansen-roach
multiregion
am-241 1 0.0 .147224e-04 end
pu-238 1 0.0 .2288e-05 end
pu-239 1 0.0 .2186e-02 end
pu-240 1 0.0 .2927e-03 end
pu-241 1 0.0 .541976e-04 end
pu-242 1 0.0 .6751e-05 end
u-235 1 0.0 .9269e-05 end
u-238 1 0.0 .6162e-02 end
o 1 0.0 .1864e-01 end
c 1 0.0 .2660e-01 end
h 1 0.0 .2432e-01 end
h 2 0.0 4.489e-2 end
c 2 0.0 3.110e-2 end
cl 2 0.0 7.240e-3 end
n 3 0.0 1.98881e-5 end
o 3 0.0 5.33497e-6 end
h 4 0.0 0.05712 end
c 4 0.0 0.03570 end
o 4 0.0 0.01428 end
cu 5 0.0 8.33333E-2 end
cd 5 0.0 4.71679E-4 end
sn 5 0.0 1.13027E-4 end
end comp
buckledslab vacuum reflected 0.0 46.0620 46.5660 end
1 13.4844 oneextermod
2 28.4844 noextermod
end zone
EXPT 1547-04; CSAS25/KENO-Va; 2/10/92
read para
gen=303 tme=60 flx=yes fdn=yes pki=yes nub=yes
end para
read geom
box type 1
cuboid 1 1 5.0900 0.0000 5.0830 0.0000 5.0900 0.0000
cuboid 2 1 5.1020 -0.0120 5.1265 -0.0435 5.1020 -0.0120
cuboid 3 1 5.1040 -0.0140 5.1285 -0.0455 5.1040 -0.0140
box type 2
cuboid 1 1 5.0900 0.0000 5.0830 0.0000 0.8908 0.0000
cuboid 2 1 5.1020 -0.0120 5.1265 -0.0435 0.9028 -0.0120
cuboid 3 1 5.1040 -0.0140 5.1285 -0.0455 0.9048 -0.0140
box type 3
cuboid 5 1 5.1040 -0.0140 5.1285 -0.0455 0.3860 0.0
cuboid 3 1 5.1040 -0.0140 5.1285 -0.0455 0.4230 -0.0370
corebdy 0 1 0.0 0.0 0.0
cuboid 4 2 0.61302E+2 -15.24 0.61806E+2 -15.24 0.422088E+02 -15.24
end geom
read array
nux=9 nuy=9 nuz=7
loop
 1 1 9 1 1 9 1 1 3 1
 3 1 9 1 1 9 1 4 4 1
 1 1 9 1 1 9 1 5 6 1
 2 1 9 1 1 9 1 7 7 1
end loop
end array
read bias
id=400 2 2 end bias

```

```
end data  
end
```

```

#csas25
EXPT 1547-05; CSAS25; 2/10/92; Hansen-Roach CROSS SECTIONS
hansen-roach
multiregion
am-241 1 0.0 .147224e-04 end
pu-238 1 0.0 .2288e-05 end
pu-239 1 0.0 .2186e-02 end
pu-240 1 0.0 .2927e-03 end
pu-241 1 0.0 .541976e-04 end
pu-242 1 0.0 .6751e-05 end
u-235 1 0.0 .9269e-05 end
u-238 1 0.0 .6162e-02 end
o 1 0.0 .1864e-01 end
c 1 0.0 .2660e-01 end
h 1 0.0 .2432e-01 end
h 2 0.0 4.489e-2 end
c 2 0.0 3.110e-2 end
cl 2 0.0 7.240e-3 end
n 3 0.0 1.98881e-5 end
o 3 0.0 5.33497e-6 end
h 4 0.0 0.05712 end
c 4 0.0 0.03570 end
o 4 0.0 0.01428 end
cu 5 0.0 8.33333E-2 end
cd 5 0.0 4.71679E-4 end
sn 5 0.0 1.13027E-4 end
end comp
buckledslab vacuum reflected 0.0 46.0620 46.5660 end
1 14.5010 oneextermod
2 29.5010 noextermod
end zone
EXPT 1547-05; CSAS25/KENO-Va; 2/10/92
read para
gen=303 tme=60 flx=yes fdn=yes pki=yes nub=yes
end para
read geom
box type 1
cuboid 1 1 5.0900 0.0000 5.0830 0.0000 5.0900 0.0000
cuboid 2 1 5.1020 -0.0120 5.1265 -0.0435 5.1020 -0.0120
cuboid 3 1 5.1040 -0.0140 5.1285 -0.0455 5.1040 -0.0140
box type 2
cuboid 1 1 5.0900 0.0000 5.0830 0.0000 2.2040 0.0000
cuboid 2 1 5.1020 -0.0120 5.1265 -0.0435 2.2160 -0.0120
cuboid 3 1 5.1040 -0.0140 5.1285 -0.0455 2.2180 -0.0140
box type 3
cuboid 5 1 5.1040 -0.0140 5.1285 -0.0455 1.0850 0.0
cuboid 3 1 5.1040 -0.0140 5.1285 -0.0455 1.1325 -0.0475
corebdy 0 1 0.0 0.0 0.0
cuboid 4 2 0.61302E+2 -15.24 0.61806E+2 -15.24 0.44242E+2 -15.24
end geom
read array
nux=9 nuy=9 nuz=7
loop
 1 1 9 1 1 9 1 1 3 1
 3 1 9 1 1 9 1 4 4 1
 1 1 9 1 1 9 1 5 6 1
 2 1 9 1 1 9 1 7 7 1
end loop
end array
read bias
id=400 2 2 end bias

```

```
end data  
end
```

```

#csas25
EXPT 1547-06; CSAS25; 2/10/92; Hansen-Roach CROSS SECTIONS
hansen-roach
multiregion
am-241 1 0.0 .147224e-04 end
pu-238 1 0.0 .2288e-05 end
pu-239 1 0.0 .2186e-02 end
pu-240 1 0.0 .2927e-03 end
pu-241 1 0.0 .541976e-04 end
pu-242 1 0.0 .6751e-05 end
u-235 1 0.0 .9269e-05 end
u-238 1 0.0 .6162e-02 end
o 1 0.0 .1864e-01 end
c 1 0.0 .2660e-01 end
h 1 0.0 .2432e-01 end
h 2 0.0 4.489e-2 end
c 2 0.0 3.110e-2 end
cl 2 0.0 7.240e-3 end
n 3 0.0 1.98881e-5 end
o 3 0.0 5.33497e-6 end
h 4 0.0 0.05712 end
c 4 0.0 0.03570 end
o 4 0.0 0.01428 end
cu 5 0.0 8.33333E-2 end
cd 5 0.0 4.71679E-4 end
sn 5 0.0 1.13027E-4 end
end comp
buckledslab vacuum reflected 0.0 46.0620 46.5660 end
1 16.0410 oneextermod
2 31.0410 noextermod
end zone
EXPT 1547-06; CSAS25/KENO-Va; 2/10/92
read para
gen=303 tme=60 flx=yes fdn=yes pki=yes nub=yes
end para
read geom
box type 1
cuboid 1 1 5.0900 0.0000 5.0830 0.0000 5.0900 0.0000
cuboid 2 1 5.1020 -0.0120 5.1265 -0.0435 5.1020 -0.0120
cuboid 3 1 5.1040 -0.0140 5.1285 -0.0455 5.1040 -0.0140
box type 2
cuboid 1 1 5.0900 0.0000 5.0830 0.0000 4.1840 0.0000
cuboid 2 1 5.1020 -0.0120 5.1265 -0.0435 4.1960 -0.0120
cuboid 3 1 5.1040 -0.0140 5.1285 -0.0455 4.1980 -0.0140
box type 3
cuboid 5 1 5.1040 -0.0140 5.1285 -0.0455 2.1600 0.0
cuboid 3 1 5.1040 -0.0140 5.1285 -0.0455 2.2200 -0.0600
corebdy 0 1 0.0 0.0 0.0
cuboid 4 2 0.61302E+2 -15.24 0.61806E+2 -15.24 0.47322E+2 -15.24
end geom
read array
nux=9 nuy=9 nuz=7
loop
 1 1 9 1 1 9 1 1 3 1
 3 1 9 1 1 9 1 4 4 1
 1 1 9 1 1 9 1 5 6 1
 2 1 9 1 1 9 1 7 7 1
end loop
end array
read bias
id=400 2 2 end bias

```

```
end data  
end
```

```

#csas25
EXPT 1547-07; CSAS25; 2/11/92; Hansen-Roach CROSS SECTIONS
hansen-roach
multiregion
am-241 1 0.0 .147224e-04 end
pu-238 1 0.0 .2288e-05 end
pu-239 1 0.0 .2186e-02 end
pu-240 1 0.0 .2927e-03 end
pu-241 1 0.0 .541976e-04 end
pu-242 1 0.0 .6751e-05 end
u-235 1 0.0 .9269e-05 end
u-238 1 0.0 .6162e-02 end
o 1 0.0 .1864e-01 end
c 1 0.0 .2660e-01 end
h 1 0.0 .2432e-01 end
h 2 0.0 4.489e-2 end
c 2 0.0 3.110e-2 end
cl 2 0.0 7.240e-3 end
n 3 0.0 1.98881e-5 end
o 3 0.0 5.33497e-6 end
h 4 0.0 0.05712 end
c 4 0.0 0.03570 end
o 4 0.0 0.01428 end
al 5 0.0 5.88742E-2 end
fe 5 0.0 2.03213E-4 end
si 5 0.0 2.309E-4 end
end comp
buckledslab vacuum reflected 0.0 46.0620 46.5660 end
1 13.2102 oneextermod
2 28.2102 noextermod
end zone
EXPT 1547-07; CSAS25/KENO-Va; 2/11/92
read para
gen=303 tme=60 flx=yes fdn=yes pki=yes nub=yes
end para
read geom
box type 1
cuboid 1 1 5.0900 0.0000 5.0830 0.0000 5.0900 0.0000
cuboid 2 1 5.1020 -0.0120 5.1265 -0.0435 5.1020 -0.0120
cuboid 3 1 5.1040 -0.0140 5.1285 -0.0455 5.1040 -0.0140
box type 2
cuboid 1 1 5.0900 0.0000 5.0830 0.0000 0.4123 0.0000
cuboid 2 1 5.1020 -0.0120 5.1265 -0.0435 0.4243 -0.0120
cuboid 3 1 5.1040 -0.0140 5.1285 -0.0455 0.4263 -0.0140
box type 3
cuboid 5 1 5.1040 -0.0140 5.1285 -0.0455 0.3160 0.0
cuboid 3 1 5.1040 -0.0140 5.1285 -0.0455 0.3530 -0.0370
corebdy 0 1 0.0 0.0 0.0
cuboid 4 2 0.61302E+2 -15.24 0.61806E+2 -15.24 0.416603E+02 -15.24
end geom
read array
nux=9 nuy=9 nuz=7
loop
 1 1 9 1 1 9 1 1 3 1
 3 1 9 1 1 9 1 4 4 1
 1 1 9 1 1 9 1 5 6 1
 2 1 9 1 1 9 1 7 7 1
end loop
end array
read bias
id=400 2 2 end bias

```

```
end data  
end
```

```

#csas25
EXPT 1547-08; CSAS28; 2/11/92; Hansen-Roach CROSS SECTIONS
hansen-roach
multiregion
am-241 1 0.0 .147224e-04 end
pu-238 1 0.0 .2288e-05 end
pu-239 1 0.0 .2186e-02 end
pu-240 1 0.0 .2927e-03 end
pu-241 1 0.0 .541976e-04 end
pu-242 1 0.0 .6751e-05 end
u-235 1 0.0 .9269e-05 end
u-238 1 0.0 .6162e-02 end
o 1 0.0 .1864e-01 end
c 1 0.0 .2660e-01 end
h 1 0.0 .2432e-01 end
h 2 0.0 4.489e-2 end
c 2 0.0 3.110e-2 end
cl 2 0.0 7.240e-3 end
n 3 0.0 1.98881e-5 end
o 3 0.0 5.33497e-6 end
h 4 0.0 0.05712 end
c 4 0.0 0.03570 end
o 4 0.0 0.01428 end
al 5 0.0 5.88742E-2 end
fe 5 0.0 2.03213E-4 end
si 5 0.0 2.309E-4 end
end comp
buckledslab vacuum reflected 0.0 46.0620 46.5660 end
1 13.8408 oneextermod
2 28.8408 noextermod
end zone
EXPT 1547-08; CSAS25/KENO-Va; 2/11/92
read para
gen=303 tme=60 flx=yes fdn=yes pki=yes nub=yes
end para
read geom
box type 1
cuboid 1 1 5.0900 0.0000 5.0830 0.0000 5.0900 0.0000
cuboid 2 1 5.1020 -0.0120 5.1265 -0.0435 5.1020 -0.0120
cuboid 3 1 5.1040 -0.0140 5.1285 -0.0455 5.1040 -0.0140
box type 2
cuboid 1 1 5.0900 0.0000 5.0830 0.0000 1.0536 0.0000
cuboid 2 1 5.1020 -0.0120 5.1265 -0.0435 1.0656 -0.0120
cuboid 3 1 5.1040 -0.0140 5.1285 -0.0455 1.0676 -0.0140
box type 3
cuboid 5 1 5.1040 -0.0140 5.1285 -0.0455 0.9610 0.0
cuboid 3 1 5.1040 -0.0140 5.1285 -0.0455 0.9855 -0.0245
corebdy 0 1 0.0 0.0 0.0
cuboid 4 2 0.61302E+2 -15.24 0.61806E+2 -15.24 0.429216E+02 -15.24
end geom
read array
nux=9 nuy=9 nuz=7
loop
1 1 9 1 1 9 1 1 3 1
3 1 9 1 1 9 1 4 4 1
1 1 9 1 1 9 1 5 6 1
2 1 9 1 1 9 1 7 7 1
end loop
end array
read bias
id=400 2 2 end bias

```

```
end data  
end
```

```

#csas25
EXPT 1547-09; CSAS28; 2/11/92; Hansen-Roach CROSS SECTIONS
hansen-roach
multiregion
am-241 1 0.0 .147224e-04 end
pu-238 1 0.0 .2288e-05 end
pu-239 1 0.0 .2186e-02 end
pu-240 1 0.0 .2927e-03 end
pu-241 1 0.0 .541976e-04 end
pu-242 1 0.0 .6751e-05 end
u-235 1 0.0 .9269e-05 end
u-238 1 0.0 .6162e-02 end
o 1 0.0 .1864e-01 end
c 1 0.0 .2660e-01 end
h 1 0.0 .2432e-01 end
h 2 0.0 4.489e-2 end
c 2 0.0 3.110e-2 end
cl 2 0.0 7.240e-3 end
n 3 0.0 1.98881e-5 end
o 3 0.0 5.33497e-6 end
h 4 0.0 0.05712 end
c 4 0.0 0.03570 end
o 4 0.0 0.01428 end
al 5 0.0 5.88742E-2 end
fe 5 0.0 2.03213E-4 end
si 5 0.0 2.309E-4 end
end comp
buckledslab vacuum reflected 0.0 46.0620 46.5660 end
1 14.847 oneextermod
2 29.847 noextermod
end zone
EXPT 1547-09; CSAS25/KENO-Va; 2/11/92
read para
gen=303 tme=60 flx=yes fdn=yes pki=yes nub=yes
end para
read geom
box type 1
cuboid 1 1 5.0900 0.0000 5.0830 0.0000 5.0900 0.0000
cuboid 2 1 5.1020 -0.0120 5.1265 -0.0435 5.1020 -0.0120
cuboid 3 1 5.1040 -0.0140 5.1285 -0.0455 5.1040 -0.0140
box type 2
cuboid 1 1 5.0900 0.0000 5.0830 0.0000 2.0360 0.0000
cuboid 2 1 5.1020 -0.0120 5.1265 -0.0435 2.0480 -0.0120
cuboid 3 1 5.1040 -0.0140 5.1285 -0.0455 2.0500 -0.0140
box type 3
cuboid 5 1 5.1040 -0.0140 5.1285 -0.0455 1.9710 0.0
cuboid 3 1 5.1040 -0.0140 5.1285 -0.0455 2.0055 -0.0345
corebdy 0 1 0.0 0.0 0.0
cuboid 4 2 0.61302E+2 -15.24 0.61806E+2 -15.24 0.44934E+2 -15.24
end geom
read array
nux=9 nuy=9 nuz=7
loop
 1 1 9 1 1 9 1 1 3 1
 3 1 9 1 1 9 1 4 4 1
 1 1 9 1 1 9 1 5 6 1
 2 1 9 1 1 9 1 7 7 1
end loop
end array
read bias
id=400 2 2 end bias

```

```
end data  
end
```

```

#csas25
EXPT 1547-10; CSAS28; 2/12/92; Hansen-Roach CROSS SECTIONS
hansen-roach
multiregion
am-241 1 0.0 5.80105E-7 end
pu-239 1 0.0 1.954E-4 end
pu-240 1 0.0 1.702E-5 end
pu-241 1 0.0 1.03449E-6 end
u-235 1 0.0 1.904E-6 end
u-238 1 0.0 1.252E-3 end
h 1 0.0 4.489E-2 end
c 1 0.0 4.412E-2 end
o 1 0.0 3.023E-3 end
h 2 0.0 4.489E-2 end
c 2 0.0 3.110E-2 end
cl 2 0.0 0.724E-2 end
n 3 0.0 1.98881e-5 end
o 3 0.0 5.33497e-6 end
h 4 0.0 0.05712 end
c 4 0.0 0.03570 end
o 4 0.0 0.01428 end
cu 5 0.0 8.44384e-2 end
o 5 0.0 1.00651e-4 end
c 5 0.0 1.78929e-5 end
cu 6 0.0 8.33333E-2 end
cd 6 0.0 4.71679E-4 end
sn 6 0.0 1.13027E-4 end
al 7 0.0 5.88742E-2 end
fe 7 0.0 2.03213E-4 end
si 7 0.0 2.309E-4 end
end comp
buckledslab vacuum reflected 0.0 46.17 46.71 end
1 11.0730 oneextermod
2 26.0730 noextermod
end zone
EXPT 1547-10; CSAS25/KENO-Va; 2/12/92
read para
gen=303 tme=60 flx=yes fdn=yes pki=yes nub=yes
end para
read geom
box type 1
cuboid 1 1 2.545 -2.545 2.545 -2.545 2.545 -2.545
cuboid 2 1 2.5605 -2.5605 2.5685 -2.5685 2.5605 -2.5605
cuboid 3 1 2.565 -2.565 2.595 -2.595 2.565 -2.565
box type 2
cuboid 1 1 2.545 -2.545 2.545 -2.545 1.70 -1.70
cuboid 2 1 2.5605 -2.5605 2.5685 -2.5685 1.7155 -1.7155
cuboid 3 1 2.565 -2.565 2.595 -2.595 1.72 -1.72
box type 3
cuboid 1 1 2.545 -2.545 2.545 -2.545 0.692 -0.692
cuboid 2 1 2.5605 -2.5605 2.5685 -2.5685 0.7075 -0.7075
cuboid 3 1 2.565 -2.565 2.595 -2.595 0.712 -0.712
box type 4
cuboid 1 1 2.545 -2.545 2.545 -2.545 0.190992 -0.190992
cuboid 2 1 2.5605 -2.5605 2.5685 -2.5685 0.206492 -0.206492
cuboid 3 1 2.565 -2.565 2.595 -2.595 .210922 -.210922
corebdy 0 1 0.0 0.0 0.0
reflector 4 2 15.0 15.0 15.0 15.0 15.0 15.0 5
end geom
read array
nux=9 nuy=9 nuz=7

```

```
loop
2 1 9 1 1 9 1 1 3 1
1 1 9 1 1 9 1 4 5 1
3 1 9 1 1 9 1 6 6 1
4 1 9 1 1 9 1 7 7 1
end loop
end array
read bias
id=400 2 2 end bias
end data
end
```

```

#csas25
EXPT 1547-11; CSAS28; 2/12/92; Hansen-Roach CROSS SECTIONS
hansen-roach
multiregion
am-241 1 0.0 5.80105E-7 end
pu-239 1 0.0 1.954E-4 end
pu-240 1 0.0 1.702E-5 end
pu-241 1 0.0 1.03449E-6 end
u-235 1 0.0 1.904E-6 end
u-238 1 0.0 1.252E-3 end
h 1 0.0 4.489E-2 end
c 1 0.0 4.412E-2 end
o 1 0.0 3.023E-3 end
h 2 0.0 4.489E-2 end
c 2 0.0 3.110E-2 end
cl 2 0.0 0.724E-2 end
n 3 0.0 1.98881e-5 end
o 3 0.0 5.33497e-6 end
h 4 0.0 0.05712 end
c 4 0.0 0.03570 end
o 4 0.0 0.01428 end
cu 5 0.0 8.44384e-2 end
o 5 0.0 1.00651e-4 end
c 5 0.0 1.78929e-5 end
cu 6 0.0 8.33333E-2 end
cd 6 0.0 4.71679E-4 end
sn 6 0.0 1.13027E-4 end
al 7 0.0 5.88742E-2 end
fe 7 0.0 2.03213E-4 end
si 7 0.0 2.309E-4 end
end comp
buckledslab vacuum reflected 0.0 46.17 46.71 end
1 11.8612 oneextermod
2 26.8612 noextermod
end zone
EXPT 1547-11; CSAS25/KENO-Va; 2/12/92
read para
gen=303 tme=60 flx=yes fdn=yes pki=yes nub=yes
end para
read geom
box type 1
cuboid 1 1 2.545 -2.545 2.545 -2.545 2.545 -2.545
cuboid 2 1 2.5605 -2.5605 2.5685 -2.5685 2.5605 -2.5605
cuboid 3 1 2.565 -2.565 2.595 -2.595 2.565 -2.565
box type 2
cuboid 1 1 2.545 -2.545 2.545 -2.545 1.70 -1.70
cuboid 2 1 2.5605 -2.5605 2.5685 -2.5685 1.7155 -1.7155
cuboid 3 1 2.565 -2.565 2.595 -2.595 1.72 -1.72
box type 3
cuboid 1 1 2.545 -2.545 2.545 -2.545 0.692 -0.692
cuboid 2 1 2.5605 -2.5605 2.5685 -2.5685 0.7075 -0.7075
cuboid 3 1 2.565 -2.565 2.595 -2.595 0.712 -0.712
box type 4
cuboid 1 1 2.545 -2.545 2.545 -2.545 0.28718 -0.28718
cuboid 2 1 2.5605 -2.5605 2.5685 -2.5685 0.30268 -0.30268
cuboid 3 1 2.565 -2.565 2.595 -2.595 0.30718 -0.30718
box type 5
cuboid 5 1 2.565 -2.565 2.595 -2.595 0.15875 -0.15875
cuboid 3 1 2.565 -2.565 2.595 -2.595 0.19525 -0.19525
corebdy 0 1 0.0 0.0 0.0
reflector 4 2 15.0 15.0 15.0 15.0 15.0 5

```

```
end geom
read array
nux=9 nuy=9 nuz=9
loop
2 1 9 1 1 9 1 1 3 1
5 1 9 1 1 9 1 4 4 1
1 1 9 1 1 9 1 5 6 1
3 1 9 1 1 9 1 7 8 1
4 1 9 1 1 9 1 9 9 1
end loop
end array
read bias
id=400 2 2 end bias
end data
end
```

```

#csas25
EXPT 1547-12; CSAS28; 2/11/92; Hansen-Roach CROSS SECTIONS
hansen-roach
multiregion
am-241 1 0.0 5.80105E-7 end
pu-239 1 0.0 1.954E-4 end
pu-240 1 0.0 1.702E-5 end
pu-241 1 0.0 1.03449E-6 end
pu-242 1 0.0 1.904E-6 end
u-238 1 0.0 1.252E-3 end
h 1 0.0 4.489E-2 end
c 1 0.0 4.412E-2 end
o 1 0.0 3.023E-3 end
h 2 0.0 4.489E-2 end
c 2 0.0 3.110E-2 end
cl 2 0.0 0.724E-2 end
n 3 0.0 1.98881e-5 end
o 3 0.0 5.33497e-6 end
h 4 0.0 0.05712 end
c 4 0.0 0.03570 end
o 4 0.0 0.01428 end
cu 5 0.0 8.44384e-2 end
o 5 0.0 1.00651e-4 end
c 5 0.0 1.78929e-5 end
cu 6 0.0 8.33333E-2 end
cd 6 0.0 4.71679E-4 end
sn 6 0.0 1.13027E-4 end
al 7 0.0 5.88742E-2 end
fe 7 0.0 2.03213E-4 end
si 7 0.0 2.309E-4 end
end comp
buckledslab vacuum reflected 0.0 46.17 46.71 end
1 12.3421 oneextermod
2 27.3421 noextermod
end zone
EXPT 1547-12; CSAS25/KENO-Va; 2/11/92
read para
gen=303 tme=60 flx=yes fdn=yes pki=yes nub=yes
end para
read geom
box type 1
cuboid 1 1 2.545 -2.545 2.545 -2.545 2.545 -2.545
cuboid 2 1 2.5605 -2.5605 2.5685 -2.5685 2.5605 -2.5605
cuboid 3 1 2.565 -2.565 2.595 -2.595 2.565 -2.565
box type 2
cuboid 1 1 2.545 -2.545 2.545 -2.545 1.70 -1.70
cuboid 2 1 2.5605 -2.5605 2.5685 -2.5685 1.7155 -1.7155
cuboid 3 1 2.565 -2.565 2.595 -2.595 1.72 -1.72
box type 3
cuboid 1 1 2.545 -2.545 2.545 -2.545 0.692 -0.692
cuboid 2 1 2.5605 -2.5605 2.5685 -2.5685 0.7075 -0.7075
cuboid 3 1 2.565 -2.565 2.595 -2.595 0.712 -0.712
box type 4
cuboid 1 1 2.545 -2.545 2.545 -2.545 0.055 -0.055
cuboid 2 1 2.5605 -2.5605 2.5685 -2.5685 0.0705 -0.0705
cuboid 3 1 2.565 -2.565 2.595 -2.595 0.075 -0.075
box type 5
cuboid 5 1 2.565 -2.565 2.595 -2.595 0.3185 -0.3185
cuboid 3 1 2.565 -2.565 2.595 -2.595 0.355 -0.355
corebdy 0 1 0.0 0.0 0.0
reflector 4 2 15.0 15.0 15.0 15.0 15.0 5

```

```
end geom
read array
nux=9 nuy=9 nuz=10
loop
2 1 9 1 1 9 1 1 3 1
5 1 9 1 1 9 1 4 4 1
1 1 9 1 1 9 1 5 6 1
3 1 9 1 1 9 1 7 9 1
4 1 9 1 1 9 1 10 10 1
end loop
end array
read bias
id=400 2 2 end bias
end data
end
```

```

#csas25
EXPT 1547-13; CSAS28; 2/11/92; Hansen-Roach CROSS SECTIONS
hansen-roach
multiregion
am-241 1 0.0 5.80105E-7 end
pu-239 1 0.0 1.954E-4 end
pu-240 1 0.0 1.702E-5 end
pu-241 1 0.0 1.03449E-6 end
u-235 1 0.0 1.904E-6 end
u-238 1 0.0 1.252E-3 end
h 1 0.0 4.489E-2 end
c 1 0.0 4.412E-2 end
o 1 0.0 3.023E-3 end
h 2 0.0 4.489E-2 end
c 2 0.0 3.110E-2 end
cl 2 0.0 0.724E-2 end
n 3 0.0 1.98881e-5 end
o 3 0.0 5.33497e-6 end
h 4 0.0 0.05712 end
c 4 0.0 0.03570 end
o 4 0.0 0.01428 end
cu 5 0.0 8.44384e-2 end
o 5 0.0 1.00651e-4 end
c 5 0.0 1.78929e-5 end
cu 6 0.0 8.33333E-2 end
cd 6 0.0 4.71679E-4 end
sn 6 0.0 1.13027E-4 end
al 7 0.0 5.88742E-2 end
fe 7 0.0 2.03213E-4 end
si 7 0.0 2.309E-4 end
end comp
buckledslab vacuum reflected 0.0 46.17 46.71 end
1 13.0547 oneextermod
2 28.0547 noextermod
end zone
EXPT 1547-13; CSAS25/KENO-Va; 2/11/92
read para
gen=303 tme=60 flx=yes fdn=yes pki=yes nub=yes
end para
read geom
box type 1
cuboid 1 1 2.545 -2.545 2.545 -2.545 2.545 -2.545
cuboid 2 1 2.5605 -2.5605 2.5685 -2.5685 2.5605 -2.5605
cuboid 3 1 2.565 -2.565 2.595 -2.595 2.565 -2.565
box type 2
cuboid 1 1 2.545 -2.545 2.545 -2.545 1.70 -1.70
cuboid 2 1 2.5605 -2.5605 2.5685 -2.5685 1.7155 -1.7155
cuboid 3 1 2.565 -2.565 2.595 -2.595 1.72 -1.72
box type 3
cuboid 1 1 2.545 -2.545 2.545 -2.545 0.692 -0.692
cuboid 2 1 2.5605 -2.5605 2.5685 -2.5685 0.7075 -0.7075
cuboid 3 1 2.565 -2.565 2.595 -2.595 0.712 -0.712
box type 4
cuboid 1 1 2.545 -2.545 2.545 -2.545 0.2315 -0.2315
cuboid 2 1 2.5605 -2.5605 2.5685 -2.5685 0.247 -0.247
cuboid 3 1 2.565 -2.565 2.595 -2.595 0.2515 -0.2515
box type 5
cuboid 5 1 2.565 -2.565 2.595 -2.595 0.645 -0.645
cuboid 3 1 2.565 -2.565 2.595 -2.595 0.675 -0.675
corebody 0 1 0.0 0.0 0.0
reflector 4 2 15.0 15.0 15.0 15.0 15.0 5

```

```
end geom
read array
nux=9 nuy=9 nuz=8
loop
2 1 9 1 1 9 1 1 1 3 1
5 1 9 1 1 9 1 4 4 1
1 1 9 1 1 9 1 5 7 1
4 1 9 1 1 9 1 8 8 1
end loop
end array
read bias
id=400 2 2 end bias
end data
end
```

```

#csas25
EXPT 1547-14; CSAS28; 2/12/92; Hansen-Roach CROSS SECTIONS
hansen-roach
multiregion
am-241 1 0.0 5.80105E-7 end
pu-239 1 0.0 1.954E-4 end
pu-240 1 0.0 1.702E-5 end
pu-241 1 0.0 1.03449E-6 end
u-235 1 0.0 1.904E-6 end
u-238 1 0.0 1.252E-3 end
h 1 0.0 4.489E-2 end
c 1 0.0 4.412E-2 end
o 1 0.0 3.023E-3 end
h 2 0.0 4.489E-2 end
c 2 0.0 3.110E-2 end
cl 2 0.0 0.724E-2 end
n 3 0.0 1.98881e-5 end
o 3 0.0 5.33497e-6 end
h 4 0.0 0.05712 end
c 4 0.0 0.03570 end
o 4 0.0 0.01428 end
cu 5 0.0 8.44384e-2 end
o 5 0.0 1.00651e-4 end
c 5 0.0 1.78929e-5 end
cu 6 0.0 8.33333E-2 end
cd 6 0.0 4.71679E-4 end
sn 6 0.0 1.13027E-4 end
al 7 0.0 5.88742E-2 end
fe 7 0.0 2.03213E-4 end
si 7 0.0 2.309E-4 end
end comp
buckledslab vacuum reflected 0.0 46.17 46.71 end
1 13.5211 oneextermod
2 28.5211 noextermod
end zone
EXPT 1547-14; CSAS25/KENO-Va; 2/12/92
read para
gen=303 tme=60 flx=yes fdn=yes pki=yes nub=yes
end para
read geom
box type 1
cuboid 1 1 2.545 -2.545 2.545 -2.545 2.545 -2.545
cuboid 2 1 2.5605 -2.5605 2.5685 -2.5685 2.5605 -2.5605
cuboid 3 1 2.565 -2.565 2.595 -2.595 2.565 -2.565
box type 2
cuboid 1 1 2.545 -2.545 2.545 -2.545 1.70 -1.70
cuboid 2 1 2.5605 -2.5605 2.5685 -2.5685 1.7155 -1.7155
cuboid 3 1 2.565 -2.565 2.595 -2.595 1.72 -1.72
box type 3
cuboid 1 1 2.545 -2.545 2.545 -2.545 0.692 -0.692
cuboid 2 1 2.5605 -2.5605 2.5685 -2.5685 0.7075 -0.7075
cuboid 3 1 2.565 -2.565 2.595 -2.595 0.712 -0.712
box type 4
cuboid 1 1 2.545 -2.545 2.545 -2.545 0.068 -0.068
cuboid 2 1 2.5605 -2.5605 2.5685 -2.5685 0.0835 -0.0835
cuboid 3 1 2.565 -2.565 2.595 -2.595 0.088 -0.088
box type 5
cuboid 5 1 2.565 -2.565 2.595 -2.595 0.9635 -0.9635
cuboid 3 1 2.565 -2.565 2.595 -2.595 1.01 -1.01
corebdy 0 1 0.0 0.0 0.0
reflector 4 2 15.0 15.0 15.0 15.0 15.0 5

```

```
end geom
read array
nux=9 nuy=9 nuz=9
loop
2 1 9 1 1 9 1 1 3 1
5 1 9 1 1 9 1 4 4 1
1 1 9 1 1 9 1 5 7 1
3 1 9 1 1 9 1 8 8 1
4 1 9 1 1 9 1 9 9 1
end loop
end array
read bias
id=400 2 2 end bias
end data
end
```

```

#csas25
EXPT 1547-15; CSAS28; 2/12/92; Hansen-Roach CROSS SECTIONS
hansen-roach
multiregion
am-241 1 0.0 5.80105E-7 end
pu-239 1 0.0 1.954E-4 end
pu-240 1 0.0 1.702E-5 end
pu-241 1 0.0 1.03449E-6 end
u-235 1 0.0 1.904E-6 end
u-238 1 0.0 1.252E-3 end
h 1 0.0 4.489E-2 end
c 1 0.0 4.412E-2 end
o 1 0.0 3.023E-3 end
h 2 0.0 4.489E-2 end
c 2 0.0 3.110E-2 end
cl 2 0.0 0.724E-2 end
n 3 0.0 1.98881e-5 end
o 3 0.0 5.33497e-6 end
h 4 0.0 0.05712 end
c 4 0.0 0.03570 end
o 4 0.0 0.01428 end
cu 5 0.0 8.44384e-2 end
o 5 0.0 1.00651e-4 end
c 5 0.0 1.78929e-5 end
cu 6 0.0 8.33333E-2 end
cd 6 0.0 4.71679E-4 end
sn 6 0.0 1.13027E-4 end
al 7 0.0 5.88742E-2 end
fe 7 0.0 2.03213E-4 end
si 7 0.0 2.309E-4 end
end comp
buckledslab vacuum reflected 0.0 46.17 46.71 end
1 13.9432 oneextermod
2 28.9432 noextermod
end zone
EXPT 1547-15; CSAS25/KENO-Va; 2/12/92
read para
gen=303 tme=60 flx=yes fdn=yes pki=yes nub=yes
end para
read geom
box type 1
cuboid 1 1 2.545 -2.545 2.545 -2.545 2.545 -2.545
cuboid 2 1 2.5605 -2.5605 2.5685 -2.5685 2.5605 -2.5605
cuboid 3 1 2.565 -2.565 2.595 -2.595 2.565 -2.565
box type 2
cuboid 1 1 2.545 -2.545 2.545 -2.545 1.70 -1.70
cuboid 2 1 2.5605 -2.5605 2.5685 -2.5685 1.7155 -1.7155
cuboid 3 1 2.565 -2.565 2.595 -2.595 1.72 -1.72
box type 3
cuboid 1 1 2.545 -2.545 2.545 -2.545 0.692 -0.692
cuboid 2 1 2.5605 -2.5605 2.5685 -2.5685 0.7075 -0.7075
cuboid 3 1 2.565 -2.565 2.595 -2.595 0.712 -0.712
box type 4
cuboid 1 1 2.545 -2.545 2.545 -2.545 0.373 -0.373
cuboid 2 1 2.5605 -2.5605 2.5685 -2.5685 0.3885 -0.3885
cuboid 3 1 2.565 -2.565 2.595 -2.595 0.393 -0.393
box type 5
cuboid 5 1 2.565 -2.565 2.595 -2.595 1.290 -1.290
cuboid 3 1 2.565 -2.565 2.595 -2.595 1.35 -1.35
corebdy 0 1 0.0 0.0 0.0
reflector 4 2 15.0 15.0 15.0 15.0 15.0 5

```

```
end geom
read array
nux=9 nuy=9 nuz=9
loop
2 1 9 1 1 9 1 1 3 1
5 1 9 1 1 9 1 4 4 1
1 1 9 1 1 9 1 5 7 1
3 1 9 1 1 9 1 8 8 1
4 1 9 1 1 9 1 9 9 1
end loop
end array
read bias
id=400 2 2 end bias
end data
end
```

```

#csas25
EXPT 1547-16; CSAS28; 2/12/92; Hansen-Roach CROSS SECTIONS
hansen-roach
multiregion
am-241 1 0.0 5.80105E-7 end
pu-239 1 0.0 1.954E-4 end
pu-240 1 0.0 1.702E-5 end
pu-241 1 0.0 1.03449E-6 end
u-235 1 0.0 1.904E-6 end
u-238 1 0.0 1.252E-3 end
h 1 0.0 4.489E-2 end
c 1 0.0 4.412E-2 end
o 1 0.0 3.023E-3 end
h 2 0.0 4.489E-2 end
c 2 0.0 3.110E-2 end
cl 2 0.0 0.724E-2 end
n 3 0.0 1.98881e-5 end
o 3 0.0 5.33497e-6 end
h 4 0.0 0.05712 end
c 4 0.0 0.03570 end
o 4 0.0 0.01428 end
cu 5 0.0 8.44384e-2 end
o 5 0.0 1.00651e-4 end
c 5 0.0 1.78929e-5 end
cu 6 0.0 8.33333E-2 end
cd 6 0.0 4.71679E-4 end
sn 6 0.0 1.13027E-4 end
al 7 0.0 5.88742E-2 end
fe 7 0.0 2.03213E-4 end
si 7 0.0 2.309E-4 end
end comp
buckledslab vacuum reflected 0.0 46.17 46.71 end
1 13.2588 oneextermod
2 28.2588 noextermod
end zone
EXPT 1547-16; CSAS25/KENO-Va; 2/12/92
read para
gen=303 tme=60 flx=yes fdn=yes pki=yes nub=yes
end para
read geom
box type 1
cuboid 1 1 2.545 -2.545 2.545 -2.545 2.545 -2.545
cuboid 2 1 2.5605 -2.5605 2.5685 -2.5685 2.5605 -2.5605
cuboid 3 1 2.565 -2.565 2.595 -2.595 2.565 -2.565
box type 2
cuboid 1 1 2.545 -2.545 2.545 -2.545 1.70 -1.70
cuboid 2 1 2.5605 -2.5605 2.5685 -2.5685 1.7155 -1.7155
cuboid 3 1 2.565 -2.565 2.595 -2.595 1.72 -1.72
box type 3
cuboid 1 1 2.545 -2.545 2.545 -2.545 0.692 -0.692
cuboid 2 1 2.5605 -2.5605 2.5685 -2.5685 0.7075 -0.7075
cuboid 3 1 2.565 -2.565 2.595 -2.595 0.712 -0.712
box type 4
cuboid 1 1 2.545 -2.545 2.545 -2.545 0.3785 -0.3785
cuboid 2 1 2.5605 -2.5605 2.5685 -2.5685 0.394 -0.394
cuboid 3 1 2.565 -2.565 2.595 -2.595 0.3985 -0.3985
box type 5
cuboid 6 1 2.565 -2.565 2.595 -2.595 0.184 -0.184
cuboid 3 1 2.565 -2.565 2.595 -2.595 0.215 -0.215
corebdy 0 1 0.0 0.0 0.0
reflector 4 2 15.0 15.0 15.0 15.0 15.0 5

```

```
end geom
read array
nux=9 nuy=9 nuz=8
loop
2 1 9 1 1 9 1 1 1 3 1
5 1 9 1 1 9 1 4 4 1
1 1 9 1 1 9 1 5 7 1
4 1 9 1 1 9 1 8 8 1
end loop
end array
read bias
id=400 2 2 end bias
end data
end
```

```

#csas25
EXPT 1547-17; CSAS28; 2/12/92; Hansen-Roach CROSS SECTIONS
hansen-roach
multiregion
am-241 1 0.0 5.80105E-7 end
pu-239 1 0.0 1.954E-4 end
pu-240 1 0.0 1.702E-5 end
pu-241 1 0.0 1.03449E-6 end
u-235 1 0.0 1.904E-6 end
u-238 1 0.0 1.252E-3 end
h 1 0.0 4.489E-2 end
c 1 0.0 4.412E-2 end
o 1 0.0 3.023E-3 end
h 2 0.0 4.489E-2 end
c 2 0.0 3.110E-2 end
cl 2 0.0 0.724E-2 end
n 3 0.0 1.98881e-5 end
o 3 0.0 5.33497e-6 end
h 4 0.0 0.05712 end
c 4 0.0 0.03570 end
o 4 0.0 0.01428 end
cu 5 0.0 8.44384e-2 end
o 5 0.0 1.00651e-4 end
c 5 0.0 1.78929e-5 end
cu 6 0.0 8.33333E-2 end
cd 6 0.0 4.71679E-4 end
sn 6 0.0 1.13027E-4 end
al 7 0.0 5.88742E-2 end
fe 7 0.0 2.03213E-4 end
si 7 0.0 2.309E-4 end
end comp
buckledslab vacuum reflected 0.0 46.17 46.71 end
1 14.6020 oneextermod
2 29.6020 noextermod
end zone
EXPT 1547-17; CSAS25/KENO-Va; 2/12/92
read para
gen=303 tme=60 flx=yes fdn=yes pki=yes nub=yes
end para
read geom
box type 1
cuboid 1 1 2.545 -2.545 2.545 -2.545 2.545 -2.545
cuboid 2 1 2.5605 -2.5605 2.5685 -2.5685 2.5605 -2.5605
cuboid 3 1 2.565 -2.565 2.595 -2.595 2.565 -2.565
box type 2
cuboid 1 1 2.545 -2.545 2.545 -2.545 1.70 -1.70
cuboid 2 1 2.5605 -2.5605 2.5685 -2.5685 1.7155 -1.7155
cuboid 3 1 2.565 -2.565 2.595 -2.595 1.72 -1.72
box type 3
cuboid 1 1 2.545 -2.545 2.545 -2.545 0.692 -0.692
cuboid 2 1 2.5605 -2.5605 2.5685 -2.5685 0.7075 -0.7075
cuboid 3 1 2.565 -2.565 2.595 -2.595 0.712 -0.712
box type 4
cuboid 1 1 2.545 -2.545 2.545 -2.545 0.349 -0.349
cuboid 2 1 2.5605 -2.5605 2.5685 -2.5685 0.3645 -0.3645
cuboid 3 1 2.565 -2.565 2.595 -2.595 0.369 -0.369
box type 5
cuboid 6 1 2.565 -2.565 2.595 -2.595 1.08 -1.08
cuboid 3 1 2.565 -2.565 2.595 -2.595 1.15 -1.15
corebdy 0 1 0.0 0.0 0.0
reflector 4 2 15.0 15.0 15.0 15.0 15.0 5

```

```
end geom
read array
nux=9 nuy=9 nuz=10
loop
2 1 9 1 1 9 1 1 3 1
5 1 9 1 1 9 1 4 4 1
1 1 9 1 1 9 1 5 7 1
3 1 9 1 1 9 1 8 9 1
4 1 9 1 1 9 1 10 10 1
end loop
end array
read bias
id=400 2 2 end bias
end data
end
```

```

#csas25
EXPT 1547-18; CSAS28; 2/12/92; Hansen-Roach CROSS SECTIONS
hansen-roach
multiregion
am-241 1 0.0 5.80105E-7 end
pu-239 1 0.0 1.954E-4 end
pu-240 1 0.0 1.702E-5 end
pu-241 1 0.0 1.03449E-6 end
u-235 1 0.0 1.904E-6 end
u-238 1 0.0 1.252E-3 end
h 1 0.0 4.489E-2 end
c 1 0.0 4.412E-2 end
o 1 0.0 3.023E-3 end
h 2 0.0 4.489E-2 end
c 2 0.0 3.110E-2 end
cl 2 0.0 0.724E-2 end
n 3 0.0 1.98881e-5 end
o 3 0.0 5.33497e-6 end
h 4 0.0 0.05712 end
c 4 0.0 0.03570 end
o 4 0.0 0.01428 end
cu 5 0.0 8.44384e-2 end
o 5 0.0 1.00651e-4 end
c 5 0.0 1.78929e-5 end
cu 6 0.0 8.33333E-2 end
cd 6 0.0 4.71679E-4 end
sn 6 0.0 1.13027E-4 end
al 7 0.0 5.88742E-2 end
fe 7 0.0 2.03213E-4 end
si 7 0.0 2.309E-4 end
end comp
buckledslab vacuum reflected 0.0 46.17 46.71 end
1 11.2612 oneextermod
2 26.2612 noextermod
end zone
EXPT 1547-18; CSAS25/KENO-Va; 2/12/92
read para
gen=303 tme=60 flx=yes fdn=yes pki=yes nub=yes
end para
read geom
box type 1
cuboid 1 1 2.545 -2.545 2.545 -2.545 2.545 -2.545
cuboid 2 1 2.5605 -2.5605 2.5685 -2.5685 2.5605 -2.5605
cuboid 3 1 2.565 -2.565 2.595 -2.595 2.565 -2.565
box type 2
cuboid 1 1 2.545 -2.545 2.545 -2.545 1.70 -1.70
cuboid 2 1 2.5605 -2.5605 2.5685 -2.5685 1.7155 -1.7155
cuboid 3 1 2.565 -2.565 2.595 -2.595 1.72 -1.72
box type 3
cuboid 1 1 2.545 -2.545 2.545 -2.545 0.692 -0.692
cuboid 2 1 2.5605 -2.5605 2.5685 -2.5685 0.7075 -0.7075
cuboid 3 1 2.565 -2.565 2.595 -2.595 0.712 -0.712
box type 4
cuboid 1 1 2.545 -2.545 2.545 -2.545 0.274 -0.274
cuboid 2 1 2.5605 -2.5605 2.5685 -2.5685 0.2895 -0.2895
cuboid 3 1 2.565 -2.565 2.595 -2.595 0.294 -0.294
box type 5
cuboid 7 1 2.565 -2.565 2.595 -2.595 0.158 -0.158
cuboid 3 1 2.565 -2.565 2.595 -2.595 0.20 -0.20
corebdy 0 1 0.0 0.0 0.0
reflector 4 2 15.0 15.0 15.0 15.0 15.0 5

```

```
end geom
read array
nux=9 nuy=9 nuz=8
loop
2 1 9 1 1 9 1 1 1 3 1
5 1 9 1 1 9 1 4 4 1
1 1 9 1 1 9 1 5 6 1
3 1 9 1 1 9 1 7 7 1
4 1 9 1 1 9 1 8 8 1
end loop
end array
read bias
id=400 2 2 end bias
end data
end
```

```

#csas25
EXPT 1547-19; CSAS28; 2/12/92; Hansen-Roach CROSS SECTIONS
hansen-roach
multiregion
am-241 1 0.0 5.80105E-7 end
pu-239 1 0.0 1.954E-4 end
pu-240 1 0.0 1.702E-5 end
pu-241 1 0.0 1.03449E-6 end
u-235 1 0.0 1.904E-6 end
u-238 1 0.0 1.252E-3 end
h 1 0.0 4.489E-2 end
c 1 0.0 4.412E-2 end
o 1 0.0 3.023E-3 end
h 2 0.0 4.489E-2 end
c 2 0.0 3.110E-2 end
cl 2 0.0 0.724E-2 end
n 3 0.0 1.98881e-5 end
o 3 0.0 5.33497e-6 end
h 4 0.0 0.05712 end
c 4 0.0 0.03570 end
o 4 0.0 0.01428 end
cu 5 0.0 8.44384e-2 end
o 5 0.0 1.00651e-4 end
c 5 0.0 1.78929e-5 end
cu 6 0.0 8.33333E-2 end
cd 6 0.0 4.71679E-4 end
sn 6 0.0 1.13027E-4 end
al 7 0.0 5.88742E-2 end
fe 7 0.0 2.03213E-4 end
si 7 0.0 2.309E-4 end
end comp
buckledslab vacuum reflected 0.0 46.17 46.71 end
1 11.3934 oneextermod
2 26.3934 noextermod
end zone
EXPT 1547-19; CSAS25/KENO-Va; 2/12/92
read para
gen=303 tme=60 flx=yes fdn=yes pki=yes nub=yes
end para
read geom
box type 1
cuboid 1 1 2.545 -2.545 2.545 -2.545 2.545 -2.545
cuboid 2 1 2.5605 -2.5605 2.5685 -2.5685 2.5605 -2.5605
cuboid 3 1 2.565 -2.565 2.595 -2.595 2.565 -2.565
box type 2
cuboid 1 1 2.545 -2.545 2.545 -2.545 1.70 -1.70
cuboid 2 1 2.5605 -2.5605 2.5685 -2.5685 1.7155 -1.7155
cuboid 3 1 2.565 -2.565 2.595 -2.595 1.72 -1.72
box type 3
cuboid 1 1 2.545 -2.545 2.545 -2.545 0.692 -0.692
cuboid 2 1 2.5605 -2.5605 2.5685 -2.5685 0.7075 -0.7075
cuboid 3 1 2.565 -2.565 2.595 -2.595 0.712 -0.712
box type 4
cuboid 1 1 2.545 -2.545 2.545 -2.545 0.3695 -0.3695
cuboid 2 1 2.5605 -2.5605 2.5685 -2.5685 0.385 -0.385
cuboid 3 1 2.565 -2.565 2.595 -2.595 0.3895 -0.3895
box type 5
cuboid 7 1 2.565 -2.565 2.595 -2.595 0.3225 -0.3225
cuboid 3 1 2.565 -2.565 2.595 -2.595 0.365 -0.365
corebdy 0 1 0.0 0.0 0.0
reflector 4 2 15.0 15.0 15.0 15.0 15.0 5

```

```
end geom
read array
nux=9 nuy=9 nuz=8
loop
2 1 9 1 1 9 1 1 3 1
5 1 9 1 1 9 1 4 4 1
1 1 9 1 1 9 1 5 6 1
3 1 9 1 1 9 1 7 7 1
4 1 9 1 1 9 1 8 8 1
end loop
end array
read bias
id=400 2 2 end bias
end data
end
```

```

#csas25
EXPT 1547-20; CSAS28; 2/12/92; Hansen-Roach CROSS SECTIONS
hansen-roach
multiregion
am-241 1 0.0 5.80105E-7 end
pu-239 1 0.0 1.954E-4 end
pu-240 1 0.0 1.702E-5 end
pu-241 1 0.0 1.03449E-6 end
u-235 1 0.0 1.904E-6 end
u-238 1 0.0 1.252E-3 end
h 1 0.0 4.489E-2 end
c 1 0.0 4.412E-2 end
o 1 0.0 3.023E-3 end
h 2 0.0 4.489E-2 end
c 2 0.0 3.110E-2 end
cl 2 0.0 0.724E-2 end
n 3 0.0 1.98881e-5 end
o 3 0.0 5.33497e-6 end
h 4 0.0 0.05712 end
c 4 0.0 0.03570 end
o 4 0.0 0.01428 end
cu 5 0.0 8.44384e-2 end
o 5 0.0 1.00651e-4 end
c 5 0.0 1.78929e-5 end
cu 6 0.0 8.33333E-2 end
cd 6 0.0 4.71679E-4 end
sn 6 0.0 1.13027E-4 end
al 7 0.0 5.88742E-2 end
fe 7 0.0 2.03213E-4 end
si 7 0.0 2.309E-4 end
end comp
buckledslab vacuum reflected 0.0 46.17 46.71 end
1 12.0674 oneextermod
2 27.0674 noextermod
end zone
EXPT 1547-20; CSAS25/KENO-Va; 2/12/92
read para
gen=303 tme=60 flx=yes fdn=yes pki=yes nub=yes
end para
read geom
box type 1
cuboid 1 1 2.545 -2.545 2.545 -2.545 2.545 -2.545
cuboid 2 1 2.5605 -2.5605 2.5685 -2.5685 2.5605 -2.5605
cuboid 3 1 2.565 -2.565 2.595 -2.595 2.565 -2.565
box type 2
cuboid 1 1 2.545 -2.545 2.545 -2.545 1.70 -1.70
cuboid 2 1 2.5605 -2.5605 2.5685 -2.5685 1.7155 -1.7155
cuboid 3 1 2.565 -2.565 2.595 -2.595 1.72 -1.72
box type 3
cuboid 1 1 2.545 -2.545 2.545 -2.545 0.692 -0.692
cuboid 2 1 2.5605 -2.5605 2.5685 -2.5685 0.7075 -0.7075
cuboid 3 1 2.565 -2.565 2.595 -2.595 0.712 -0.712
box type 4
cuboid 1 1 2.545 -2.545 2.545 -2.545 0.3565 -0.3565
cuboid 2 1 2.5605 -2.5605 2.5685 -2.5685 0.372 -0.372
cuboid 3 1 2.565 -2.565 2.595 -2.595 0.3765 -0.3765
box type 5
cuboid 7 1 2.565 -2.565 2.595 -2.595 0.9915 -0.9915
cuboid 3 1 2.565 -2.565 2.595 -2.595 1.03 -1.03
corebdy 0 1 0.0 0.0 0.0
reflector 4 2 15.0 15.0 15.0 15.0 15.0 5

```

```
end geom
read array
nux=9 nuy=9 nuz=9
loop
2 1 9 1 1 9 1 1 1 3 1
5 1 9 1 1 9 1 4 4 1
1 1 9 1 1 9 1 5 6 1
3 1 9 1 1 9 1 7 8 1
4 1 9 1 1 9 1 9 9 1
end loop
end array
read bias
id=400 2 2 end bias
end data
end
```

```

#csas25
EXPT 1547-21; CSAS28; 2/12/92; Hansen-Roach CROSS SECTIONS
hansen-roach
multiregion
am-241 1 0.0 5.80105E-7 end
pu-239 1 0.0 1.954E-4 end
pu-240 1 0.0 1.702E-5 end
pu-241 1 0.0 1.03449E-6 end
u-235 1 0.0 1.904E-6 end
u-238 1 0.0 1.252E-3 end
h 1 0.0 4.489E-2 end
c 1 0.0 4.412E-2 end
o 1 0.0 3.023E-3 end
h 2 0.0 4.489E-2 end
c 2 0.0 3.110E-2 end
cl 2 0.0 0.724E-2 end
n 3 0.0 1.98881e-5 end
o 3 0.0 5.33497e-6 end
h 4 0.0 0.05712 end
c 4 0.0 0.03570 end
o 4 0.0 0.01428 end
cu 5 0.0 8.44384e-2 end
o 5 0.0 1.00651e-4 end
c 5 0.0 1.78929e-5 end
cu 6 0.0 8.33333E-2 end
cd 6 0.0 4.71679E-4 end
sn 6 0.0 1.13027E-4 end
al 7 0.0 5.88742E-2 end
fe 7 0.0 2.03213E-4 end
si 7 0.0 2.309E-4 end
end comp
buckledslab vacuum reflected 0.0 46.17 46.71 end
1 12.3753 oneextermod
2 27.3753 noextermod
end zone
EXPT 1547-21; CSAS25/KENO-Va; 2/12/92
read para
gen=303 tme=60 flx=yes fdn=yes pki=yes nub=yes
end para
read geom
box type 1
cuboid 1 1 2.545 -2.545 2.545 -2.545 2.545 -2.545
cuboid 2 1 2.5605 -2.5605 2.5685 -2.5685 2.5605 -2.5605
cuboid 3 1 2.565 -2.565 2.595 -2.595 2.565 -2.565
box type 2
cuboid 1 1 2.545 -2.545 2.545 -2.545 1.70 -1.70
cuboid 2 1 2.5605 -2.5605 2.5685 -2.5685 1.7155 -1.7155
cuboid 3 1 2.565 -2.565 2.595 -2.595 1.72 -1.72
box type 3
cuboid 1 1 2.545 -2.545 2.545 -2.545 0.692 -0.692
cuboid 2 1 2.5605 -2.5605 2.5685 -2.5685 0.7075 -0.7075
cuboid 3 1 2.565 -2.565 2.595 -2.595 0.712 -0.712
box type 4
cuboid 1 1 2.545 -2.545 2.545 -2.545 0.079 -0.079
cuboid 2 1 2.5605 -2.5605 2.5685 -2.5685 0.0945 -0.0945
cuboid 3 1 2.565 -2.565 2.595 -2.595 0.099 -0.099
box type 5
cuboid 7 1 2.565 -2.565 2.595 -2.595 1.338 -1.338
cuboid 3 1 2.565 -2.565 2.595 -2.595 1.375 -1.375
corebdy 0 1 0.0 0.0 0.0
reflector 4 2 15.0 15.0 15.0 15.0 15.0 5

```

```
end geom
read array
nux=9 nuy=9 nuz=10
loop
2 1 9 1 1 9 1 1 3 1
5 1 9 1 1 9 1 4 4 1
1 1 9 1 1 9 1 5 6 1
3 1 9 1 1 9 1 7 9 1
4 1 9 1 1 9 1 10 10 1
end loop
end array
read bias
id=400 2 2 end bias
end data
end
```

```

#csas25
EXPT 1547-22; CSAS28; 2/12/92; Hansen-Roach CROSS SECTIONS
hansen-roach
multiregion
am-241 1 0.0 5.80105E-7 end
pu-239 1 0.0 1.954E-4 end
pu-240 1 0.0 1.702E-5 end
pu-241 1 0.0 1.03449E-6 end
u-235 1 0.0 1.904E-6 end
u-238 1 0.0 1.252E-3 end
h 1 0.0 4.489E-2 end
c 1 0.0 4.412E-2 end
o 1 0.0 3.023E-3 end
h 2 0.0 4.489E-2 end
c 2 0.0 3.110E-2 end
cl 2 0.0 0.724E-2 end
n 3 0.0 1.98881e-5 end
o 3 0.0 5.33497e-6 end
h 4 0.0 0.05712 end
c 4 0.0 0.03570 end
o 4 0.0 0.01428 end
cu 5 0.0 8.44384e-2 end
o 5 0.0 1.00651e-4 end
c 5 0.0 1.78929e-5 end
cu 6 0.0 8.33333E-2 end
cd 6 0.0 4.71679E-4 end
sn 6 0.0 1.13027E-4 end
al 7 0.0 5.88742E-2 end
fe 7 0.0 2.03213E-4 end
si 7 0.0 2.309E-4 end
end comp
buckledslab vacuum reflected 0.0 46.17 46.71 end
1 11.8155 oneextermod
2 26.8155 noextermod
end zone
EXPT 1547-22; CSAS25/KENO-Va; 2/12/92
read para
gen=303 tme=60 flx=yes fdn=yes pki=yes nub=yes
end para
read geom
box type 1
cuboid 1 1 2.545 -2.545 2.545 -2.545 2.545 -2.545
cuboid 2 1 2.5605 -2.5605 2.5685 -2.5685 2.5605 -2.5605
cuboid 3 1 2.565 -2.565 2.595 -2.595 2.565 -2.565
box type 2
cuboid 1 1 2.545 -2.545 2.545 -2.545 1.70 -1.70
cuboid 2 1 2.5605 -2.5605 2.5685 -2.5685 1.7155 -1.7155
cuboid 3 1 2.565 -2.565 2.595 -2.595 1.72 -1.72
box type 3
cuboid 1 1 2.545 -2.545 2.545 -2.545 0.692 -0.692
cuboid 2 1 2.5605 -2.5605 2.5685 -2.5685 0.7075 -0.7075
cuboid 3 1 2.565 -2.565 2.595 -2.595 0.712 -0.712
box type 4
cuboid 1 1 2.545 -2.545 2.545 -2.545 0.1745 -0.1745
cuboid 2 1 2.5605 -2.5605 2.5685 -2.5685 0.19 -0.19
cuboid 3 1 2.565 -2.565 2.595 -2.595 0.1945 -0.1945
box type 5
cuboid 5 1 2.565 -2.565 2.595 -2.595 0.1685 -0.1685
cuboid 3 1 2.565 -2.565 2.595 -2.595 0.20 -0.20
corebdy 0 1 0.0 0.0 0.0
reflector 4 2 15.0 15.0 15.0 15.0 15.0 5

```

```
end geom
read array
nux=9 nuy=9 nuz=9
loop
2 1 9 1 1 9 1 1 3 1
1 1 9 1 1 9 1 4 4 1
5 1 9 1 1 9 1 5 5 1
1 1 9 1 1 9 1 6 6 1
3 1 9 1 1 9 1 7 8 1
4 1 9 1 1 9 1 9 9 1
end loop
end array
read bias
id=400 2 2 end bias
end data
end
```

```

#csas25
EXPT 1547-23; CSAS28; 2/12/92; Hansen-Roach CROSS SECTIONS
hansen-roach
multiregion
am-241 1 0.0 5.80105E-7 end
pu-239 1 0.0 1.954E-4 end
pu-240 1 0.0 1.702E-5 end
pu-241 1 0.0 1.03449E-6 end
u-235 1 0.0 1.904E-6 end
u-238 1 0.0 1.252E-3 end
h 1 0.0 4.489E-2 end
c 1 0.0 4.412E-2 end
o 1 0.0 3.023E-3 end
h 2 0.0 4.489E-2 end
c 2 0.0 3.110E-2 end
cl 2 0.0 0.724E-2 end
n 3 0.0 1.98881e-5 end
o 3 0.0 5.33497e-6 end
h 4 0.0 0.05712 end
c 4 0.0 0.03570 end
o 4 0.0 0.01428 end
cu 5 0.0 8.44384e-2 end
o 5 0.0 1.00651e-4 end
c 5 0.0 1.78929e-5 end
cu 6 0.0 8.33333E-2 end
cd 6 0.0 4.71679E-4 end
sn 6 0.0 1.13027E-4 end
al 7 0.0 5.88742E-2 end
fe 7 0.0 2.03213E-4 end
si 7 0.0 2.309E-4 end
end comp
buckledslab vacuum reflected 0.0 46.17 46.71 end
1 13.3938 oneextermod
2 28.3938 noextermod
end zone
EXPT 1547-23; CSAS25/KENO-Va; 2/12/92
read para
gen=303 tme=60 flx=yes fdn=yes pki=yes nub=yes
end para
read geom
box type 1
cuboid 1 1 2.545 -2.545 2.545 -2.545 2.545 -2.545
cuboid 2 1 2.5605 -2.5605 2.5685 -2.5685 2.5605 -2.5605
cuboid 3 1 2.565 -2.565 2.595 -2.595 2.565 -2.565
box type 2
cuboid 1 1 2.545 -2.545 2.545 -2.545 1.70 -1.70
cuboid 2 1 2.5605 -2.5605 2.5685 -2.5685 1.7155 -1.7155
cuboid 3 1 2.565 -2.565 2.595 -2.595 1.72 -1.72
box type 3
cuboid 1 1 2.545 -2.545 2.545 -2.545 0.692 -0.692
cuboid 2 1 2.5605 -2.5605 2.5685 -2.5685 0.7075 -0.7075
cuboid 3 1 2.565 -2.565 2.595 -2.595 0.712 -0.712
box type 4
cuboid 1 1 2.545 -2.545 2.545 -2.545 0.475 -0.475
cuboid 2 1 2.5605 -2.5605 2.5685 -2.5685 0.4915 -0.4915
cuboid 3 1 2.565 -2.565 2.595 -2.595 0.496 -0.496
box type 5
cuboid 6 1 2.565 -2.565 2.595 -2.595 0.184 -0.184
cuboid 3 1 2.565 -2.565 2.595 -2.595 0.215 -0.215
corebdy 0 1 0.0 0.0 0.0
reflector 4 2 15.0 15.0 15.0 15.0 15.0 5

```

```
end geom
read array
nux=9 nuy=9 nuz=8
loop
2 1 9 1 1 9 1 1 1 3 1
1 1 9 1 1 9 1 4 4 1
5 1 9 1 1 9 1 5 5 1
1 1 9 1 1 9 1 6 7 1
4 1 9 1 1 9 1 8 8 1
end loop
end array
read bias
id=400 2 2 end bias
end data
end
```

```

#csas25
EXPT 1547-24; CSAS28; 2/12/92; Hansen-Roach CROSS SECTIONS
hansen-roach
multiregion
am-241 1 0.0 5.80105E-7 end
pu-239 1 0.0 1.954E-4 end
pu-240 1 0.0 1.702E-5 end
pu-241 1 0.0 1.03449E-6 end
u-235 1 0.0 1.904E-6 end
u-238 1 0.0 1.252E-3 end
h 1 0.0 4.489E-2 end
c 1 0.0 4.412E-2 end
o 1 0.0 3.023E-3 end
h 2 0.0 4.489E-2 end
c 2 0.0 3.110E-2 end
cl 2 0.0 0.724E-2 end
n 3 0.0 1.98881e-5 end
o 3 0.0 5.33497e-6 end
h 4 0.0 0.05712 end
c 4 0.0 0.03570 end
o 4 0.0 0.01428 end
cu 5 0.0 8.44384e-2 end
o 5 0.0 1.00651e-4 end
c 5 0.0 1.78929e-5 end
cu 6 0.0 8.33333E-2 end
cd 6 0.0 4.71679E-4 end
sn 6 0.0 1.13027E-4 end
al 7 0.0 5.88742E-2 end
fe 7 0.0 2.03213E-4 end
si 7 0.0 2.309E-4 end
end comp
buckledslab vacuum reflected 0.0 46.17 46.71 end
1 12.5864 oneextermod
2 27.5864 noextermod
end zone
EXPT 1547-24; CSAS25/KENO-Va; 2/12/92
read para
gen=303 tme=60 flx=yes fdn=yes pki=yes nub=yes
end para
read geom
box type 1
cuboid 1 1 2.545 -2.545 2.545 -2.545 2.545 -2.545
cuboid 2 1 2.5605 -2.5605 2.5685 -2.5685 2.5605 -2.5605
cuboid 3 1 2.565 -2.565 2.595 -2.595 2.565 -2.565
box type 2
cuboid 1 1 2.545 -2.545 2.545 -2.545 1.70 -1.70
cuboid 2 1 2.5605 -2.5605 2.5685 -2.5685 1.7155 -1.7155
cuboid 3 1 2.565 -2.565 2.595 -2.595 1.72 -1.72
box type 3
cuboid 1 1 2.545 -2.545 2.545 -2.545 0.692 -0.692
cuboid 2 1 2.5605 -2.5605 2.5685 -2.5685 0.7075 -0.7075
cuboid 3 1 2.565 -2.565 2.595 -2.595 0.712 -0.712
box type 4
cuboid 1 1 2.545 -2.545 2.545 -2.545 0.2315 -0.2315
cuboid 2 1 2.5605 -2.5605 2.5685 -2.5685 0.247 -0.247
cuboid 3 1 2.565 -2.565 2.595 -2.595 0.2515 -0.2515
box type 5
cuboid 6 1 2.565 -2.565 2.595 -2.595 0.184 -0.184
cuboid 3 1 2.565 -2.565 2.595 -2.595 0.215 -0.215
corebdy 0 1 0.0 0.0 0.0
reflector 4 2 15.0 15.0 15.0 15.0 15.0 5

```

```
end geom
read array
nux=9 nuy=9 nuz=10
loop
2 1 9 1 1 9 1 1 3 1
1 1 9 1 1 9 1 4 5 1
5 1 9 1 1 9 1 6 6 1
3 1 9 1 1 9 1 7 9 1
4 1 9 1 1 9 1 10 10 1
end loop
end array
read bias
id=400 2 2 end bias
end data
end
```

```

#csas25
EXPT 1547-25; CSAS28; 2/12/92; Hansen-Roach CROSS SECTIONS
hansen-roach
multiregion
am-241 1 0.0 5.80105E-7 end
pu-239 1 0.0 1.954E-4 end
pu-240 1 0.0 1.702E-5 end
pu-241 1 0.0 1.03449E-6 end
u-235 1 0.0 1.904E-6 end
u-238 1 0.0 1.252E-3 end
h 1 0.0 4.489E-2 end
c 1 0.0 4.412E-2 end
o 1 0.0 3.023E-3 end
h 2 0.0 4.489E-2 end
c 2 0.0 3.110E-2 end
cl 2 0.0 0.724E-2 end
n 3 0.0 1.98881e-5 end
o 3 0.0 5.33497e-6 end
h 4 0.0 0.05712 end
c 4 0.0 0.03570 end
o 4 0.0 0.01428 end
cu 5 0.0 8.44384e-2 end
o 5 0.0 1.00651e-4 end
c 5 0.0 1.78929e-5 end
cu 6 0.0 8.33333E-2 end
cd 6 0.0 4.71679E-4 end
sn 6 0.0 1.13027E-4 end
al 7 0.0 5.88742E-2 end
fe 7 0.0 2.03213E-4 end
si 7 0.0 2.309E-4 end
end comp
buckledslab vacuum reflected 0.0 46.17 46.71 end
1 12.6833 oneextermod
2 27.6833 noextermod
end zone
EXPT 1547-25; CSAS25/KENO-Va; 2/12/92
read para
gen=303 tme=60 flx=yes fdn=yes pki=yes nub=yes
end para
read geom
box type 1
cuboid 1 1 2.545 -2.545 2.545 -2.545 2.545 -2.545
cuboid 2 1 2.5605 -2.5605 2.5685 -2.5685 2.5605 -2.5605
cuboid 3 1 2.565 -2.565 2.595 -2.595 2.565 -2.565
box type 2
cuboid 1 1 2.545 -2.545 2.545 -2.545 1.70 -1.70
cuboid 2 1 2.5605 -2.5605 2.5685 -2.5685 1.7155 -1.7155
cuboid 3 1 2.565 -2.565 2.595 -2.595 1.72 -1.72
box type 3
cuboid 1 1 2.545 -2.545 2.545 -2.545 0.692 -0.692
cuboid 2 1 2.5605 -2.5605 2.5685 -2.5685 0.7075 -0.7075
cuboid 3 1 2.565 -2.565 2.595 -2.595 0.712 -0.712
box type 4
cuboid 1 1 2.545 -2.545 2.545 -2.545 0.3015 -0.3015
cuboid 2 1 2.5605 -2.5605 2.5685 -2.5685 0.317 -0.317
cuboid 3 1 2.565 -2.565 2.595 -2.595 0.3215 -0.3215
box type 5
cuboid 5 1 2.565 -2.565 2.595 -2.595 0.1685 -0.1685
cuboid 3 1 2.565 -2.565 2.595 -2.595 0.185 -0.185
box type 6
cuboid 5 1 2.565 -2.565 2.595 -2.595 0.1685 -0.1685

```

```
cuboid 3 1 2.565 -2.565 2.595 -2.595 0.185 -0.185
corebdy 0 1 0.0 0.0 0.0
reflector 4 2 15.0 15.0 15.0 15.0 15.0 15.0 5
end geom
read array
nux=9 nuy=9 nuz=11
loop
2 1 9 1 1 9 1 1 3 1
5 1 9 1 1 9 1 4 4 1
1 1 9 1 1 9 1 5 5 1
6 1 9 1 1 9 1 6 6 1
1 1 9 1 1 9 1 7 7 1
3 1 9 1 1 9 1 8 10 1
4 1 9 1 1 9 1 11 11 1
end loop
end array
read bias
id=400 2 2 end bias
end data
end
```

```

#csas25
EXPT 1547-26; CSAS28; 2/13/92; Hansen-Roach CROSS SECTIONS
hansen-roach
multiregion
am-241 1 0.0 5.80105E-7 end
pu-239 1 0.0 1.954E-4 end
pu-240 1 0.0 1.702E-5 end
pu-241 1 0.0 1.03449E-6 end
u-235 1 0.0 1.904E-6 end
u-238 1 0.0 1.252E-3 end
h 1 0.0 4.489E-2 end
c 1 0.0 4.412E-2 end
o 1 0.0 3.023E-3 end
h 2 0.0 4.489E-2 end
c 2 0.0 3.110E-2 end
cl 2 0.0 0.724E-2 end
n 3 0.0 1.98881e-5 end
o 3 0.0 5.33497e-6 end
h 4 0.0 0.05712 end
c 4 0.0 0.03570 end
o 4 0.0 0.01428 end
cu 5 0.0 8.44384e-2 end
o 5 0.0 1.00651e-4 end
c 5 0.0 1.78929e-5 end
cu 6 0.0 8.33333E-2 end
cd 6 0.0 4.71679E-4 end
sn 6 0.0 1.13027E-4 end
al 7 0.0 5.88742E-2 end
fe 7 0.0 2.03213E-4 end
si 7 0.0 2.309E-4 end
end comp
buckledslab vacuum reflected 0.0 46.17 46.71 end
1 15.2151 oneextermod
2 30.2151 noextermod
end zone
EXPT 1547-26; CSAS25/KENO-Va; 2/13/92
read para
gen=303 tme=60 flx=yes fdn=yes pki=yes nub=yes
end para
read geom
box type 1
cuboid 1 1 2.545 -2.545 2.545 -2.545 2.545 -2.545
cuboid 2 1 2.5605 -2.5605 2.5685 -2.5685 2.5605 -2.5605
cuboid 3 1 2.565 -2.565 2.595 -2.595 2.565 -2.565
box type 2
cuboid 1 1 2.545 -2.545 2.545 -2.545 1.70 -1.70
cuboid 2 1 2.5605 -2.5605 2.5685 -2.5685 1.7155 -1.7155
cuboid 3 1 2.565 -2.565 2.595 -2.595 1.72 -1.72
box type 3
cuboid 1 1 2.545 -2.545 2.545 -2.545 0.692 -0.692
cuboid 2 1 2.5605 -2.5605 2.5685 -2.5685 0.7075 -0.7075
cuboid 3 1 2.565 -2.565 2.595 -2.595 0.712 -0.712
box type 4
cuboid 1 1 2.545 -2.545 2.545 -2.545 0.292 -0.292
cuboid 2 1 2.5605 -2.5605 2.5685 -2.5685 0.3075 -0.3075
cuboid 3 1 2.565 -2.565 2.595 -2.595 0.312 -0.312
box type 5
cuboid 5 1 2.565 -2.565 2.595 -2.595 0.645 -0.645
cuboid 3 1 2.565 -2.565 2.595 -2.595 0.665 -0.665
box type 6
cuboid 5 1 2.565 -2.565 2.595 -2.595 0.645 -0.645

```

```
cuboid 3 1 2.565 -2.565 2.595 -2.595 0.665 -0.665
corebdy 0 1 0.0 0.0 0.0
reflector 4 2 15.0 15.0 15.0 15.0 15.0 15.0 5
end geom
read array
nux=9 nuy=9 nuz=12
loop
2 1 9 1 1 9 1 1 3 1
5 1 9 1 1 9 1 4 4 1
1 1 9 1 1 9 1 5 5 1
6 1 9 1 1 9 1 6 6 1
1 1 9 1 1 9 1 7 8 1
3 1 9 1 1 9 1 9 11 1
4 1 9 1 1 9 1 12 12 1
end loop
end array
read bias
id=400 2 2 end bias
end data
end
```

```

#csas25
EXPT 1547-27; CSAS28; 2/13/92; Hansen-Roach CROSS SECTIONS
hansen-roach
multiregion
am-241 1 0.0 5.80105E-7 end
pu-239 1 0.0 1.954E-4 end
pu-240 1 0.0 1.702E-5 end
pu-241 1 0.0 1.03449E-6 end
u-235 1 0.0 1.904E-6 end
u-238 1 0.0 1.252E-3 end
h 1 0.0 4.489E-2 end
c 1 0.0 4.412E-2 end
o 1 0.0 3.023E-3 end
h 2 0.0 4.489E-2 end
c 2 0.0 3.110E-2 end
cl 2 0.0 0.724E-2 end
n 3 0.0 1.98881e-5 end
o 3 0.0 5.33497e-6 end
h 4 0.0 0.05712 end
c 4 0.0 0.03570 end
o 4 0.0 0.01428 end
cu 5 0.0 8.44384e-2 end
o 5 0.0 1.00651e-4 end
c 5 0.0 1.78929e-5 end
cu 6 0.0 8.33333E-2 end
cd 6 0.0 4.71679E-4 end
sn 6 0.0 1.13027E-4 end
al 7 0.0 5.88742E-2 end
fe 7 0.0 2.03213E-4 end
si 7 0.0 2.309E-4 end
end comp
buckledslab vacuum reflected 0.0 46.17 46.71 end
1 16.0613 oneextermod
2 31.0613 noextermod
end zone
EXPT 1547-27; CSAS25/KENO-Va; 2/13/92
read para
gen=303 tme=60 flx=yes fdn=yes pki=yes nub=yes
end para
read geom
box type 1
cuboid 1 1 2.545 -2.545 2.545 -2.545 2.545 -2.545
cuboid 2 1 2.5605 -2.5605 2.5685 -2.5685 2.5605 -2.5605
cuboid 3 1 2.565 -2.565 2.595 -2.595 2.565 -2.565
box type 2
cuboid 1 1 2.545 -2.545 2.545 -2.545 1.70 -1.70
cuboid 2 1 2.5605 -2.5605 2.5685 -2.5685 1.7155 -1.7155
cuboid 3 1 2.565 -2.565 2.595 -2.595 1.72 -1.72
box type 3
cuboid 1 1 2.545 -2.545 2.545 -2.545 0.692 -0.692
cuboid 2 1 2.5605 -2.5605 2.5685 -2.5685 0.7075 -0.7075
cuboid 3 1 2.565 -2.565 2.595 -2.595 0.712 -0.712
box type 4
cuboid 1 1 2.545 -2.545 2.545 -2.545 0.0645 -0.0645
cuboid 2 1 2.5605 -2.5605 2.5685 -2.5685 0.08 -0.08
cuboid 3 1 2.565 -2.565 2.595 -2.595 0.0845 -0.0845
box type 5
cuboid 5 1 2.565 -2.565 2.595 -2.595 0.9635 -0.9635
cuboid 3 1 2.565 -2.565 2.595 -2.595 0.99 -0.99
box type 6
cuboid 5 1 2.565 -2.565 2.595 -2.595 0.9635 -0.9635

```

```
cuboid 3 1 2.565 -2.565 2.595 -2.595 0.99 -0.99
corebdy 0 1 0.0 0.0 0.0
reflector 4 2 15.0 15.0 15.0 15.0 15.0 15.0 5
end geom
read array
nux=9 nuy=9 nuz=11
loop
2 1 9 1 1 9 1 1 3 1
5 1 9 1 1 9 1 4 4 1
1 1 9 1 1 9 1 5 5 1
6 1 9 1 1 9 1 6 6 1
1 1 9 1 1 9 1 7 9 1
3 1 9 1 1 9 1 10 10 1
4 1 9 1 1 9 1 11 11 1
end loop
end array
read bias
id=400 2 2 end bias
end data
end
```

```

#csas25
EXPT 1547-28; CSAS28; 2/13/92; Hansen-Roach CROSS SECTIONS
hansen-roach
multiregion
am-241 1 0.0 5.80105E-7 end
pu-239 1 0.0 1.954E-4 end
pu-240 1 0.0 1.702E-5 end
pu-241 1 0.0 1.03449E-6 end
u-235 1 0.0 1.904E-6 end
u-238 1 0.0 1.252E-3 end
h 1 0.0 4.489E-2 end
c 1 0.0 4.412E-2 end
o 1 0.0 3.023E-3 end
h 2 0.0 4.489E-2 end
c 2 0.0 3.110E-2 end
cl 2 0.0 0.724E-2 end
n 3 0.0 1.98881e-5 end
o 3 0.0 5.33497e-6 end
h 4 0.0 0.05712 end
c 4 0.0 0.03570 end
o 4 0.0 0.01428 end
cu 5 0.0 8.44384e-2 end
o 5 0.0 1.00651e-4 end
c 5 0.0 1.78929e-5 end
cu 6 0.0 8.33333E-2 end
cd 6 0.0 4.71679E-4 end
sn 6 0.0 1.13027E-4 end
al 7 0.0 5.88742E-2 end
fe 7 0.0 2.03213E-4 end
si 7 0.0 2.309E-4 end
end comp
buckledslab vacuum reflected 0.0 46.17 46.71 end
1 16.7277 oneextermod
2 31.7277 noextermod
end zone
EXPT 1547-28; CSAS25/KENO-Va; 2/13/92
read para
gen=303 tme=60 flx=yes fdn=yes pki=yes nub=yes
end para
read geom
box type 1
cuboid 1 1 2.545 -2.545 2.545 -2.545 2.545 -2.545
cuboid 2 1 2.5605 -2.5605 2.5685 -2.5685 2.5605 -2.5605
cuboid 3 1 2.565 -2.565 2.595 -2.595 2.565 -2.565
box type 2
cuboid 1 1 2.545 -2.545 2.545 -2.545 1.70 -1.70
cuboid 2 1 2.5605 -2.5605 2.5685 -2.5685 1.7155 -1.7155
cuboid 3 1 2.565 -2.565 2.595 -2.595 1.72 -1.72
box type 3
cuboid 1 1 2.545 -2.545 2.545 -2.545 0.692 -0.692
cuboid 2 1 2.5605 -2.5605 2.5685 -2.5685 0.7075 -0.7075
cuboid 3 1 2.565 -2.565 2.595 -2.595 0.712 -0.712
box type 4
cuboid 1 1 2.545 -2.545 2.545 -2.545 0.046 -0.046
cuboid 2 1 2.5605 -2.5605 2.5685 -2.5685 0.0615 -0.0615
cuboid 3 1 2.565 -2.565 2.595 -2.595 0.066 -0.066
box type 5
cuboid 5 1 2.565 -2.565 2.595 -2.595 1.2825 -1.2825
cuboid 3 1 2.565 -2.565 2.595 -2.595 1.34 -1.34
box type 6
cuboid 5 1 2.565 -2.565 2.595 -2.595 1.2825 -1.2825

```

```
cuboid 3 1 2.565 -2.565 2.595 -2.595 1.34 -1.34
corebdy 0 1 0.0 0.0 0.0
reflector 4 2 15.0 15.0 15.0 15.0 15.0 15.0 5
end geom
read array
nux=9 nuy=9 nuz=12
loop
2 1 9 1 1 9 1 1 3 1
5 1 9 1 1 9 1 4 4 1
1 1 9 1 1 9 1 5 5 1
6 1 9 1 1 9 1 6 6 1
1 1 9 1 1 9 1 7 9 1
3 1 9 1 1 9 1 10 11 1
4 1 9 1 1 9 1 12 12 1
end loop
end array
read bias
id=400 2 2 end bias
end data
end
```

```

#csas25
EXPT 1547-29; CSAS28; 2/13/92; Hansen-Roach CROSS SECTIONS
hansen-roach
multiregion
am-241 1 0.0 5.80105E-7 end
pu-239 1 0.0 1.954E-4 end
pu-240 1 0.0 1.702E-5 end
pu-241 1 0.0 1.03449E-6 end
u-235 1 0.0 1.904E-6 end
u-238 1 0.0 1.252E-3 end
h 1 0.0 4.489E-2 end
c 1 0.0 4.412E-2 end
o 1 0.0 3.023E-3 end
h 2 0.0 4.489E-2 end
c 2 0.0 3.110E-2 end
cl 2 0.0 0.724E-2 end
n 3 0.0 1.98881e-5 end
o 3 0.0 5.33497e-6 end
h 4 0.0 0.05712 end
c 4 0.0 0.03570 end
o 4 0.0 0.01428 end
cu 5 0.0 8.44384e-2 end
o 5 0.0 1.00651e-4 end
c 5 0.0 1.78929e-5 end
cu 6 0.0 8.33333E-2 end
cd 6 0.0 4.71679E-4 end
sn 6 0.0 1.13027E-4 end
al 7 0.0 5.88742E-2 end
fe 7 0.0 2.03213E-4 end
si 7 0.0 2.309E-4 end
end comp
buckledslab vacuum reflected 0.0 46.17 46.71 end
1 15.5091 oneextermod
2 30.5091 noextermod
end zone
EXPT 1547-29; CSAS25/KENO-Va; 2/13/92
read para
gen=303 tme=60 flx=yes fdn=yes pki=yes nub=yes
end para
read geom
box type 1
cuboid 1 1 2.545 -2.545 2.545 -2.545 2.545 -2.545
cuboid 2 1 2.5605 -2.5605 2.5685 -2.5685 2.5605 -2.5605
cuboid 3 1 2.565 -2.565 2.595 -2.595 2.565 -2.565
box type 2
cuboid 1 1 2.545 -2.545 2.545 -2.545 1.70 -1.70
cuboid 2 1 2.5605 -2.5605 2.5685 -2.5685 1.7155 -1.7155
cuboid 3 1 2.565 -2.565 2.595 -2.595 1.72 -1.72
box type 3
cuboid 1 1 2.545 -2.545 2.545 -2.545 0.692 -0.692
cuboid 2 1 2.5605 -2.5605 2.5685 -2.5685 0.7075 -0.7075
cuboid 3 1 2.565 -2.565 2.595 -2.595 0.712 -0.712
box type 4
cuboid 1 1 2.545 -2.545 2.545 -2.545 0.1655 -0.1655
cuboid 2 1 2.5605 -2.5605 2.5685 -2.5685 0.181 -0.181
cuboid 3 1 2.565 -2.565 2.595 -2.595 0.1855 -0.1855
box type 5
cuboid 6 1 2.565 -2.565 2.595 -2.595 0.184 -0.184
cuboid 3 1 2.565 -2.565 2.595 -2.595 0.205 -0.205
box type 6
cuboid 6 1 2.565 -2.565 2.595 -2.595 0.177 -0.177

```

```
cuboid 3 1 2.565 -2.565 2.595 -2.595 0.195 -0.195
corebdy 0 1 0.0 0.0 0.0
reflector 4 2 15.0 15.0 15.0 15.0 15.0 15.0 5
end geom
read array
nux=9 nuy=9 nuz=10
loop
2 1 9 1 1 9 1 1 3 1
5 1 9 1 1 9 1 4 4 1
1 1 9 1 1 9 1 5 5 1
6 1 9 1 1 9 1 6 6 1
1 1 9 1 1 9 1 7 9 1
4 1 9 1 1 9 1 10 10 1
end loop
end array
read bias
id=400 2 2 end bias
end data
end
```

```

#csas25
EXPT 1547-30; CSAS28; 2/13/92; Hansen-Roach CROSS SECTIONS
hansen-roach
multiregion
am-241 1 0.0 5.80105E-7 end
pu-239 1 0.0 1.954E-4 end
pu-240 1 0.0 1.702E-5 end
pu-241 1 0.0 1.03449E-6 end
u-235 1 0.0 1.904E-6 end
u-238 1 0.0 1.252E-3 end
h 1 0.0 4.489E-2 end
c 1 0.0 4.412E-2 end
o 1 0.0 3.023E-3 end
h 2 0.0 4.489E-2 end
c 2 0.0 3.110E-2 end
cl 2 0.0 0.724E-2 end
n 3 0.0 1.98881e-5 end
o 3 0.0 5.33497e-6 end
h 4 0.0 0.05712 end
c 4 0.0 0.03570 end
o 4 0.0 0.01428 end
cu 5 0.0 8.44384e-2 end
o 5 0.0 1.00651e-4 end
c 5 0.0 1.78929e-5 end
cu 6 0.0 8.33333E-2 end
cd 6 0.0 4.71679E-4 end
sn 6 0.0 1.13027E-4 end
al 7 0.0 5.88742E-2 end
fe 7 0.0 2.03213E-4 end
si 7 0.0 2.309E-4 end
end comp
buckledslab vacuum reflected 0.0 46.17 46.71 end
1 11.4439 oneextermod
2 26.4439 noextermod
end zone
EXPT 1547-30; CSAS25/KENO-Va; 2/13/92
read para
gen=303 tme=60 flx=yes fdn=yes pki=yes nub=yes
end para
read geom
box type 1
cuboid 1 1 2.545 -2.545 2.545 -2.545 2.545 -2.545
cuboid 2 1 2.5605 -2.5605 2.5685 -2.5685 2.5605 -2.5605
cuboid 3 1 2.565 -2.565 2.595 -2.595 2.565 -2.565
box type 2
cuboid 1 1 2.545 -2.545 2.545 -2.545 1.70 -1.70
cuboid 2 1 2.5605 -2.5605 2.5685 -2.5685 1.7155 -1.7155
cuboid 3 1 2.565 -2.565 2.595 -2.595 1.72 -1.72
box type 3
cuboid 1 1 2.545 -2.545 2.545 -2.545 0.692 -0.692
cuboid 2 1 2.5605 -2.5605 2.5685 -2.5685 0.7075 -0.7075
cuboid 3 1 2.565 -2.565 2.595 -2.595 0.712 -0.712
box type 4
cuboid 1 1 2.545 -2.545 2.545 -2.545 0.406 -0.406
cuboid 2 1 2.5605 -2.5605 2.5685 -2.5685 0.4215 -0.4215
cuboid 3 1 2.565 -2.565 2.595 -2.595 0.426 -0.426
box type 5
cuboid 7 1 2.565 -2.565 2.595 -2.595 0.158 -0.158
cuboid 3 1 2.565 -2.565 2.595 -2.595 0.17 -0.17
box type 6
cuboid 7 1 2.565 -2.565 2.595 -2.595 0.1585 -0.1585

```

```
cuboid 3 1 2.565 -2.565 2.595 -2.595 0.17 -0.17
corebdy 0 1 0.0 0.0 0.0
reflector 4 2 15.0 15.0 15.0 15.0 15.0 15.0 5
end geom
read array
nux=9 nuy=9 nuz=9
loop
2 1 9 1 1 9 1 1 3 1
5 1 9 1 1 9 1 4 4 1
1 1 9 1 1 9 1 5 5 1
6 1 9 1 1 9 1 6 6 1
1 1 9 1 1 9 1 7 7 1
3 1 9 1 1 9 1 8 8 1
4 1 9 1 1 9 1 9 9 1
end loop
end array
read bias
id=400 2 2 end bias
end data
end
```

```

#csas25
EXPT 1547-31; CSAS28; 2/13/92; Hansen-Roach CROSS SECTIONS
hansen-roach
multiregion
am-241 1 0.0 5.80105E-7 end
pu-239 1 0.0 1.954E-4 end
pu-240 1 0.0 1.702E-5 end
pu-241 1 0.0 1.03449E-6 end
u-235 1 0.0 1.904E-6 end
u-238 1 0.0 1.252E-3 end
h 1 0.0 4.489E-2 end
c 1 0.0 4.412E-2 end
o 1 0.0 3.023E-3 end
h 2 0.0 4.489E-2 end
c 2 0.0 3.110E-2 end
cl 2 0.0 0.724E-2 end
n 3 0.0 1.98881e-5 end
o 3 0.0 5.33497e-6 end
h 4 0.0 0.05712 end
c 4 0.0 0.03570 end
o 4 0.0 0.01428 end
cu 5 0.0 8.44384e-2 end
o 5 0.0 1.00651e-4 end
c 5 0.0 1.78929e-5 end
cu 6 0.0 8.33333E-2 end
cd 6 0.0 4.71679E-4 end
sn 6 0.0 1.13027E-4 end
al 7 0.0 5.88742E-2 end
fe 7 0.0 2.03213E-4 end
si 7 0.0 2.309E-4 end
end comp
buckledslab vacuum reflected 0.0 46.17 46.71 end
1 13.5315 oneextermod
2 28.5315 noextermod
end zone
EXPT 1547-31; CSAS25/KENO-Va; 2/13/92
read para
gen=303 tme=60 flx=yes fdn=yes pki=yes nub=yes
end para
read geom
box type 1
cuboid 1 1 2.545 -2.545 2.545 -2.545 2.545 -2.545
cuboid 2 1 2.5605 -2.5605 2.5685 -2.5685 2.5605 -2.5605
cuboid 3 1 2.565 -2.565 2.595 -2.595 2.565 -2.565
box type 2
cuboid 1 1 2.545 -2.545 2.545 -2.545 1.70 -1.70
cuboid 2 1 2.5605 -2.5605 2.5685 -2.5685 1.7155 -1.7155
cuboid 3 1 2.565 -2.565 2.595 -2.595 1.72 -1.72
box type 3
cuboid 1 1 2.545 -2.545 2.545 -2.545 0.692 -0.692
cuboid 2 1 2.5605 -2.5605 2.5685 -2.5685 0.7075 -0.7075
cuboid 3 1 2.565 -2.565 2.595 -2.595 0.712 -0.712
box type 4
cuboid 1 1 2.545 -2.545 2.545 -2.545 0.0755 -0.0755
cuboid 2 1 2.5605 -2.5605 2.5685 -2.5685 0.091 -0.091
cuboid 3 1 2.565 -2.565 2.595 -2.595 0.0955 -0.0955
box type 5
cuboid 7 1 2.565 -2.565 2.595 -2.595 1.314 -1.314
cuboid 3 1 2.565 -2.565 2.595 -2.595 1.34 -1.34
box type 6
cuboid 7 1 2.565 -2.565 2.595 -2.595 1.3145 -1.3145

```

```
cuboid 3 1 2.565 -2.565 2.595 -2.595 1.345 -1.345
corebdy 0 1 0.0 0.0 0.0
reflector 4 2 15.0 15.0 15.0 15.0 15.0 15.0 5
end geom
read array
nux=9 nuy=9 nuz=10
loop
2 1 9 1 1 9 1 1 3 1
5 1 9 1 1 9 1 4 4 1
1 1 9 1 1 9 1 5 5 1
6 1 9 1 1 9 1 6 6 1
1 1 9 1 1 9 1 7 8 1
3 1 9 1 1 9 1 9 9 1
4 1 9 1 1 9 1 10 10 1
end loop
end array
read bias
id=400 2 2 end bias
end data
end
```

```
#csas25
EXPT 1677-02; CSAS25; 2/4/92; Hansen-Roach CROSS SECTIONS
hansen-roach
multiregion
am-241 1 0.0 3.511e-7 end
pu-239 1 0.0 2.578e-4 end
pu-240 1 0.0 2.257e-5 end
pu-241 1 0.0 1.756e-6 end
o 1 0.0 1.974e-3 end
u-238 1 0.0 6.604e-4 end
u-235 1 0.0 1.008e-5 end
h 1 0.0 4.468e-2 end
c 1 0.0 4.537e-2 end
o 2 0.0 1.428e-2 end
h 2 0.0 5.712e-2 end
c 2 0.0 3.570e-2 end
end comp
buckledslab vacuum reflected 0.0 35.63 35.63 end
1 11.975 oneextermod
2 26.975 noextermod
end zone
EXPT 1677-02; CSAS25/KENO-Va; 2/4/92
read para
gen=303 tme=60 flx=yes fdn=yes pki=yes nub=yes
end para
read geom
cuboid 1 1 35.63 0.0 35.63 0.0 23.95 0.0
cuboid 2 2 50.63 -15.0 50.63 -15.0 38.95 -15.0
end geom
read bias
id=400 2 2 end bias
end data
end
```

```
#csas25
EXPT 1677-03; CSAS25; 1/31/92; Hansen-Roach CROSS SECTIONS
hansen-roach
multiregion
am-241 1 0.0 3.511e-7 end
pu-239 1 0.0 2.578e-4 end
pu-240 1 0.0 2.257e-5 end
pu-241 1 0.0 1.756e-6 end
o 1 0.0 1.974e-3 end
u-238 1 0.0 6.604e-4 end
u-235 1 0.0 1.008e-5 end
h 1 0.0 4.468e-2 end
c 1 0.0 4.537e-2 end
o 2 0.0 1.428e-2 end
h 2 0.0 5.712e-2 end
c 2 0.0 3.570e-2 end
end comp
buckledslab vacuum reflected 0.0 40.72 40.72 end
1 10.11 oneextermod
2 30.47 noextermod
end zone
EXPT 1677-03; CSAS25/KENO-Va; 1/31/92
read para
gen=303 tme=60 flx=yes fdn=yes pki=yes nub=yes
end para
read geom
cuboid 1 1 40.72 0.0 40.72 0.0 20.22 0.0
cuboid 2 2 55.72 -15.0 55.72 -15.0 35.22 -15.0
end geom
read bias
id=400 2 2 end bias
end data
end
```

```
#csas25
EXPT 1677-04; CSAS25; 2/4/92; Hansen-Roach CROSS SECTIONS
hansen-roach
multiregion
am-241 1 0.0 3.511e-7 end
pu-239 1 0.0 2.578e-4 end
pu-240 1 0.0 2.257e-5 end
pu-241 1 0.0 1.756e-6 end
o 1 0.0 1.974e-3 end
u-238 1 0.0 6.604e-4 end
u-235 1 0.0 1.008e-5 end
h 1 0.0 4.468e-2 end
c 1 0.0 4.537e-2 end
o 2 0.0 1.428e-2 end
h 2 0.0 5.712e-2 end
c 2 0.0 3.570e-2 end
end comp
buckledslab vacuum reflected 0.0 45.81 50.90 end
1 8.57 oneextermod
2 23.57 noextermod
end zone
EXPT 1677-04; CSAS25/KENO-Va; 2/4/92
read para
gen=303 tme=60 flx=yes fdn=yes pki=yes nub=yes
end para
read geom
cuboid 1 1 50.90 0.0 45.81 0.0 17.14 0.0
cuboid 2 2 65.90 -15.0 60.81 -15.0 32.14 -15.0
end geom
read bias
id=400 2 2 end bias
end data
end
```

```
#csas25
EXPT 1677-05; CSAS25; 2/4/92; Hansen-Roach CROSS SECTIONS
hansen-roach
multiregion
am-241 1 0.0 3.511e-7 end
pu-239 1 0.0 2.578e-4 end
pu-240 1 0.0 2.257e-5 end
pu-241 1 0.0 1.756e-6 end
o 1 0.0 1.974e-3 end
u-238 1 0.0 6.604e-4 end
u-235 1 0.0 1.008e-5 end
h 1 0.0 4.468e-2 end
c 1 0.0 4.537e-2 end
o 2 0.0 1.428e-2 end
h 2 0.0 5.712e-2 end
c 2 0.0 3.570e-2 end
end comp
buckledslab vacuum reflected 0.0 61.08 50.90 end
1 7.765 oneextermod
2 22.765 noextermod
end zone
EXPT 1677-05; CSAS25/KENO-Va; 2/4/92
read para
gen=303 tme=60 flx=yes fdn=yes pki=yes nub=yes
end para
read geom
cuboid 1 1 61.08 0.0 50.90 0.0 15.53 0.0
cuboid 2 2 76.08 -15.0 65.90 -15.0 30.53 -15.0
end geom
read bias
id=400 2 2 end bias
end data
end
```

```
#csas25
EXPT 1677-06; CSAS25; 2/4/92; Hansen-Roach CROSS SECTIONS
hansen-roach
multiregion
am-241 1 0.0 3.511e-7 end
pu-239 1 0.0 2.578e-4 end
pu-240 1 0.0 2.257e-5 end
pu-241 1 0.0 1.756e-6 end
o 1 0.0 1.974e-3 end
u-238 1 0.0 6.604e-4 end
u-235 1 0.0 1.008e-5 end
h 1 0.0 4.468e-2 end
c 1 0.0 4.537e-2 end
o 2 0.0 1.428e-2 end
h 2 0.0 5.712e-2 end
c 2 0.0 3.570e-2 end
end comp
buckledslab vacuum reflected 0.0 61.08 55.99 end
1 7.58 oneextermod
2 22.58 noextermod
end zone
EXPT 1677-06; CSAS25/KENO-Va; 2/4/92
read para
gen=303 tme=60 flx=yes fdn=yes pki=yes nub=yes
end para
read geom
cuboid 1 1 61.08 0.0 55.99 0.0 15.16 0.0
cuboid 2 2 76.08 -15.0 70.99 -15.0 30.16 -15.0
end geom
read bias
id=400 2 2 end bias
end data
end
```

```
#csas25
EXPT 1677-07; CSAS25; 2/4/92; Hansen-Roach CROSS SECTIONS
hansen-roach
multiregion
am-241 1 0.0 3.511e-7 end
pu-239 1 0.0 2.578e-4 end
pu-240 1 0.0 2.257e-5 end
pu-241 1 0.0 1.756e-6 end
o 1 0.0 1.974e-3 end
u-238 1 0.0 6.604e-4 end
u-235 1 0.0 1.008e-5 end
h 1 0.0 4.468e-2 end
c 1 0.0 4.537e-2 end
o 2 0.0 1.428e-2 end
h 2 0.0 5.712e-2 end
c 2 0.0 3.570e-2 end
end comp
buckledslab vacuum reflected 0.0 66.17 61.08 end
1 7.215 oneextermod
2 22.215 noextermod
end zone
EXPT 1677-07; CSAS25/KENO-Va; 2/4/92
read para
gen=303 tme=60 flx=yes fdn=yes pki=yes nub=yes
end para
read geom
cuboid 1 1 66.17 0.0 61.08 0.0 14.43 0.0
cuboid 2 2 81.17 -15.0 76.08 -15.0 29.43 -15.0
end geom
read bias
id=400 2 2 end bias
end data
end
```

```
#csas25
EXPT 1677-08; CSAS25; 2/4/92; Hansen-Roach CROSS SECTIONS
hansen-roach
multiregion
am-241 1 0.0 3.511e-7 end
pu-239 1 0.0 2.578e-4 end
pu-240 1 0.0 2.257e-5 end
pu-241 1 0.0 1.756e-6 end
o 1 0.0 1.974e-3 end
u-238 1 0.0 6.604e-4 end
u-235 1 0.0 1.008e-5 end
h 1 0.0 4.468e-2 end
c 1 0.0 4.537e-2 end
o 2 0.0 1.428e-2 end
h 2 0.0 5.712e-2 end
c 2 0.0 3.570e-2 end
end comp
buckledslab vacuum reflected 0.0 50.90 50.90 end
1 8.245 oneextermod
2 23.245 noextermod
end zone
EXPT 1677-08; CSAS25/KENO-Va; 2/4/92
read para
gen=303 tme=60 flx=yes fdn=yes pki=yes nub=yes
end para
read geom
cuboid 1 1 50.90 0.0 50.90 0.0 16.49 0.0
cuboid 2 2 65.90 -15.0 65.90 -15.0 31.49 -15.0
end geom
read bias
id=400 2 2 end bias
end data
end
```

```
#csas25
EXPT 1677-09; CSAS25; 2/4/92; Hansen-Roach CROSS SECTIONS
hansen-roach
multiregion
am-241 1 0.0 3.511e-7 end
pu-239 1 0.0 2.578e-4 end
pu-240 1 0.0 2.257e-5 end
pu-241 1 0.0 1.756e-6 end
o 1 0.0 1.974e-3 end
u-238 1 0.0 6.604e-4 end
u-235 1 0.0 1.008e-5 end
h 1 0.0 4.468e-2 end
c 1 0.0 4.537e-2 end
end comp
buckledslab vacuum reflected 0.0 45.81 40.72 end
1 17.99 noextermod
end zone
EXPT 1677-09; CSAS25/KENO-Va; 2/4/92
read para
gen=303 tme=60 flx=yes fdn=yes pki=yes nub=yes
end para
read geom
cuboid 1 1 45.81 0.0 40.72 0.0 37.98 0.0
end geom
end data
end
```

```
#csas25
EXPT 1677-10; CSAS25; 2/4/92; Hansen-Roach CROSS SECTIONS
hansen-roach
multiregion
am-241 1 0.0 3.511e-7 end
pu-239 1 0.0 2.578e-4 end
pu-240 1 0.0 2.257e-5 end
pu-241 1 0.0 1.756e-6 end
o 1 0.0 1.974e-3 end
u-238 1 0.0 6.604e-4 end
u-235 1 0.0 1.008e-5 end
h 1 0.0 4.468e-2 end
c 1 0.0 4.537e-2 end
end comp
buckledslab vacuum reflected 0.0 40.72 42.24 end
1 20.36 noextermod
end zone
EXPT 1677-10; CSAS25/KENO-Va; 2/4/92
read para
gen=303 tme=60 flx=yes fdn=yes pki=yes nub=yes
end para
read geom
cuboid 1 1 40.72 0.0 40.72 0.0 42.24 0.0
end geom
end data
end
```

The file ROOT.EXE in the ROOT directory and the file SECTION6.EXE in the SECTION6.DIR directory are self-extracting archives.

To re-create the original files, just execute those two files. The .EXE files and this file can then be deleted.